

**FUNCTIONAL STUDY OF AMINO ACIDS AT N- AND
C-TERMINI OF CYT2Aa2 TOXIN**

SIRIYA THAMMACHAT

**A THESIS SUBMITTED IN PARTIAL FULFILLMENT
OF THE REQUIREMENTS FOR
THE DEGREE OF DOCTOR OF PHILOSOPHY
(MOLECULAR GENETICS AND GENETIC ENGINEERING)
FACULTY OF GRADUATE STUDIES
MAHIDOL UNIVERSITY
2010**

COPYRIGHT OF MAHIDOL UNIVERSITY

Thesis
entitled
**FUNCTIONAL STUDY OF AMINO ACIDS AT N- AND
C-TERMINI OF CYT2Aa2 TOXIN**

.....
Miss Siriya Thammachat
Candidate

.....
Assoc. Prof. Chartchai Krittanai, Ph.D.
Major-advisor

.....
Asst. Prof. Boonhiang Promdonkoy, Ph.D.
Co-advisor

.....
Asst. Prof. Gerd Katzenmeier, Ph.D.
Co-advisor

.....
Asst. Prof. Panadda Boonserm, Ph.D.
Co-advisor

.....
Prof. Banchong Mahaisavariya, M.D.
Dip. Thai Board of Orthopedics
Dean
Faculty of Graduate Studies
Mahidol University

.....
Assoc. Prof. Apinunt Udomkit, Ph.D.
Program Director
Doctor of Philosophy in Molecular
Genetics and Genetic Engineering
Institute of Molecular Biosciences
Mahidol University

Thesis
entitled
**FUNCTIONAL STUDY OF AMINO ACIDS AT N- AND
C-TERMINI OF CYT2Aa2 TOXIN**

was submitted to the Faculty of Graduate Studies, Mahidol University for the degree
of Doctor of Philosophy (Molecular Genetics and Genetic Engineering)

on
June 21, 2010

.....
Miss Siriya Thammachat
Candidate

.....
Assoc. Prof. Apinunt Udomkit, Ph.D.
Chair

..... Assoc. Prof. Chartchai Krittanai, Ph.D. Member Asst. Prof. Panadda Boonserm, Ph.D. Member
--	--

..... Assoc. Prof. Wannapong Triampo, Ph.D. Member Asst. Prof. Boonhiang Promdonkoy, Ph.D. Member
--	--

..... Prof. Banchong Mahaisavariya, M.D. Dip. Thai Board of Orthopedics Dean Faculty of Graduate Studies Mahidol University Prof. Prasert Auewarakul, M.D. Dr. med. Director Institute of Molecular Biosciences Mahidol University
--	--

ACKNOWLEDGEMENTS

My Ph.D. thesis was successful because there are valuable suggestions and strong support from my major advisor, Assoc. Prof. Chartchai Krittanai and my co-advisors, Asst. Prof. Boonhiang Promdonkoy, Asst. Prof. Panadda Boonserm. I am very appreciated them in their valuable help and guidance for my research.

I would like to gratefully thank Dr. Apichai Bourchookarn, Dr. Anchane Sangcharoen, Mrs. Nuanwan Pungtanom, Miss Somruathai Kidsanguan, Mr. Suparat Taengchaiyaphum, Dr. Phattara-orn Havanapan, and Miss Wanwarang Pathaichindachote for their encouragement, assistance, and discussion including the knowledge of laboratory.

This study was supported by the Royal Golden Jubilee Ph.D. program from the Thailand Research Fund (TRF) and the scholarship from National Center for Genetic Engineering and Biotechnology, NSTDA during 2006-2007.

I would like to thank all staffs and my friends for assistance, their precious and memorable friendship. Finally, I would like to express my deepest appreciation and thankfulness to my family for their entirely love, support and encouragement in my life.

Siriya Thammachat

FUNCTIONAL STUDY OF AMINO ACIDS AT N-AND C-TERMINI OF CYT2Aa2 TOXIN

SIRIYA THAMMACHAT 4837245 MBMG/D

Ph.D. (MOLECULAR GENETICS AND GENETIC ENGINEERING)

THESIS ADVISORY COMMITTEE: CHARTCHAI KRITTANAI, Ph.D.,
BOONHIANG PROMDONKOY, Ph.D., PANADDA BOONSERM, Ph.D., GERD
KATZENMEIER, Ph.D.

ABSTRACT

Cyt2Aa2 is a 29 kDa cytolytic protein produced by *Bacillus thuringiensis* supsp. *darmstadiensis* during the sporulation stage. This protein exerts lethal activity against mosquito larvae *in vivo* and broad-range activity *in vitro*. To become a 25 kDa active toxin, a proteolytic processing of N-and C-termini is required. This study aims to investigate a functional role of amino acids on the N-terminus (position 1-40) and the C-terminus (position 229-259) of Cyt2Aa2. A number of mutant toxins with destabilizing interactions between these two terminal fragments or two monomers were generated and analyzed in comparison with the wild-type Cyt2Aa2. Results show that substitution by alanine at positions R25, P27, and I31, and by leucine at position D39 and the deletion of 22 amino acids at the C-terminus (N238-N259) did not affect the structure and function of the toxin. On the other hand, alanine substitution at L33, N230, and I233 affected protein conformation and toxicity. C-terminal truncation from S229 and I233 dramatically reduced protein production and toxicity and affected the tertiary structure of Cyt2Aa2. Results suggest that amino acids located at β 1 on the N-terminus and α F on the C-terminus play important roles during structural folding, dimerization, and inclusion formation. Amino acid replacement and deletion of these regions could lead to protein misfolding which causes an inability in the protein to maintain its biological activities.

KEY WORDS: *Bacillus thuringiensis* / MUTAGENESIS/ AMINO ACID/
Cyt2Aa2/ MOSQUITO LARVICIDAL TOXICITY

94 pages

การศึกษาบทบาทและหน้าที่ของกรดอะมิโนบนปลายด้านหมู่อะมิโนและด้านหมู่คาร์บอกซีของ
โปรตีน Cyt2Aa2

FUNCTIONAL STUDY OF AMINO ACIDS AT N- AND C-TERMINI OF CYT2Aa2 TOXIN

สิริยา ธรรมชาติ 4837245 MBMG/D

ปร.ด. (อนุพันธุศาสตร์และพันธุวิศวกรรมศาสตร์)

คณะกรรมการที่ปรึกษาวิทยานิพนธ์ : ชาติชาย กฤตชัย, Ph.D. บุญเสียง พรหมคอนกอย, Ph.D.,
ปนัดดา บุญเสริม, Ph.D., GERD KATZENMEIER, Ph.D.

บทคัดย่อ

Cyt2Aa2 เป็นโปรตีนที่มีขนาดเริ่มต้น 29 กิโลดาลตัน พบได้ใน *Bacillus thuringiensis* สายพันธุ์ *darmstadensis* โปรตีนชนิดนี้จำเป็นต้องถูกตัดด้วยเอ็นไซม์ที่บริเวณปลายด้านอะมิโนและด้านคาร์บอกซีจึงจะสามารถออกฤทธิ์ฆ่าลูกน้ำยุงและทำให้เชื้อหุ้มของเซลล์หลายชนิดแตกได้ในหลอดทดลอง งานวิจัยนี้ได้สร้างโปรตีนกลายพันธุ์ที่มีการเปลี่ยนแปลงของกรดอะมิโนที่ตำแหน่งบนปลายด้านอะมิโน (ตำแหน่ง 1-40) และคาร์บอกซี (ตำแหน่ง 229-259) โดยวิธีการก่อกลายพันธุ์ที่ตำแหน่งจำเพาะและทำการศึกษาวเคราะห์คุณสมบัติต่างๆของโปรตีนกลายพันธุ์ทั้งหมดเปรียบเทียบกับโปรตีนต้นแบบ พบว่าโปรตีนกลายพันธุ์ที่ถูกแทนที่ด้วยอะลานีนที่อาร์จินิน25 โพรลีน27 ไอโซลิวซีน31 และลิวซีนที่แอสพาร์เตต39 และที่ถูกตัดทางด้านปลายคาร์บอกซีจากแอสพาราจิน238ยังคงมีโครงสร้างและคุณสมบัติในการออกฤทธิ์เทียบเท่ากับโปรตีนต้นแบบ ในขณะที่โปรตีนกลายพันธุ์ที่ถูกแทนที่ด้วยอะลานีนที่ลิวซีน33 แอสพาราจิน230และไอโซลิวซีน233 มีโครงสร้างที่แตกต่างไปจากเดิมและมีประสิทธิภาพในการออกฤทธิ์ลดลง นอกจากนี้โปรตีนกลายพันธุ์ที่ถูกตัดทางด้านปลายคาร์บอกซีจากเซอรีน229 และไอโซลิวซีน233 มีการผลิตโปรตีนและออกฤทธิ์ได้น้อยลง อีกทั้งยังมีโครงสร้างชั้นตติยภูมิที่แตกต่างไปจากโปรตีนต้นแบบ ผลการทดลองชี้ให้เห็นว่ากรดอะมิโนที่ปลายด้านอะมิโนและคาร์บอกซีของโปรตีนCyt2Aa2 มีบทบาทสำคัญในการสร้างโปรตีนในเซลล์ การรักษาเสถียรภาพของโครงสร้างโปรตีน การละลายของโปรตีน ความสามารถในการถูกตัดด้วยเอ็นไซม์และประสิทธิภาพในการออกฤทธิ์ของโปรตีน

CONTENTS

	Page
ACKNOWLEDGEMENTS	iii
ABSTRACT (ENGLISH)	iv
ABSTRACT (THAI)	v
LIST OF TABLES	ix
LIST OF FIGURES	x
LIST OF ABBREVIATION	xii
CHAPTER I INTRODUCTION	1
1.1 <i>Bacillus thuringiensis</i>	1
1.2 <i>Bt</i> toxins	3
1.3 Cytolytic toxin	3
1.4 Cyt2Aa2 toxin	3
CHAPTER II OBJECTIVES	20
CHAPTER III MATERIALS	21
3.1 Chemicals	21
3.2 Enzymes and accessory buffers	21
3.3 Bacteria strain	23
3.4 Culture media	23
3.5 Oligonucleotide primers	23
3.6 Miscellaneous	26
CHAPTER IV METHODS	27
4.1 Plasmid extraction	27
4.2 Agarose gel electrophoresis	28

CONTENT (cont.)

	Page
4.3 Site-directed mutagenesis	28
4.4 Competent cells preparation by CaCl ₂	32
4.5 Transformation of DNA plasmid into competent cell	32
4.6 Restriction enzyme analysis	32
4.7 Automated DNA sequencing	33
4.8 Expression level of protein	33
4.9 Expression and partial purification of protein	33
4.10 Protein quantification by Bradford's assay	34
4.11 SDS-PAGE analysis	34
4.12 Western blot analysis	36
4.13 Protein solubilization	36
4.14 Proteolytic processing by Proteinase K	37
4.15 Mosquito larvicidal activity assay	37
4.16 Haemolytic activity assay	37
4.17 Toxin oligomerization assay	38
4.18 Protein purification	38
4.19 Intrinsic fluorescence spectrometry	39
4.20 Dynamic light scattering	39
CHAPTER V RESULTS	40
5.1 Site-directed mutagenesis	40
5.2 Protein expression and identification	40
5.3 Solubilization and proteinase K processing	48
5.4 Mosquito larvicidal toxicity	48

CONTENT (cont.)

	Page
5.5 Haemolytic activity	55
5.6 Protoxin dimerization	55
5.7 Toxin oligomerization	55
5.8 Intrinsic fluorescence spectroscopy	63
5.9 Dynamic light scattering	63
CHAPTER VI DISCUSSION	72
CHAPTER VII SUMMARY	85
REFERENCES	86
BIOGRAPHY	93

LIST OF TABLES

Table	Page
1.1 List of <i>cyt</i> genes from several <i>Bacillus thuringiensis</i> strains	4
3.1 List of endonuclease restriction enzymes and their recognition sites	22
3.2 Primer sequences for site-directed mutagenesis	24
4.1 Temperature cycling parameters for site-directed mutagenesis	31
4.2 Composition of SDS-polyacrylamide gel	35
5.1 Mosquito larvicidal toxicity of Cyt2Aa2 and mutant proteins	54
5.2 Haemolysis end-point of Cyt2Aa2 and mutant proteins	56
6.1 List of truncated mutants of Cyt2Aa2 toxin	84

LIST OF FIGURES

Figure	Page
1.1 Electron micrograph of <i>Bacillus thuringiensis</i> subsp. <i>israelensis</i>	2
1.2 Phylogram of Cyt toxin family	5
1.3 The structure of Cyt2Aa1 monomer from <i>Bacillus thuringiensis</i> subsp. <i>kyushuensis</i>	7
1.4 Predicted secondary structure of Cyt1Aa1 protein	8
1.5 The crystal structure of activated Cyt2Ba monomer	9
1.6 Alignment of amino acid sequences of six Cyt proteins from different subspecies of <i>Bacillus thuringiensis</i>	10
1.7 Nucleotide and deduced amino acid sequences of Cyt2Aa2 toxin	12
1.8 Topology diagram of Cyt2A protein	13
1.9 The structure of Cyt2A protoxin (dimer)	14
1.10 The two proposed mechanisms of Cyt toxin	17
1.11 Proposed oligomeric pore structure of Cyt2Aa1 protein	18
4.1 Overview of QuikChange™ site-directed mutagenesis method (Stratagene)	30
5.1 PCR products of all mutants	41
5.2 Expression level of mutants and Cyt2Aa2	42
5.3 Protein profile of all mutants and Cyt2Aa2 on 15% polyacrylamide gel	44
5.4 Partially purified inclusion of D39L mutant and Cyt2Aa2	46
5.5 Partially purified inclusion of mutant and Cyt2Aa2	47
5.6 Partially purified inclusion of truncated mutants and Cyt2Aa2	49
5.7 Western blot analysis of Cyt2Aa2 and mutant inclusion	50
5.8 Protoxin and proteinase K activated product of Cyt2Aa2 protein	51
5.9 Solubilization in 50 mM Na ₂ CO ₃ /NaHCO ₃ buffer pH 9.5 and proteinase K activation of mutants	52
5.10 Protein solubilization and proteolytic processing of S229stop and Cyt2Aa2	53

LIST OF FIGURES (cont.)

Figure	Page
5.11 Haemolytic activity of mutant and Cyt2Aa2 proteins	57
5.12 Cyt2Aa2 and mutant protoxins in presence and absence of reducing agent on 12.5 % polyacrylamide gel	59
5.13 Cyt2Aa2 and truncated protoxins in presence and absence of reducing agent on 12.5 % polyacrylamide gel	60
5.14 Toxin oligomerization test of Cyt2Aa2 toxin	61
5.15 Toxin oligomerization test of D39L toxin compared with Cyt2Aa2 toxin	62
5.16 Intrinsic fluorescence spectra of mutants compared with Cyt2Aa2	64
5.17 Size distribution profile of mutants and Cyt2Aa2 protoxin in 50 mM Na ₂ CO ₃ /NaHCO ₃ buffer, pH 9.5	69
6.1 H-bond pattern in β -sheet of two monomers and van der Waals contacts on dimer interface of Cyt2 protein	74
6.2 The H-bond interaction between I31 and L33 of Cyt2 protoxin	75
6.3 H-bond between α F of two monomers	77
6.4 H-bond network between D39, L33 and N241 in Cyt2A monomer	82

LIST OF ABBREVIATIONS

% (w/w)	percent weight by weight
% T	percent of gel
Amp	Ampicillin
ANS	8-anilinonaphthalene-1-sulfonic acid
a.u.	arbitrary unit
BSA	bovine serum albumin
bp	base pairs
°C	degree Celsius
Cry	crystal
Cyt	cytolytic
DNA	Deoxyribonucleic acid
DTT	1,4-dithiothreitol
<i>E. coli</i>	<i>Eschericia coli</i>
EDTA	ethylenediamine tetraamino acid
<i>et al.</i>	and others
EtBr	ethidium bromide
g	gram(s)
hr	hour(s)
IPTG	isopropyl-β-D-thiogalactopyranoside
kb	kilobase(s)
kDa	kilodalton(s)
LB	Luria-Bertani medium
M	molar (mol/l)
mg	milligram(s)
min	minute(s)

LIST OF ABBREVIATIONS (cont.)

ml	milliliter(s)
mM	millimolar
MW	molecular weight
μg	microgram(s)
nm	nanometer(s)
N-terminus	amino terminus
C-terminus	carboxyl terminus
OD ₆₀₀	optical density at 600 nm
OD ₅₄₀	optical density at 540 nm
psi	pound per square inch
rpm	revolution per minute
UV	ultraviolet

CHAPTER I

INTRODUCTION

1.1 *Bacillus thuringiensis*

Bacillus thuringiensis (*Bt*) is a rod-shaped, catalase-positive, gram-positive bacterium. It can be found in many habitats including soil [1] and plant leaves [2]. The genome size of *Bacillus thuringiensis* strains is approximately at 2.4 to 5.7 million bp [3] and contains a large variety of transposable elements [4]. During the stationary phase of its growth cycle, *Bacillus thuringiensis* produces parasporal crystal proteins [4], as shown in **figure 1.1**. The crystalline proteins can be classified into 2 major classes which are Cry and Cyt proteins [5]. Surprisingly, both of them were found to be toxic to insect larvae. Its insecticidal activities are highly offensive to the order of *Lepidoptera* (moths and butterflies), *Blattodea* (cockroaches), *Coleoptera* (beetles), *Diptera* (flies and mosquitoes), *Hymenoptera* (bees and wasps), Homoptera, Orthoptera, and Mallophaga [6-10]. However, they are harmless to humans, vertebrates and plants [11]. They are very friendly to the environment because they are easily and completely biodegradable [11]. Currently, *Bt* toxin is a good choice to develop to be bio-pesticides for commercial in agriculture and forestry fields [4, 11-13]. For example, it was studied to control of sheep blowfly species (*Lucilia cuprina*, *L. sericata*, and *Calliphora stygia*) instead of chemical insecticides [12, 14]. In medical field, it can be used to control mosquitoes and blackflies which are vectors of serious human diseases, such as dengue fever and river blindness [11]. Moreover, it was applied in the development of transgenic insect-resistant plants [11]. In the present, several strains of *B. thuringiensis* have been classified into 55 serotypes based on their H flagellar antigens [15]. Individual subspecies produce a range of different toxins with differing insect specificities and can also be grouped into different pathotypes on the basis of their insect targets [16].

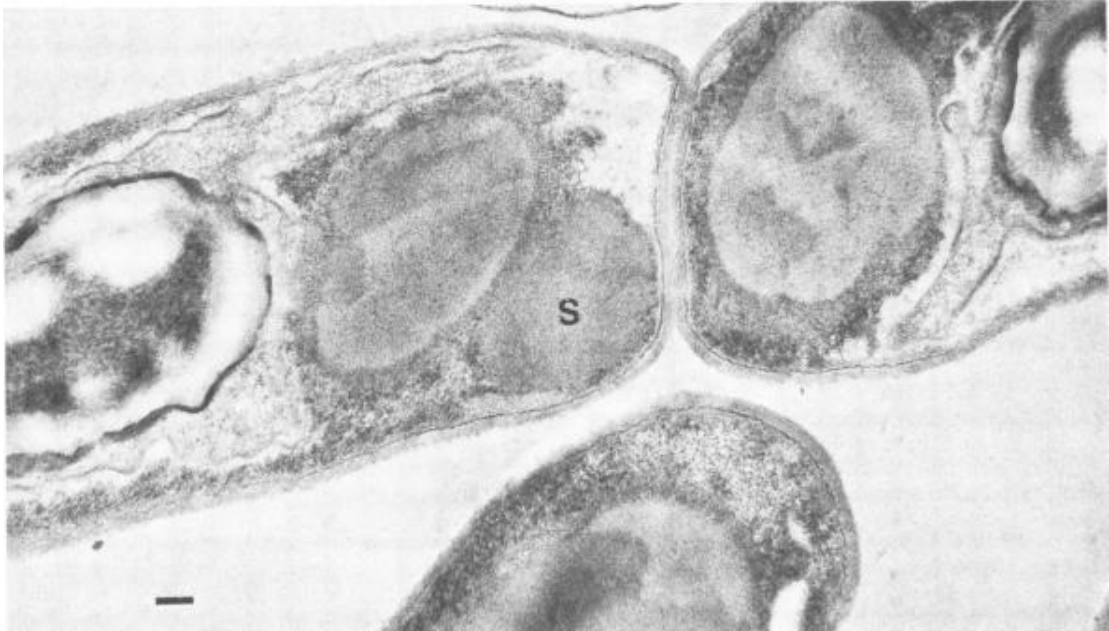


Figure 1.1: Electron micrograph of *Bacillus thuringiensis* subsp. *israelensis*
(Bar, 0.1 μm ; x 138, 600)

Bacillus thuringiensis subsp. *israelensis* produces parasporal inclusion (S) during sporulation stage [17].

1.2 *Bt* toxin

The crystal proteins are produced from *Bacillus thuringiensis* during sporulation phase of life cycle known as δ -endotoxins [4]. Based on amino acid sequences, crystal proteins have been distinguished to two major families which are Crystal (Cry) and Cytolytic (Cyt) toxins [5, 15]. Cry and Cyt toxins are expected to have similar mode of action but they also have differences in many aspects. Firstly, Cyt toxin is highly toxic to Dipteran larvae, whereas Cry toxin is specifically toxic to various insect orders, Lepidoptera, Coleoptera, Hymenoptera, Diptera [18, 19]. Secondly, Cyt toxin shows broad-range activity to a variety of eukaryotic cells and erythrocytes *in vitro* [20-23] but Cry toxin requires specific-receptors for protein binding [18, 20-23]. Finally, Cyt toxin (25-28 kDa) is smaller than Cry toxin [24]. Cyt toxin is a single domain protein that is entirely different protein structure from Cry toxin [25]. In contrast, Cry toxin is large and composed of three domains. Cyt toxins have been found in a variety of mosquitocidal *B. thuringiensis* strains [20] which are *Bacillus thuringiensis* (Bt) subspecies *israelensis* [26], *kyushuensis* [24], *fukuokaensis* [27], *jegathesan* [28], *darmstadiensis* [29] and *meddellin* [30]. In addition, some strains of *B. thuringiensis* produce pesticidal proteins during vegetative growth called Vegetative Insecticidal Proteins (VIPs) [31]. The VIPs are not parasporal crystal proteins but they are secreted from the cell. The VIPs exhibit their toxicity against lepidopteran insect pest [31].

1.3 Cytolytic toxin

Cyt proteins can be divided into 2 subtypes which are Cyt1 (CytA) and Cyt2 (CytB) proteins. The entomocidal delta-endotoxins Cyt1 and Cyt2 are produced in many strains of *Bacillus thuringiensis* as shown in **table 1.1**. The phylogenetic tree of phylogenetic is shown in **figure 1.2** [32]. The alignment of amino acid sequences of Cyt1 and Cyt2 proteins demonstrated a 39% identity and 70% similarity [24]. The proteases cleavage sites of Cyt1 and Cyt2 are found at matching positions on the sequence alignment and were equally haemolytic *in vitro* [33]. They are also similar in amino acid sequence, predicted secondary structure, and alpha-helical content. The

Table 1.1: List of *cyt* genes from several *Bacillus thuringiensis* strains [34]

Gene	Subspecies	Access No. [Reference]
<i>cyt1Aa1</i>	<i>israelensis</i>	X03182 [26]
<i>cyt1Aa2</i>	<i>israelensis</i>	X04338 [35]
<i>cyt1Aa3</i>	<i>morrisoni</i> PG14	Y00135 [36]
<i>cyt1Aa4</i>	<i>morrisoni</i> PG14	M35968 [37]
<i>cyt1Ab1</i>	<i>medellin</i>	X98793 [38]
<i>cyt1Ba1</i>	<i>neoleonensis</i>	U37196 [39]
<i>cyt2Aa1</i>	<i>kyushuensis</i>	Z14147 [24]
<i>cyt2Aa2</i>	<i>darmstadiensis</i>	AF472606 [40]
<i>cyt2Ba1</i>	<i>israelensis</i>	U52043 [41]
<i>cyt2Ba2</i>	<i>morrisoni</i> PG14	AF020789[25]
<i>cyt2Ba3</i>	<i>fukuokaensis</i>	AF022884[25]
<i>cyt2Ba4</i>	<i>morrisoni</i> HD12	AF022885[25]
<i>cyt2Ba5</i>	<i>morrisoni</i> HD518	AF022886[25]
<i>cyt2Ba6</i>	<i>morrisoni</i> serovar <i>tenebrionis</i>	AF034926[25]
<i>cyt2Ba7</i>	strain T301	AF215645 [42]
<i>cyt2Bb1</i>	<i>jegathesan</i>	U82519 [20]
<i>cyt2Bc1</i>	<i>medellin</i>	AJ251979 [43]

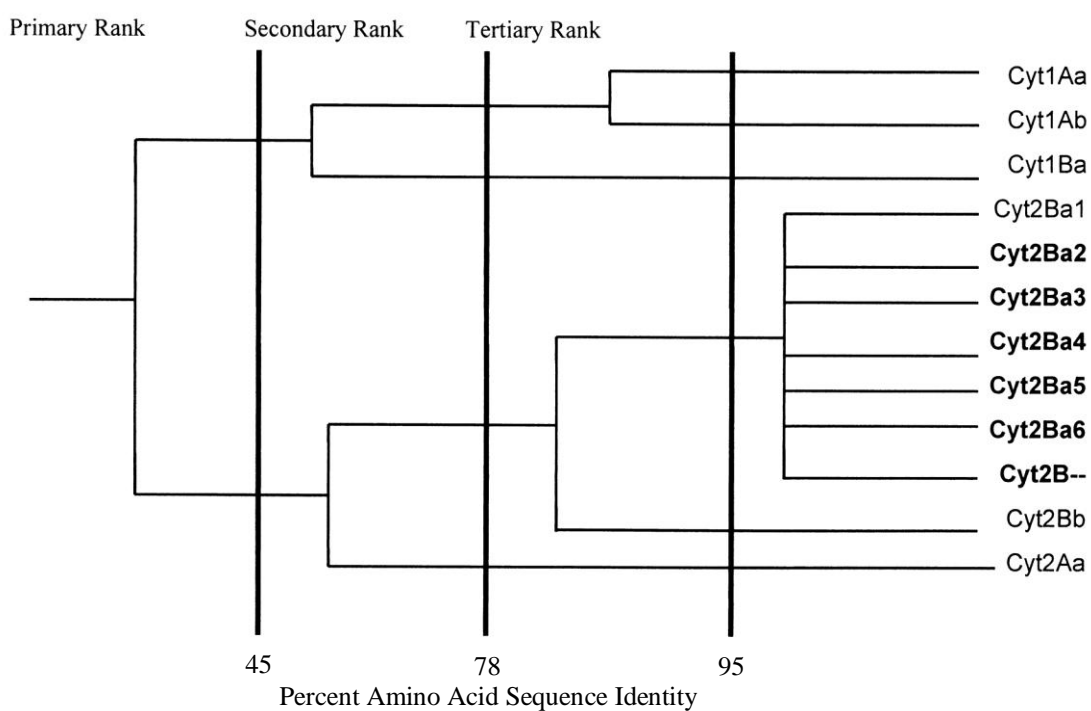


Figure 1.2: Phylogram of Cyt toxin family

The figure illustrates the relationship between Cyt toxins. Thicker vertical lines divide the four levels of nomenclature ranks. Protein names in boldface indicate that the central region of the genes has been used for comparison [32].

only obvious difference is an additional fifteen residue at C-terminus of Cyt2 that may facilitate high expression and inclusions formation in an acrySTALLIFEROUS without a 20 kDa helper protein which is essential for Cyt1 inclusion formation [33]. The 20 kDa helper protein was proposed to improve expression of Cyt1 protein in *E. coli* cells through post-transcriptional regulation of *cyt1* gene [44]. Some studies suggested that the helper protein does not affect on post-transcription and translational initiation [45]. It may bind to nascent Cyt1 polypeptide to prevent from degradation [46].

After Li et al. [25] obtained X-ray crystallographic structure of Cyt2Aa1 shown in **figure 1.3** (in absence of lipid), Cyt1Aa1 structure as **figure 1.4** was created using the Swiss-Pdb Viewer 3.1 software and expected to be similar to Cyt2Aa1. Cyt1Aa1 was predicted to have two outer α -helix hairpins (helices A-B and C-D) flanking a core of mixed β -sheet (strands 1 to 7). In addition, the study revealed that activated Cyt2Ba toxin is composed of a six β -sheets surrounded by two outer α -helix layers (helices 1-5) as shown in **figure 1.5** [47]. From **figure 1.6**, an alignment result of amino acid sequences of six Cyt proteins from various subspecies of *B. thuringiensis* showed four blocks with high similarity scores and high statistical significance. Comparison of **figures 1.3-1.6** indicates that the four blocks are (i) helix A (consensus sequence YILQAIQLANAFQGALDP), (ii) the loop after helix D plus beta strand 4 (TFTNLNTQKDEAWIFW), (iii) beta strand 5 and beta strand 6 (TNYYYNVLFIAIQNEDTGGVMACVPIGFE), and (iv) strand 6a and the following loop (LFFTIKDSARY) [48].

1.4 Cyt2Aa2 toxin

Cyt1Aa toxin isolated from *Bacillus thuringiensis* subsp. *israelensis* is the first cytolytic toxin that was discovered and thoroughly characterized [32, 49]. Cyt2Aa1 produced from *Bacillus thuringiensis* subsp. *kyushuensis* is another cytolytic toxin [20, 24, 26] that can exhibit toxicity against mosquito larvae and show broad-range activity *in vitro* [50]. A cytolytic protein isolated from *B. thuringiensis* subsp. *darmstadiensis* (Btd 73E10-2) showed an immunological cross-reactivity with anti-Cyt2Aa1 antibody but did not react with anti-Cyt1Aa1 antibody [50, 51]. It can imply

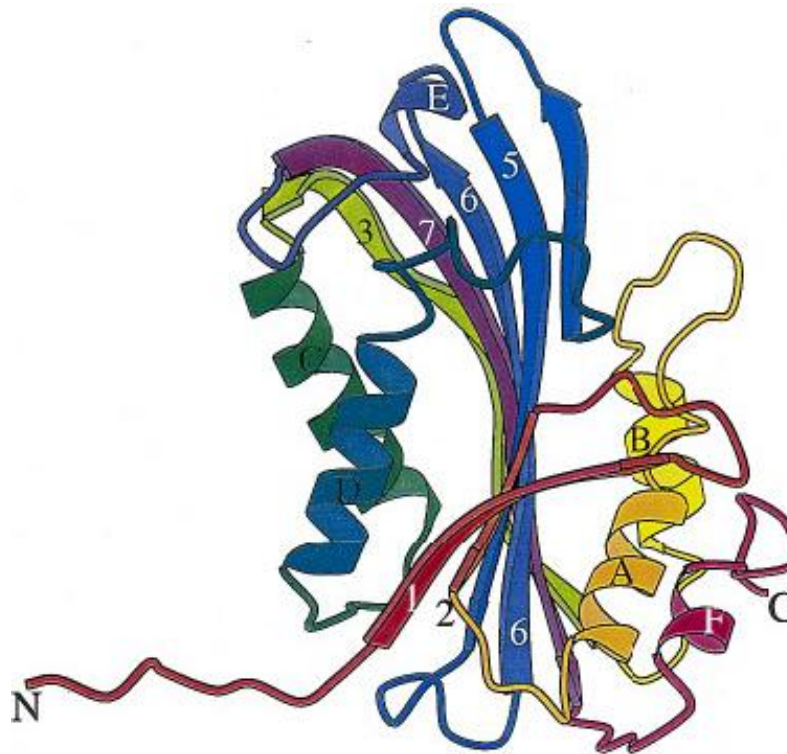


Figure 1.3: The structure of Cyt2Aa1 monomer from *Bacillus thuringiensis* subsp. *kyushuensis* prepared by MOLSCRIPT [25]

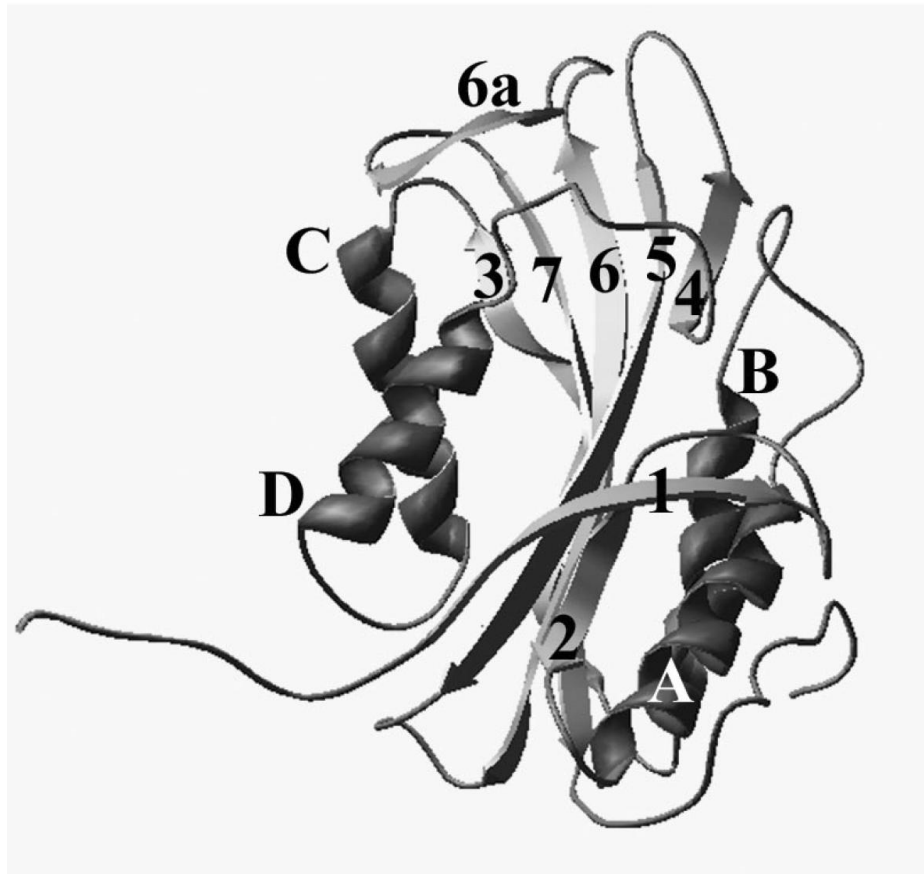


Figure 1.4: Predicted secondary structure of Cyt1Aa1 protein created with Swiss-PdbViewer 3.1

The structure was predicted based on the X-ray crystallographic structure of Cyt2Aa1 protein [25]. The α -helices are marked by letters, and β -strands are numbered [48].

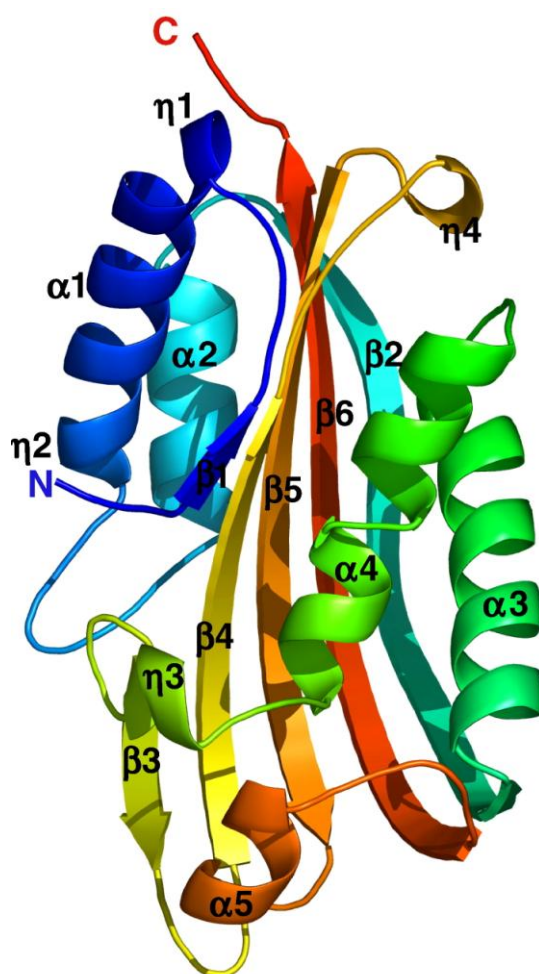


Figure 1.5: Crystal structure of activated Cyt2Ba monomer created with PyMOL [47]

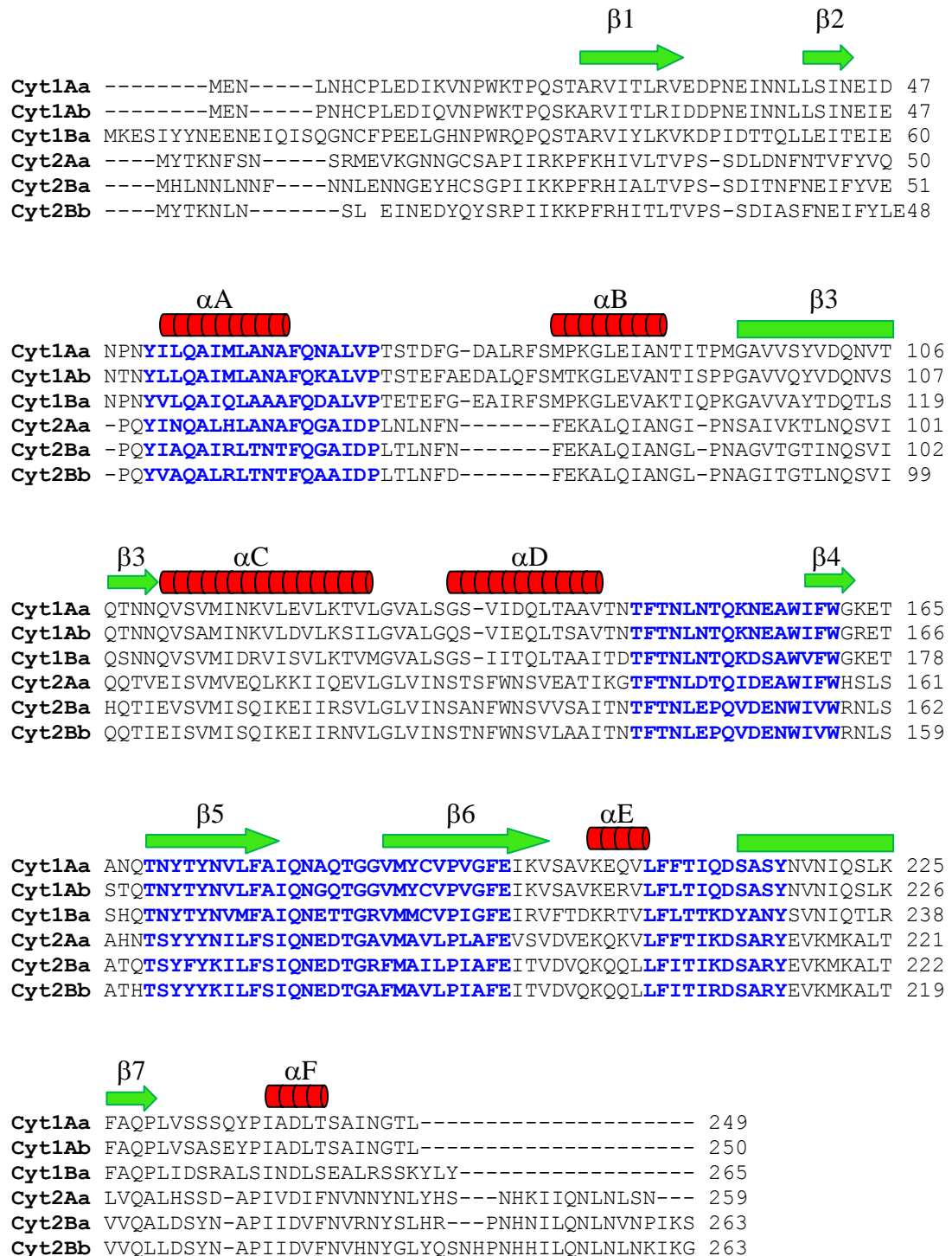


Figure 1.6: Alignment of amino acid sequences of six Cyt proteins from different subspecies of *B. thuringiensis* generated by BioEdit program: Highly conserved blocks are in blue letter.

that *B. thuringiensis* subsp. *darmstadiensis* contains a *cyt2A*-like gene. The gene was cloned into *E. coli* cell and then verified DNA sequences. DNA sequence analysis showed that the gene is 854 bp containing an open reading frame translating to 259 amino acids shown in **figure 1.7** [40]. The cloned gene was designated *cyt2Aa2*. *cyt2Aa2* can be expressed in *Escherichia coli* system as inclusion bodies which could be solubilized in alkaline buffer. The 28 k-Da protoxin was processed by proteinase K resulting in 25-kDa (T34-F237) and 23-kDa (S38-S228) activated fragments that is similar to Cyt2Ba toxin. The structure of the endogenously cleaved Cyt2Ba monomer is from T41 to S228. Cyt2Aa2 toxin is highly toxic to *Culex quinquefasciatus* and *Aedes aegypti* larvae and it can lyse sheep erythrocytes [40].

From X-ray crystallographic experiment of unprocessed Cyt2A protein, it showed that Cyt2A is a single domain protein of α/β architecture that is composed of six α -helices and seven β -sheets as shown in **figure 1.3** [25]. The two α -helices are in outer layer and a mixed β -sheet is in the middle of the protein structure (**figure 1.8**) [25]. Cyt2A toxin structure is similar to volvatoxin A2 (VVA2), a cardiotoxin produced by a straw mushroom *Volvariella volvacea* [52]. The α -helices have the amphipathic property, the hydrophobic residues face against the β -sheet while the polar and charge residues point out to the environment. The β -strands have shown strongly left-handed twist and amphipathic character in some of the β -sheets.

Cyt2A protoxin is generally in a dimer form by intertwining their N-terminal arms after proteolysis processing of N- and C-terminal parts, and it will be released to monomeric molecule [24]. The N-terminal part of protoxin Cyt2A is involved with dimerization between two molecules by intertwining with another N-terminal end from another molecule [25]. The protoxin dimers have been produced to stabilize secondary structure of the protoxin molecules. Five areas of the monomeric surface are possible to provide the interaction between each other as shown in **figure 1.9** [25]. Firstly, hydrogen bonds between F28 to P36 of $\beta'1$ and N44 to Y48 of $\beta1$ and $\beta2$ in another molecule. Secondly, the salt bridge and van der Waals interactions of loop $_{\alpha D, \beta 4}$, loop $_{\beta 1, \beta 2}$, loop $_{\alpha A, \alpha B}$ with the region before $\beta1$ of another monomer. Thirdly, the interactions between loop $_{\beta 7, \alpha F}$ and αF , Asn230 in loop $_{\beta 7, \alpha F}$ and Val234 in

```

TAATTTAAAAGGAGGATCATAATATGTATACTAAAAATTTTAGTAATTCAGAATGGAAG 60
      M Y T K N F S N S R M E V 13

TAAAAGGTAATAACGGGTGTTCTGCACCTATTATTAGAAAACCATTTAAACATATTGTAT 120
      K G N N G C S A P I I R K P F K H I V L 33

TAACGGTTCATCCAGTGATTTAGATAATTTTAATACAGTCTTTTATGTACAACCACAAT 180
      T V P S S D L D N F N T V F Y V Q P Q Y 53

ACATTAATCAGGCTCTTCATTTAGCAAATGCTTTTCAAGGGGCTATAGACCCACTTAATT 240
      I N Q A L H L A N A F Q G A I D P L N L 73

TAAATTTCAATTTTGTAAAAGGCACCTCAAATTGCAAATGGTATTCCTAATTCTGCAATTG 300
      N F N F E K A L Q I A N G I P N S A I V 93

TAAAACTCTTAATCAAAGTGTTATACAGCAAACAGTTGAAATTTTCAGTTATGGTTGAGC 360
      K T L N Q S V I Q Q T V E I S V M V E Q 113

AACTTAAAAAGATTATTCAAGAGGTTTTAGGACTTGTTATTAACAGTACTAGTTTTTGGGA 420
      L K K I I Q E V L G L V I N S T S F W N 133

ATTCGGTAGAAGCTACAATTAAAGGCACATTTACAAATTTAGACACTCAAATAGATGAAG 480
      S V E A T I K G T F T N L D T Q I D E A 153

CATGGATTTTTTGGCATAGTTTATCCGCCCACAATACAAGTTATTATTATAATATTTTAT 540
      W I F W H S L S A H N T S Y Y Y N I L F 173

TTTCTATTCAAAATGAAGATACAGGTGCAGTTATGGCAGTATTACCTTTAGCATTTGAGG 600
      S I Q N E D T G A V M A V L P L A F E V 193

TTTCTGTGGATGTTGAAAAACAAAAGTATTATTCTTTACAATAAAAGATAGTGCACGAT 660
      S V D V E K Q K V L F F T I K D S A R Y 213

ATGAAGTTAAAATGAAAGCTTTGACTTTAGTTCAAGCTCTACATTCCTCTAATGCCCCAA 720
      E V K M K A L T L V Q A L H S S N A P I 233

TTGTAGATATATTTAATGTTAATAACTATAATTTATACCATTCTAATCATAAGATTATTC 780
      V D I F N V N N Y N L Y H S N H K I I Q 253

AAAATTTAAATTTATCGAATTGATGTTTGATTCTTAAATATCTATTTTTCAAATAAAAAT 840
      N L N L S N * 259

CCTTAATTTTATTC 854

```

Figure 1.7: Nucleotide and deduced amino acid sequences of Cyt2Aa2 toxin (GenBank accession no. AF472606) [40]

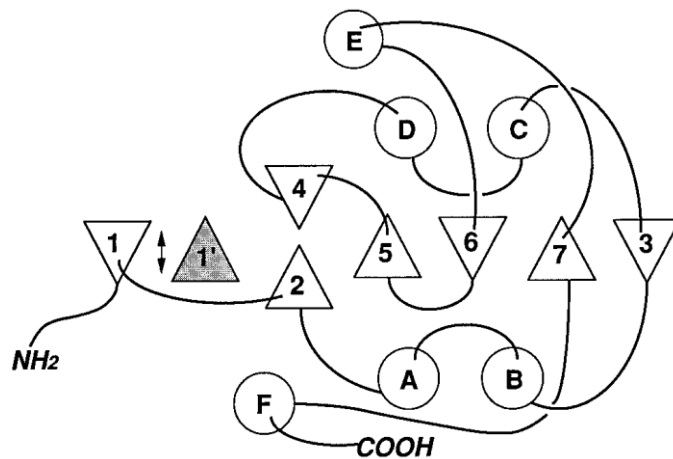


Figure 1.8: Topology diagram of Cyt2A protein [25]

The figure shows conformation of the Cyt2A toxin. Helix hairpins A-B and C-D are in the outer layer and a mixed β -sheet is in the middle of protein structure. α -helices are represented by circle and β -sheets are represented by the triangles.

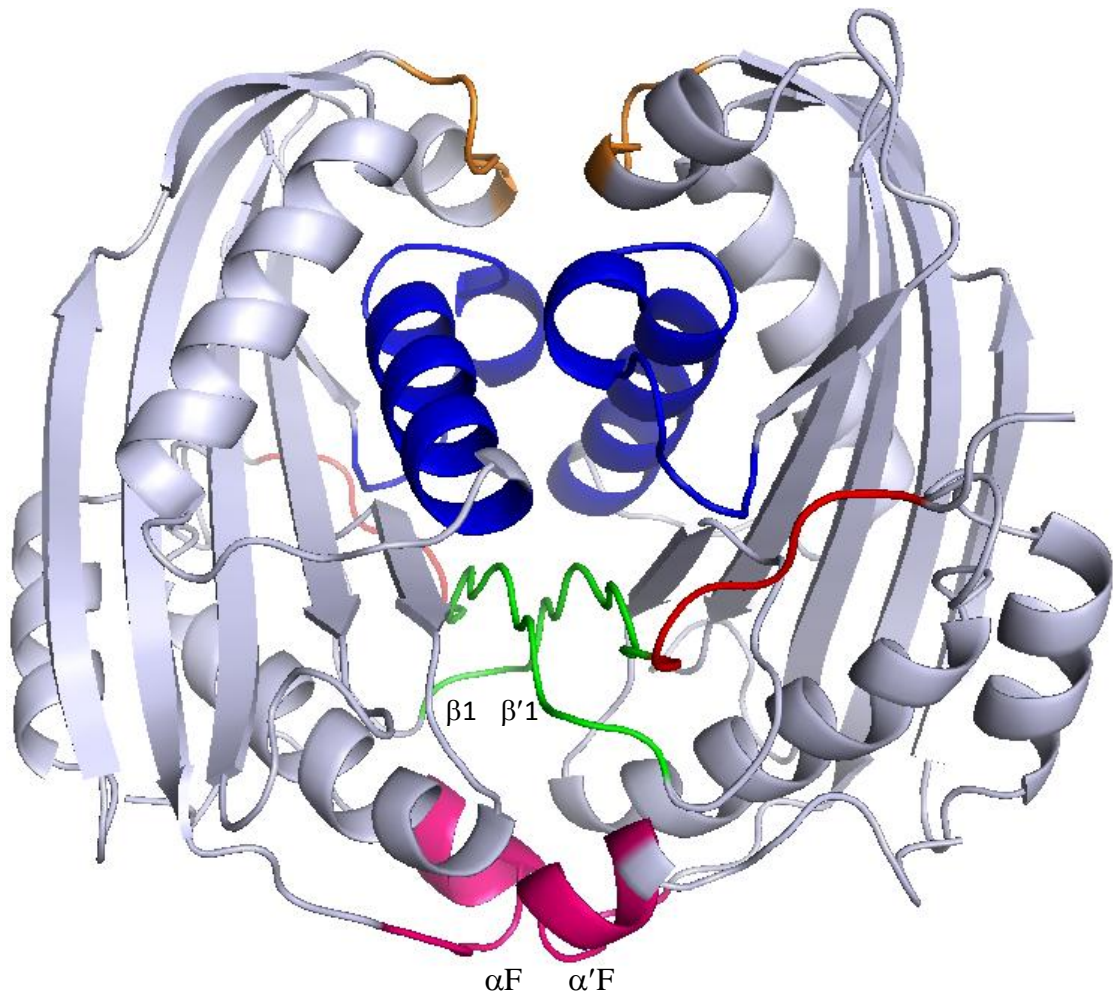


Figure 1.9: The structure of Cyt2A protoxin (dimer) created by PyMOL

The figure shows dimeric structure of Cyt2A protoxins. Two monomers interact to each other between five areas as previously described [25]. The five areas are colored in red, green, pink, blue, and orange.

α F form hydrogen bonds with each other similar to Ala231 in loop $_{\beta 7, \alpha F}$ and Ile233 in α F. The next is between α D and loop $_{\alpha D, \beta 4}$ which are salt bridged between Lys140 and Asp147. The last area is between loop $_{\alpha E, \beta 7}$ that form the salt bridge of each molecule [25]. In addition, Cyt2A toxin has an extra 15 residue at C-terminal sequence that make a difference from Cyt1A [24]. The additional amino acids of Cyt2A have been suggested to be proteolysis preventing residues.

Toxin mechanism

Cry and Cyt toxins are in a class of bacterial toxins known as pore-forming toxins (PFT). There are two main groups of PFT: (i) the α -helical toxins, in which α -helix regions form the trans-membrane pore, such as the colicins, exotoxin A, diphtheria toxin and also the Cry three-domain toxins [53]. (ii) the β -barrel toxins, that insert into the membrane by forming a β -barrel composed of β -sheet hairpins from each monomer [53]. For instance; aerolysin, α -hemolysin, anthrax protective antigen, cholesterol-dependent toxins as the perfringolysin O and the Cyt toxins [53].

The proposed mechanism of action of crystalline Cry and Cyt toxins are composed of 1) the solubilization of crystalline protoxin in the larval mid-gut, 2) the processing of toxin by mid-gut proteases, and 3) binding to the mid-gut epithelium cell membrane and forming of the lytic pore. Firstly, *Bacillus thuringiensis* crystalline inclusions are ingested by the susceptible insect larvae. Insecticidal δ -endotoxins produced as protoxins could be solubilized in the insect mid-gut lumen due to its characteristic high pH and reducing conditions [54]. The soluble protoxins are then processed by many mid-gut protease enzymes to be converted into active form [55-57]. Next, the active toxin recognizes specific receptor or epithelial cell surface. After that the activated toxins insert into the membrane and form the lytic pore causing imbalance osmotic pressure, cell swelling and leading to cell lysis [4, 54, 58].

The previous studies with multilamellar liposomes [51] and planar lipid bilayers [21] have demonstrated that CytA interacts with phospholipids as previous suggested by Thomas and Ellar [59]. The cytolytic action of the protein is thus largely caused by a nonspecific protein-lipid interaction, with a very limited role of specific surface receptors. This is in clear contrast to the postulated receptor-mediated

insecticidal action of species-specific Cry δ -endotoxins [60]. Until now, the molecular mechanism is still unclear.

Generally, Cyt toxins are synthesized as protoxins and small parts of the N-terminus and C-terminus are removed to activate the toxin [25, 56, 61]. In the case of Cyt2Aa, 33 to 37 amino acid residues and 22 to 30 amino acid residues from the N-terminal and the C-terminal ends are removed by protease enzymes in the mid-gut tract of mosquito larvae producing a monomeric protein as 25 and 23 kDa active toxins [11, 33, 40]. The active toxin will bind to mid-gut receptor on brush border of susceptible membrane and form the oligomeric complexes. The ion channels or pores are then generated by insertion of the toxin into apical membrane resulting to osmotic balance disruption, swelling and lysis of the cells - so called colloidal osmotic lysis. Eventually, the vulnerable larvae die because of stopping ingestion [1, 11, 12].

At the toxin binding step, two possible hypotheses that are relevant to mode of action of toxin (**figure 1.10**) were hypothesized which are detergent-like model [37] and pore forming model [62]. The detergent-like model proposed that Cyt toxins aggregate on the membrane surface and cause large non-specific defects in lipid packing. Intracellular molecules can release to the outside-a mechanism similar to the so-called carpet model formulated for antimicrobial peptides by Shai [63]. The aggregates may even completely destroy the membrane in a detergent-like manner, resulting in the complete absence of a vesicle. Importantly, the detergent-like action requires neither stoichiometric toxin assemblies nor stable penetration of the toxin across the lipid bilayer [48].

Another model is pore-forming model. Cyt activated toxins insert into cell membrane and form oligomer to generate a pore in lipid bilayers. Diameter of the pore was expected to be 1-2 nm. The pore-forming mechanism for Cyt δ -endotoxins is thought to involve a hinge movement of helices, followed by insertion of the underlying long amphiphilic β -strands ($\beta 5$, $\beta 6$ and $\beta 7$) into the lipid bilayers, leaving the helices exposed and span on the membrane surface (**figure 1.11**) [25, 64, 65].

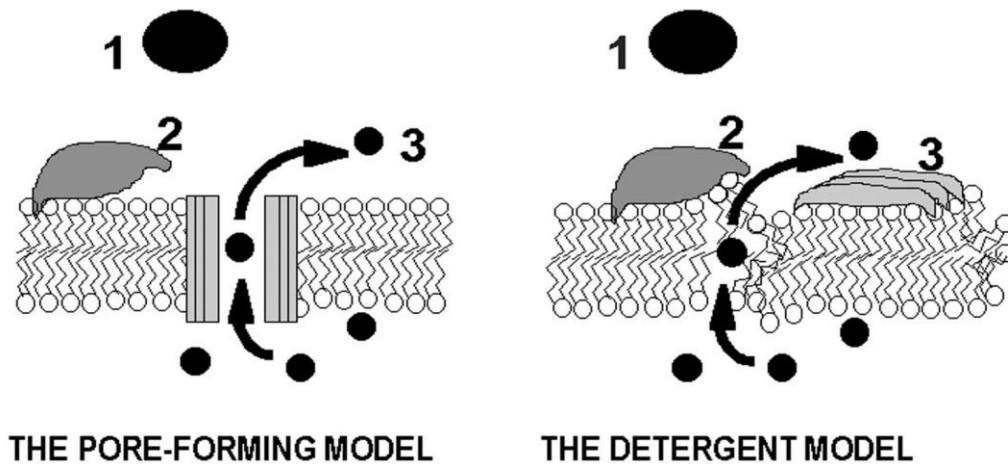


Figure 1.10: The two proposed mechanisms of Cyt toxin [48]

1) An active toxin diffuses in the extracellular phase, 2) The active toxin changes conformation and binds to phospholipid bilayers, 3) Toxin molecules insert into the membrane and form the transmembrane pore or aggregate on the lipid membrane leading to the membrane fragmentation and releasing of toxin-lipid complexes.

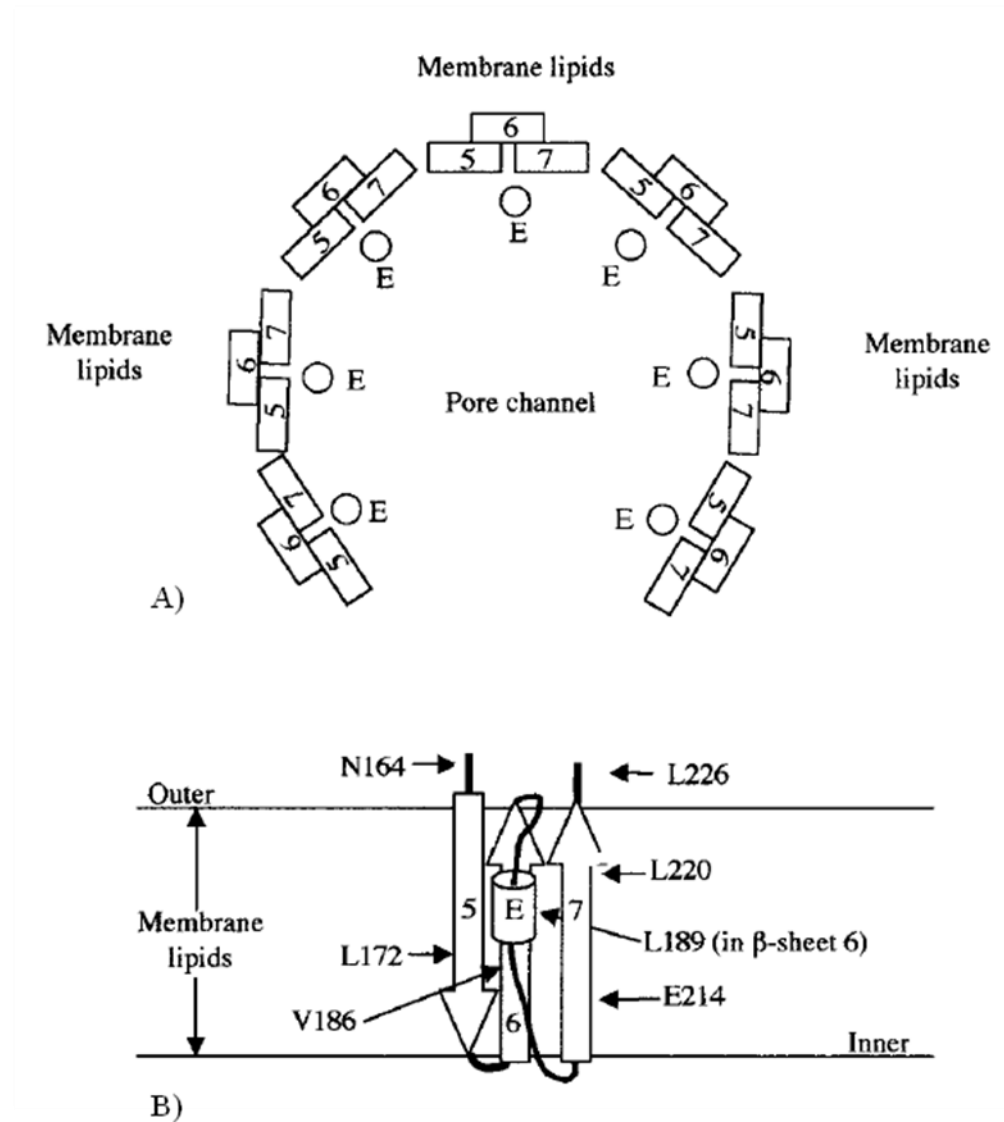


Figure 1.11: Proposed oligomeric pore structure of Cyt2Aa1 protein [65]

A) The top view of oligomeric pore structure that formed by β 5, β 6 and β 7, B) The side view of the pore and locations amino acid residues that expected to involve in pore formation.

In aqueous buffer Cyt toxins are resistant to proteolytic processing [24]. By contrast, after incubation with liposomes they developed new cleavage sites for 11 different proteases, and these sites are confined to the helices and the proposed hinge regions [25, 66]. This study supports pore-forming model that showed a major conformational change in the presence of a lipid bilayer and indicated protection of $\beta 5$ - $\beta 7$ fragments from proteolytic processing [64].

Synergism

Cyt δ -endotoxins produced by some strains of *Bacillus thuringiensis* exhibit a broad spectrum activity against a variety of eukaryotic cells *in vitro* but highly specific towards dipteran insects *in vivo*. The resistance in lepidopteran insect could be found, when using *Bt* toxin [67]. Cyt1Aa suppresses the resistance of *Culex quinquefasciatus* Cry-resistant population [68] and Cyt1Aa protein synergizes Cry11Aa toxicity by functioning as a receptor molecule [69]. Moreover, co-expression of Cyt2Aa2 and Cry4Ba toxins increased toxicities against *Culex quinquefasciatus* and *Aedes aegypti* larvae. This result suggested that these two toxins have synergistic activity toward two species of mosquito larvae [70].

CHAPTER II

OBJECTIVE

Cyt toxins are cytolytic proteins produced by some species of *B. thurigiensis*. The toxin is active against mosquito larvae such as *Aedes aegypti*; a vector for a dengue virus caused a dengue fever. Many people died from this disease so, it is a serious problem in tropical countries, such as Thailand. According to the benefit of Cyt toxins, they have been widely studied in all aspects including a toxin mechanism. Cyt protein is produced as “protoxin” and formed crystalline inclusion inside the cell. Upon ingestion by susceptible larvae, the inclusion is solubilized in the alkaline condition of the insect gut. To activate the protein function, amino acids at N- and C-termini of the protoxin will be removed by the gut proteases. This thesis aims to investigate the functional significances of amino acids located around $\beta 1$ at N-terminus and around αF at C-terminus of Cyt2Aa2. Amino acids in these regions are removed during proteolytic processing to yield the active toxin. Therefore, they should not involve with toxin activity. However, they might play important role to stabilize the protoxin conformation. Without these regions, the toxin structure may collapse and unable to exhibit any activity.

CHAPTER III

MATERIALS

3.1 Chemicals

Ampicillin	Sigma
Cetyl Trimethyl Ammonium Bromide (CTAB)	Sigma
Colloidal Coomassie Brilliant Blue R-250	Sigma
1,4-Dithiothreitol (DTT)	Sigma
Isopropyl- β -D-Thiogalactopyranoside (IPTG)	Sigma

Other chemicals and reagents were purchased from a variety of companies (BIO-RAD, Merck and Sigma).

3.2 Enzymes and Accessory Buffers

Restriction endonucleases and other enzymes were purchased from the following companies:

<i>Pfu</i> DNA polymerase	Promega
<i>DpnI</i>	Promega
Proteinase K	Sigma
RNase A	Sigma
PMSF	Sigma

Restriction enzymes used in this experiment are listed in **table 3.1**.

Table 3.1: List of restriction enzymes and their recognition sites

Restriction Enzymes	Recognition site (5'-3')	Incubation temperature	Reaction buffer*	Suppliers
<i>Xho</i> I	C↓TCGAG	37°C	Buffer D	Promega
<i>Dde</i> I	C↓TNAG	37°C	Buffer D	Promega
<i>Sca</i> I	AGT↓ACT	37°C	Buffer K	Promega
<i>Pvu</i> II	CAG↓CTG	37°C	Buffer B	Promega
<i>Sau</i> 96I	G↓GNCC	37°C	Buffer C	Promega
<i>Hind</i> III	A↓AGCTT	37°C	Buffer E	Promega
<i>Nla</i> IV	GGN↓NCC	37°C	Buffer 4	NEB

The enzyme-buffers were supplied by the enzyme manufacturers.

3.3 Bacterial Strain

Escherichia coli strain JM109 [recA1 supE44 endA1 hsdR17 gyrA96 rclA1 thiΔ (lac-proAB) F' (traD36 proAB⁺ lacI^q lacZΔM15] containing pGEM-Cyt2Aa2 plasmid [40] was obtained from Dr. Boonhiang Promdonkoy (National Center for Genetic Engineering and Biotechnology). The plasmid was used as a template for site-directed mutagenesis and protein expression.

3.4 Culture Media

Luria-Bertani medium (LB)

LB broth for the culture of *Escherichia coli* contains 1% (w/v) tryptone, 0.5% (w/v) yeast extract and 1% (w/v) NaCl. LB agar was prepared by adding 1.5% (w/v) of Bacto-agar (GIBCO BRL) into LB broth. The media were sterilized by autoclaving at 121 °C, 15 psi. for 30 min. Ampicillin was added into the selected media to a final concentration of 100 µg/ml when media were cool down to approximately 50 °C.

3.5 Oligonucleotide primers

In this study, the synthetic oligonucleotides were designed from the recombinant plasmid pGEM-Cyt2Aa2 containing *cyt2Aa2* gene (850 bp) by Vector NTI8 program and purchased from Prologo Singapore Pty Ltd. The sequences of all oligonucleotide primers were shown in **table 3.2** with the restriction enzymes.

Table 3.2: Primer sequences for site-directed mutagenesis

Mutants	Primer Sequences (5'-3')	Restriction enzymes
D39L	5'-CATCCAGTCTCTTAGATAATTTTAATACAG-3' 5'-CTGTATTAAAATTATCTAAGAGACTGGATG-3'	<i>DdeI</i> Appear
S229stop	5'-AAGCTCTACATTCCCTGAGATGCCCC-3' 5'-GGGGCATCTCAGGAATGTAGAGCTT-3'	<i>DdeI</i> Appear
R25A	5'-GGGTGCTCAGCACCTATTATTGCAAAACC-3' 5'-GGTTTGTCAATAATAGGTGCTGAGCACCC-3'	<i>DdeI</i> Appear
P27A	5'-CTATTATTAGAAAAGCTTTTAAACATATTG-3' 5'-CAATATGTTTAAAGCTTTTCTAATAATAG-3'	<i>HindIII</i> Appear
I31A	5'-CATTTAAACATGCAGTACTAACGGTTCCAT-3' 5'-GAACCGTTAGTACTGCATGTTTAAATGGTT-3'	<i>ScaI</i> Appear
L33A	5'-TAAACATATTGTAGCAACCGTTCCATCCAG-3' 5'-CTGGATGGAACGGTTGCTACAATATGTTTA-3'	<i>NlaIV</i> Disappear

“▼” = Specific cleavage site

XXXX = Recognition sequence

Table 3.2: (Cont.) Primer sequences for site-directed mutagenesis

Mutants	Primer Sequences (5'-3')	Restriction enzymes
N230A	5'-AAGCTCTACATTCCTCTGCG <u>GGCCCA</u> ATTG-3' 5'-CAATTG <u>GGGCC</u> GCAGAGGAATGTAGAGCTT-3'	<i>Sau96I</i> Appear
I233A	5'-TCCTCTAATGCCCC <u>CAGCTG</u> TAGATATATTT-3' 5'-AAATATATCTAC <u>CAGCT</u> GGGGCATTAGAGGA-3'	<i>PvuII</i> Appear
I233stop	5'-CCTCTAATGCCCC <u>CTTAGG</u> TAGATATATTTA-3' 5'-TAAATATATCTAC <u>CCTAAG</u> GGGCATTAGAGG-3'	<i>DdeI</i> Appear
N238stop	TAATTAAAAGGAGGATCATAATATG <u>CTCGAGT</u> CAAAATATATCTACAATTGGGG	<i>XhoI</i> Appear

“▼” = Specific cleavage site

XXXX = Recognition sequence

3.6 Miscellaneous

Alkaline phosphatase-conjugated anti-rabbit IgG	Sigma
Bio-Rad Protein assay (Bradford's reagent)	Bio-Rad
Deoxyribonucleotide triphosphate (dNTPs)	Amersham Pharmacia Biotech
Standard DNA markers	Biolabs
SDS-PAGE molecular weight standards, Broad range	Bio-Rad
Membrane filter tube	Eppendorf
Superdex 200 (HR 10/30) column	Amercham Pharmacia Biotech
QIAgen Spin Miniprep Kit	QIAGEN
Skimmed milk	Carnation
Sheep blood	National Laboratory Animal Center, Mahidol University
<i>Aedes aegypti</i>	Institute of Molecular Biosciences, Mahidol University

CHAPTER IV

METHODS

4.1 Plasmid extraction

QIAgen kit

E. coli strain JM109 cells harboring pGEM-Cyt2Aa2 plasmids were collected by centrifugation at 10,600 g for 1 minute and resuspended in 250 µl Buffer P1 before transferred to a microcentrifuge tube. The 250 µl Buffer P2 was added and mixed thoroughly by inverting the tube 4-6 times. The 350 µl Buffer N3 was mixed immediately and thoroughly and then it was centrifuged at 17,900 g for 10 minutes. The supernatant was applied to the QIAprep spin column and centrifuged for 1 minute. The QIAprep spin column was washed by adding 0.5 ml Buffer PB and centrifuged for 1 minute. The 0.75 ml Buffer PE was added to the column and centrifuged and discarded the flow-through. To remove residual wash buffer, it was centrifuged again and discarded the flow-through. The 50 µl of sterile distilled water was added into the QIAprep spin column and left for 1 minute at room temperature. Centrifugation for 1 minute to elute DNA is the last step.

CTAB method

A single colony of *E. coli* strain JM109 containing pGEM-Cyt2Aa2 plasmid was inoculated in 3 ml of LB broth and shaken at 37 °C with 250 rpm for 16-18 hrs. The cell pellet was collected at 10,600 g for 1 min in microcentrifuge tube before resuspended in 200 µl of STET buffer (8% sucrose, 5% Triton-X 100, 50 mM EDTA, 50 mM Tris-HCl, pH 8.0). Lysozyme was added at 0.1 mg/ml final concentration and then the mixture was incubated at room temperature for 10 min. It

was boiled for 30-45 sec. and centrifuged at 15,300 g for 15 min. The white pellet was removed by sterile toothpick and then added 5 µl of ribonuclease A (10 mg/ml) to the supernatant. After incubated at 37 °C for 15-30 min, plasmid DNA was recovered by adding a 20 µl of 5% CTAB solution (Cetyl Trimethyl Ammonium Bromide) and left at room temperature for 15-30 min. The mixture was centrifuged at 15,300 g to collect the pellet and then it was resuspended with 300 µl of 1.2 M NaCl by vigorously vortex. A 300 µl of chloroform was added with vigorously inverted for 30 sec and centrifuged at 15,300 g for 5 min to remove protein. Clear aqueous phase was transferred into a new microcentrifuge tube. DNA was precipitated after adding 2 volume of absolute ethanol and incubated at room temperature for 5 min and centrifuged at 15,300 g for 15 min. The DNA pellet was washed twice with 500 µl of 70% ethanol. A dried DNA pellet was dissolved in 20 µl of sterile distilled water.

4.2 Agarose gel electrophoresis

The percentage of an agarose gel was prepared depending on size of DNA. Agarose powder was added in 1xTBE and boiled to obtain the clear solution. When the temperature of this solution cooled down to 60 °C, it was poured into an electrophoretic tray to solidify at room temperature. The DNA sample was mixed with 6xDNA loading dye before loaded into the well of the agarose gel that containing 1xTBE buffer in the tank. The constant volt was applied at 80-90 Volts to perform the agarose gel electrophoresis. After the electrophoresis was completed, the gel was stained with ethidium bromide for 3 min and destained in distilled water for 5-10 min. The DNA band on this agarose gel was visualized under UV light and then taken a photograph.

4.3 Site-directed mutagenesis

Cyt2Aa2 toxin gene from *Bacillus thuringiensis* subsp. *darmstadiensis* cloned and expressed in *Escherichia coli* was obtained from Dr. B. Promdonkoy [40]. In

vitro site-directed mutagenesis using PCR based method (QuikChange™) as shown in **figure 4.1** were carried out to generate Cyt2Aa2 mutants. Mutagenic primers were designed using Vector NTI8 program. The pGEM®-T EASY containing the wild type gene was used as a template for mutagenesis. The high fidelity polymerase, *Pfu* DNA polymerase was employed in PCR reaction. The template was eliminated by adding 1 µl of *DpnI* enzyme directly to PCR products and then incubated at 37 °C for 3 hours. The 5 µl of digested PCR product was analyzed in 1 % agarose gel electrophoresis. The mutagenic plasmids were transformed into *E. coli* JM109 competent cells to produce mutant colonies. The restriction enzyme analysis was performed for screening mutants based on their recognition site incorporated in the mutagenic primers and automated DNA sequencing was used to confirm the mutagenic DNA sequence.

PCR reactions were prepared in 200 µl PCR tubes and performed as shown in **table 4.1**. PCR reaction mixture (50 µl) was consisted of :

DNA template	20-50 ng
10 mM dNTP mix (2.5 mM each)	1 µl
Forward and reverse primers	10 pmole each
10x <i>Pfu</i> buffer	5 µl
<i>Pfu</i> DNA polymerase	0.5 µl
Sterile distilled water added to final volume	50 µl

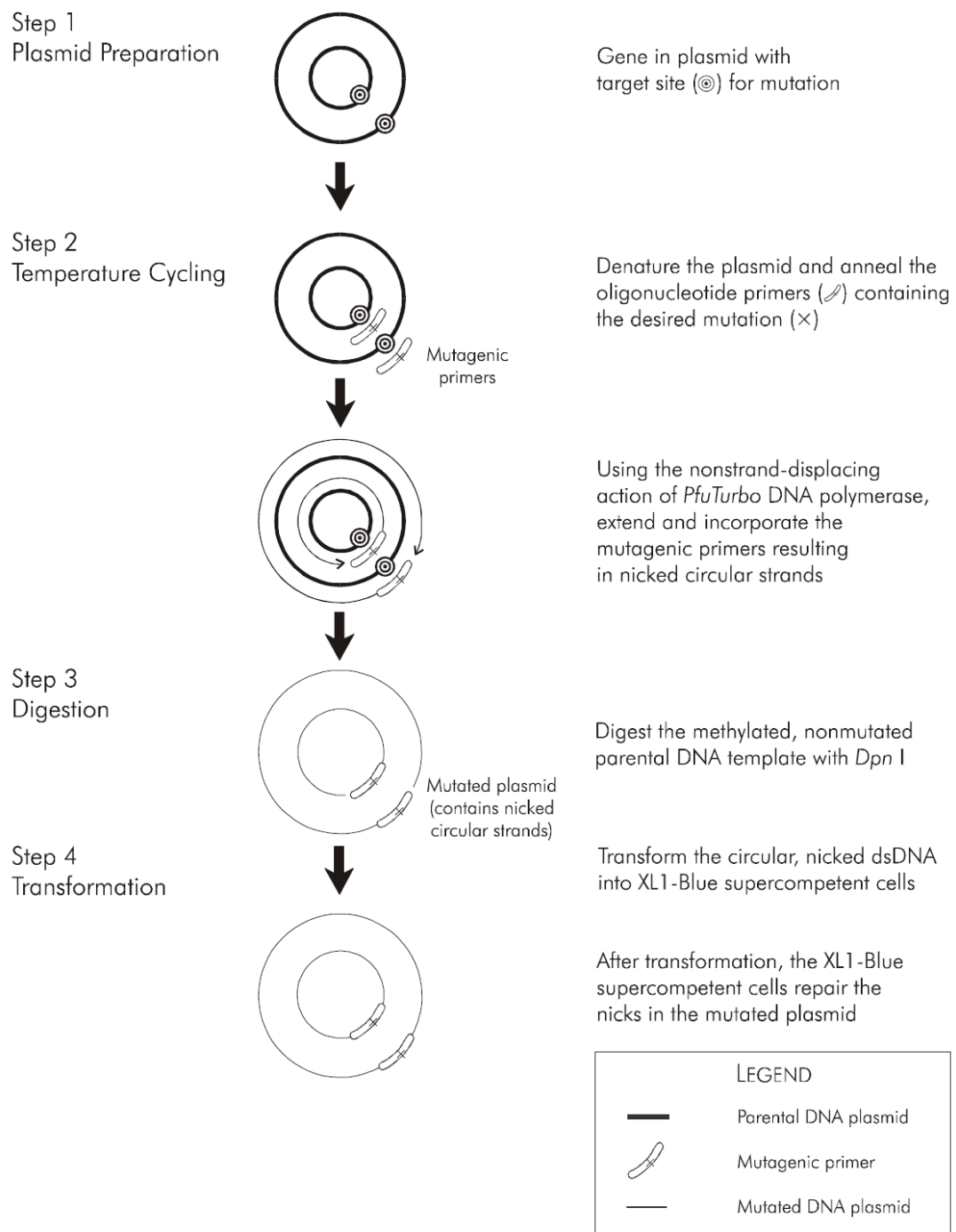


Figure 4.1: Overview of the QuikChange® site-directed mutagenesis method (Stratagene)

Table 4.1: Temperature cycling parameters for site-directed mutagenesis.

Primer set	Template	Segment	Cycle	Temperature	Time
Mutagenic forward And Mutagenic reverse	pGEM-Cyt2Aa	1	1	95°C	1 minute
		2	25	95°C	30 seconds
				Ta °C	30 seconds
				68°C	8 minutes
		3	1	68°C	8 minutes

Ta is annealing temperature depending on each mutagenic primer sets.

4.4 Competent cells preparation by CaCl₂

A single colony of *E. coli* strain JM109 was picked into LB broth and cultured at 37 °C with 250 rpm shaking overnight. The 1 % inoculation was performed in LB broth and then incubated at 37 °C for 2.5 hours until OD₆₀₀ reached 0.3-0.4. The supernatant was removed after centrifugation at 1,700 g, 4 °C for 10 min. A 10 ml of 0.1 M CaCl₂ was slightly added into the cell pellet and kept on ice for 10 min before spinning at 1,700 g, 4 °C for 10 min. The cell pellet was resuspended with 2 ml of CaCl₂ and then added glycerol 30% (v/v) before aliquot 200 µl into the new tube and stored at -80 °C.

4.5 Transformation of plasmid DNA into competent cells

The 10-30 ng of *DpnI*-digested PCR product was added in 200 µl of competent cells. The mixture was chilled on ice for 30 min before placed in 42 °C for 90 sec and immediately chilled on ice 2-5 min. A 800 µl of LB broth was added and incubated at 37 °C with 250 rpm shaking for 1 hour. The transformed cell was collected at 2,700 g, 4 °C for 2 min. The 800 µl of supernatant was removed before 200 µl of resuspended cell was spreaded on LB agar plate containing 100 µg/ml of ampicillin. The transformed cell plate was incubated at 37 °C for 16-20 hours.

4.6 Restriction enzyme analysis

Restriction enzyme analysis was used to screen the correct clones. After obtaining DNA plasmids from CTAB method, the specific enzyme that designed in the mutagenic primer was added into the microcentrifuge tube containing the appropriate buffer and DNA plasmids. The final reaction volume was adjusted by adding sterile distilled water and then incubated at 37 °C for 3 hours or depending on the best condition of each enzyme.

4.7 Automated DNA sequencing

The extracted DNA from QIAGEN kit was submitted to perform DNA sequencing by MegaBACETM1030 Automated DNA sequencer (Amersham Pharmacia Biotech, USA). The results were aligned in Vector NTI8 program to compare with their wild type and confirm a right mutation position (nucleotides).

4.8 Expression level of proteins

Both wild type and mutagenic colonies were incubated in LB broth containing 0.1 mg/ml ampicillin and grown at 37°C with 250 rpm shaking for 16-20 hrs. The overnight culture was transferred into fresh LB broth containing 0.1mg/ml ampicillin to make up 1% innoculum and further incubated at 37°C with 250 rpm shaking. When OD₆₀₀ of the cell culture was 0.3-0.5, the expression would be induced by IPTG at final concentration of 0.1 mM. The 1 OD of *E.coli* cells were collected by centrifugation at 10,600 g, 4 °C for 1 min. The cell pellet was resuspended with 50 µl of distilled water and 20 µl of 4X sample buffer. The sample was sonicated for 10 min and heated at 95 °C for 5 min. The 0.1 OD was subjected to analyze on polyacrylamide gel.

4.9 Expression and partial purification of protein

The *E. coli* harboring wild type and mutant plasmids was grown at 37 °C until OD₆₀₀ of culture reached 0.3–0.4. Protein was expressed by adding 0.1 mM IPTG and incubated at 37 °C for 5 hours. The *E. coli* cell expressing mutant protein was collected by centrifugation with Sorvall F-16/250 rotor at 6,000 rpm, 4 °C for 20 minutes and then resuspended in distilled water. Lysozyme (100 mg/ml) 20 µl was added into the resuspended cells and left for 5-10 min at room temperature. To obtain inclusions, the *E. coli* cells were lysed by French Pressure Cell at 18,000 psi. Inclusions were collected by centrifugation at 6,654 g, 4 °C for 15 min and washed

with sterile distilled water 2 times. The inclusion was dissolved in 3 ml of sterile distilled water and aliquot into 1.5 ml microcentrifuge tube.

4.10 Protein quantification by Bradford's assay

Concentrations of proteins were determined by the method of Bradford (Bradford, 1976) using the Bio-Rad protein assay kit and BSA as a standard. The 300 μ l of Bradford reagent was mixed with 10 μ l of protein sample in the well of 96-well titer plate. The concentration of protein was measured by Bradford assay in SoftMax program.

4.11 SDS-PAGE analysis

SDS-PAGE analysis is the method to investigate a protein profile depending on molecular weight.

Sample preparation

The protein was mixed with 4x sample buffer (0.5 M Tris-HCl pH 7.5, 10% SDS, glycerol, 0.5% w/v bromophenol blue, and distilled water) and heated at 95 °C for 5 min before loaded into the well of SDS-PAGE gel.

SDS-PAGE preparation

SDS-PAGE is composed of two layers which are a stacking gel and a separating gel. The list of SDS-PAGE composition was shown in **table 4.2**. The separating gel was firstly prepared. All compositions of separating gel were added into a beaker and then were rinsed into the space between the two mirrors. After complete polymerization, the stacking solution was then prepared in the same mixture of separating solution, excepting 1.5 M Tris-HCl pH 6.8 solution. A comb was put in the stacking gel to create the well.

Table 4.2: Composition of SDS-polyacrylamide gel

Contents	Separating gel		Stacking gel	
	12.5%	15%	4%	6%
Distilled water (ml)	3.2	2.3	1.8	1.6
1.5 M Tris-HCl pH 8.8 (ml)	2.5	2.5	-	-
0.5 M Tris-HCl pH 6.8 (ml)	-	-	0.75	0.75
30% Acrylamide (ml)	4.17	5	0.4	0.6
10% SDS (μl)	100	100	30	30
10% APS (μl)	100	100	30	30
TEMED (μl)	5	5	2	2
Total Volume (ml)	10	10	3	3

4.12 Western blot analysis

Semi-dry blot analysis

Protein samples were separated on 15% SDS-PAGE. A polyvinylidene difluoride (PVDF) transfer membrane (Amersham Biosciences) and 6 whatman paper were cut in the same size of SDS-PAGE gel. The PVDF membrane was rinsed with methanol and washed with sterile distilled water for 3 times. The PVDF membrane and whatman paper were soaked in transfer buffer for 10 min. The 3 whatman paper, PVDF membrane, SDS-PAGE gel and the rest of 3 whatman paper were placed at Mini Trans-Blot[®] electrophoresis transfer cell (BIO-RAD). To transfer the protein to the membrane, the constant current at 300 amp was applied for 1 hour after that the membrane was soaked in Paunceau S and then washed with milliQ for 2-3 times. A 10 ml of 5% (w/v) skim milk in 1x PBS buffer, pH 7.4 was added to the membrane and shaken for 2 times before the membrane was blocked overnight with 10 ml of 5% skim milk at 4 °C. In the next step, A 1 µl of Cyt primary antibody mixed in 10 ml of 5% skim milk was added to the membrane incubated at 4 °C for 1 hour. The membrane was washed three times with 10 ml of 1x PBS containing 0.1% tween-20 for 5 minutes each time. The membrane was shaken in 10 ml of 5% skim milk for 30 minutes with 1 µl of α -rabbit secondary antibody linked with horseradish peroxidase or alkaline phosphatase and then washed with 10 ml of 5% TBST for 5 minutes 5 times. Protein-antibody complexes were visualized by ECL Plus Detection Reagent (Amersham Bioscience) or the combination of BCIP (5-Bromo-4-Chloro-3'-Indolyphosphate p-Toluidine Salt) and NBT (Nitro-Blue Tetrazolium Chloride).

4.13 Protein solubilization

The inclusion was solubilized in 1 ml of 50 mM Na₂CO₃/NaHCO₃ pH 9.8 and incubated at 37 °C for 1 hour. To obtain the solubilized protein, the sample was centrifuged at 15,300 g for 10 min and the supernatant was taken to the new microcentrifuge tube.

4.14 Proteolytic processing by proteinase K

The proteolytic processing is required to activate Cyt2Aa2, 1% (w/w) proteinase K was added into solubilized protoxin and incubated at 37 °C for 1 hour. To stop the activity of proteinase K enzyme, phenylmethanesulphonylfluoride (PMSF) was added into the mixture to final concentration 4 mM.

4.15 Mosquito larvicidal activity assay

The inclusion was diluted with distilled water as two-fold serial dilutions from 500 to 0.25 µg/ml and each concentration was prepared in duplication. To test the activity, the 2nd instar *Aedes aegypti* larvae (10 larvae/well) were fed with diluted inclusion. A mortality of larvae was recorded after 24 hours and then LC₅₀ was calculated (50% lethal concentration) by using Probit program. Each experiment was repeated at least 3 times.

4.16 Haemolytic activity assay

Preparation of sheep red blood cells

Normal sheep blood in Alsevers solution was purchased from National Laboratory Animal Center, Mahidol University, Salaya Campus. In washing step, 7 ml of PBS buffer (8 mM Na₂HPO₄, 1.5 mM KH₂PO₄, 140 mM NaCl, 2.7 mM KCl, pH 7.4) was slowly added into 3 ml of sheep blood kept on ice and centrifuged at 3,000 rpm, 4 °C for 5 minutes using AR-500 rotor (TOMY MX-301). The supernatant was removed and if the supernatant is pink or red, this step should be performed again until it is clear.

Haemolytic assay

Toxin samples (500µg/ml) 100 µl were diluted in two-fold serial dilutions with PBS buffer 100 µl and were mixed with 2% of sheep red blood cells 100 µl and

left at room temperature. The end-point of haemolysis was monitored after 24 hours. The end-point is the lowest concentration that can lyse the red blood cells.

4.17 Toxin oligomerization assay

Liposome preparation

The 100 mg/ml egg yolk phosphatidyl choline: 50 mg/ml cholesterol: 10 mg/ml stearyl amine = 4:3:1 in molar ratio were mixed in a small glass bottle. The mixture was purged with nitrogen gas until it dried before solubilized with PBS buffer pH 7.4 and aliquoted 100 µl to each microcentrifuge tube. 900 µl of PBS buffer pH 7.4 was added into microcentrifuge tube containing 100 µl of multilamellar liposome vesicles. The mixture was sonicated for 30 minutes at 20-25 °C.

Oligomerization assay

Protoxin or activated toxin (2-10 µg) was incubated with liposome suspension in PBS buffer pH 7.4 at room temperature for 2 hours. After centrifugation at 15,300 g for 20 min, samples were then loaded on 10% SDS-PAGE to examine the pattern of toxin.

4.18 Protein purification

Toxin purification was performed by size exclusion chromatography (superdex200) using AKTA purifier system (Amersham Biosciences). The collected purified protein was separated by their sizes. The column was equilibrated with 50 mM of carbonate buffer pH 9.5 at the flow rate 0.4 ml/min. The protein sample was centrifuged at 10,000 rpm for 1 min before applied to the column.

4.19 Intrinsic fluorescence spectroscopy

Changes in intrinsic fluorescence can be used to monitor structural changes. The 400 μ l of purified toxin was added into a quartz cuvette and then placed the sample in Jasco FP-6300 machine. The protein sample was excited at 280 nm and the emission spectra were scanned from 300-550 nm. The protein emission spectra were corrected with a buffer spectrum. Excitation and emission slit width are 2.5 nm. Each experiment was repeated at least 2 times.

4.20 Dynamic Light Scattering (DLS)

Dynamic Light Scattering technique used to determine the size distribution profile of particles in solution. The particles move randomly in solution and the moving particles of various sizes show the different frequency of the scattered light when the light passes through the solution. The 1 ml of 0.1-0.4 μ g/ml purified protoxin in carbonate buffer pH 9.5 was added into cuvette and then analyzed by Zetasizer machine (National Metal and Materials Technology Center, Thailand).

CHAPTER V

RESULTS

5.1 Site-directed mutagenesis

The PCR products of all mutants could be observed about 3.85 kb after analyzed on agarose gel (**figure 5.1**). Extracted DNA plasmids were digested with restriction enzymes as shown in **table 3.1** and were analyzed on 1.2% agarose gel before being visualized under UV light. The digested DNA fragments of mutants by endonuclease restriction enzyme were similar to the digested DNA pattern that was predicted from Vector NTI program. Then the full-length of *cyt2Aa2* gene of selected recombinant clones were confirmed by automated DNA sequencing and the results showed the mutation as expected.

5.2 Protein expression and identification

Cyt2Aa2 and mutant proteins were expressed upon 5 hours by induction with 0.1 mM IPTG and 0.1 OD of cell lysates were used to determine the protein expression level after analyzing on 12.5% SDS-PAGE gel. Expression levels of R25A, P27A, I31A, D39L, and I233A mutants were similar to those of wild type and protein bands could be observed at 29 kDa, whereas L33A, N230A, truncated S229stop and I233stop gave lower expression level than wild type (**figure 5.2**). Truncated mutants were found to give lower expression level than Cyt2Aa2. After cell collection and centrifugation, inclusion bodies were separated from the whole cells. The result showed that all mutants could produce proteins as inclusions in *E. coli* system (**figure 5.3**). The inclusions were resuspended with distilled water before analyzing on 12.5% polyacrylamide gel. Inclusions of R25A, P27A, I31A, L33A, D39L, N230A, and I233A mutants showed similar molecular weight as Cyt2Aa2 (**figure 5.4 and 5.5**). Truncated S229stop, I233stop and N238stop proteins were

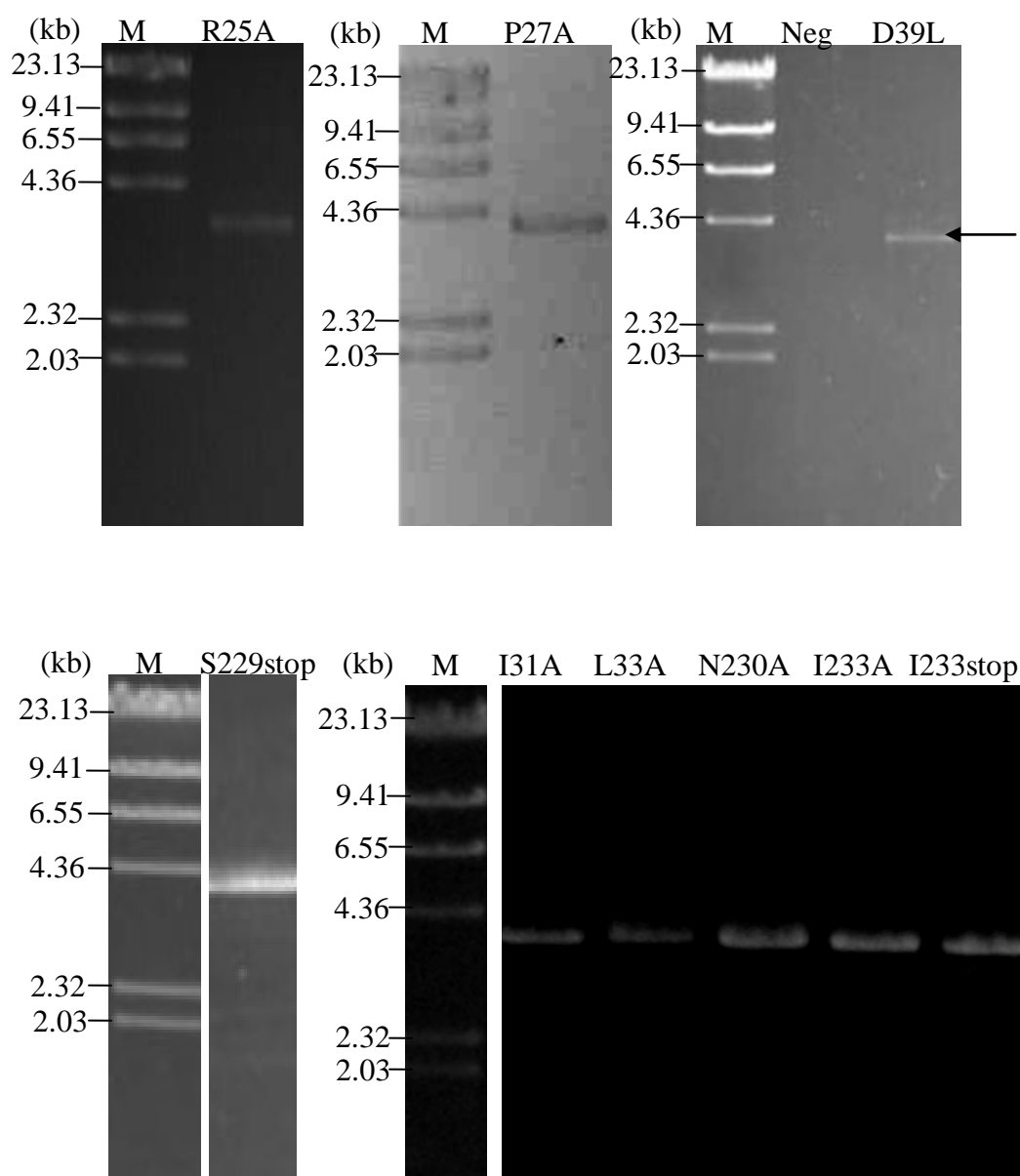


Figure 5.1: PCR products of all mutants

The PCR reaction was performed under optimum temperature using specific primer, dNTPs, and high fidelity enzyme (*pfu* DNA polymerase). An arrow indicates PCR product that was observed at 3.85 kb as expected on 1.2% agarose gel. M is λ /HindIII DNA marker and Neg is negative control that perform without the specific primer.

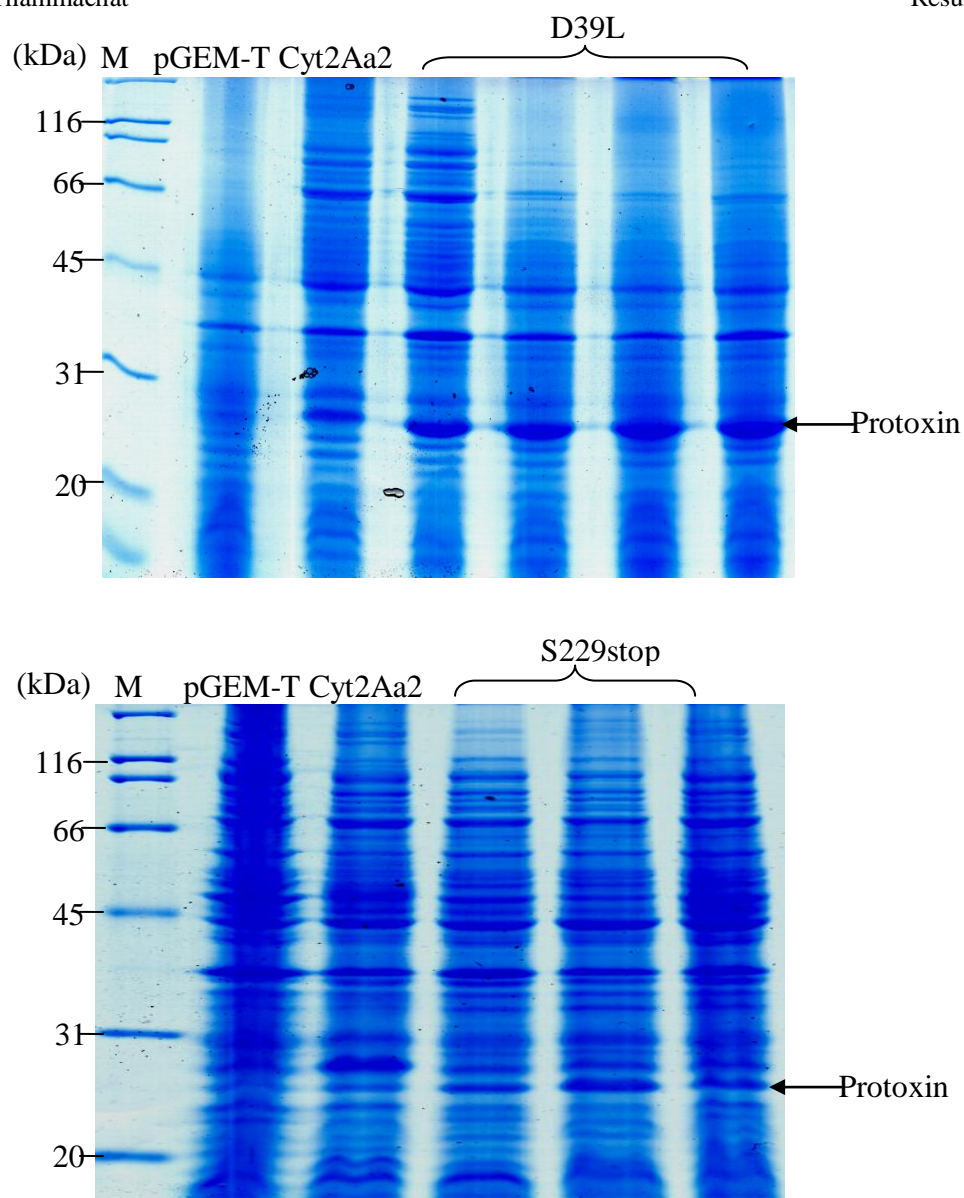


Figure 5.2: Expression level of mutants and Cyt2Aa2

Recombinant *E. coli* cells carrying pGEM[®]-T Easy were analyzed on 15% polyacrylamide gel. The arrows indicate the band of protoxin. M is broad-range protein marker. pGEM-T lane is loaded with total lysate from cell carrying pGEM[®]-T Easy vector.

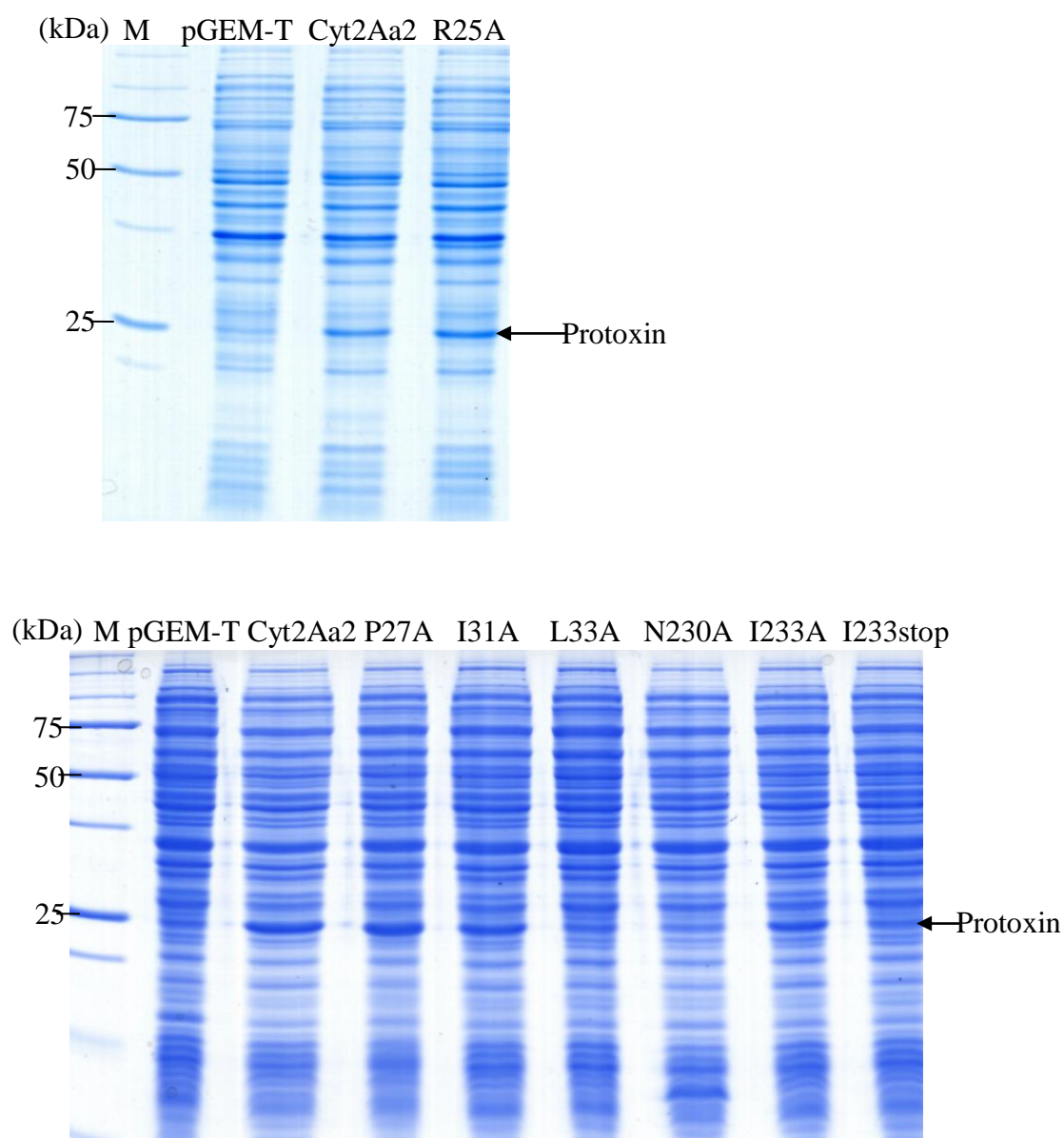


Figure 5.2: (Cont.) Expression level of mutants and Cyt2Aa2

Recombinant *E. coli* cells carrying pGEM[®]-T Easy were analyzed on 15% polyacrylamide gel. The arrows indicate the band of prototoxin. M is precision protein marker. pGEM-T lane is loaded with total lysate from cells carrying pGEM[®]-T Easy vector.

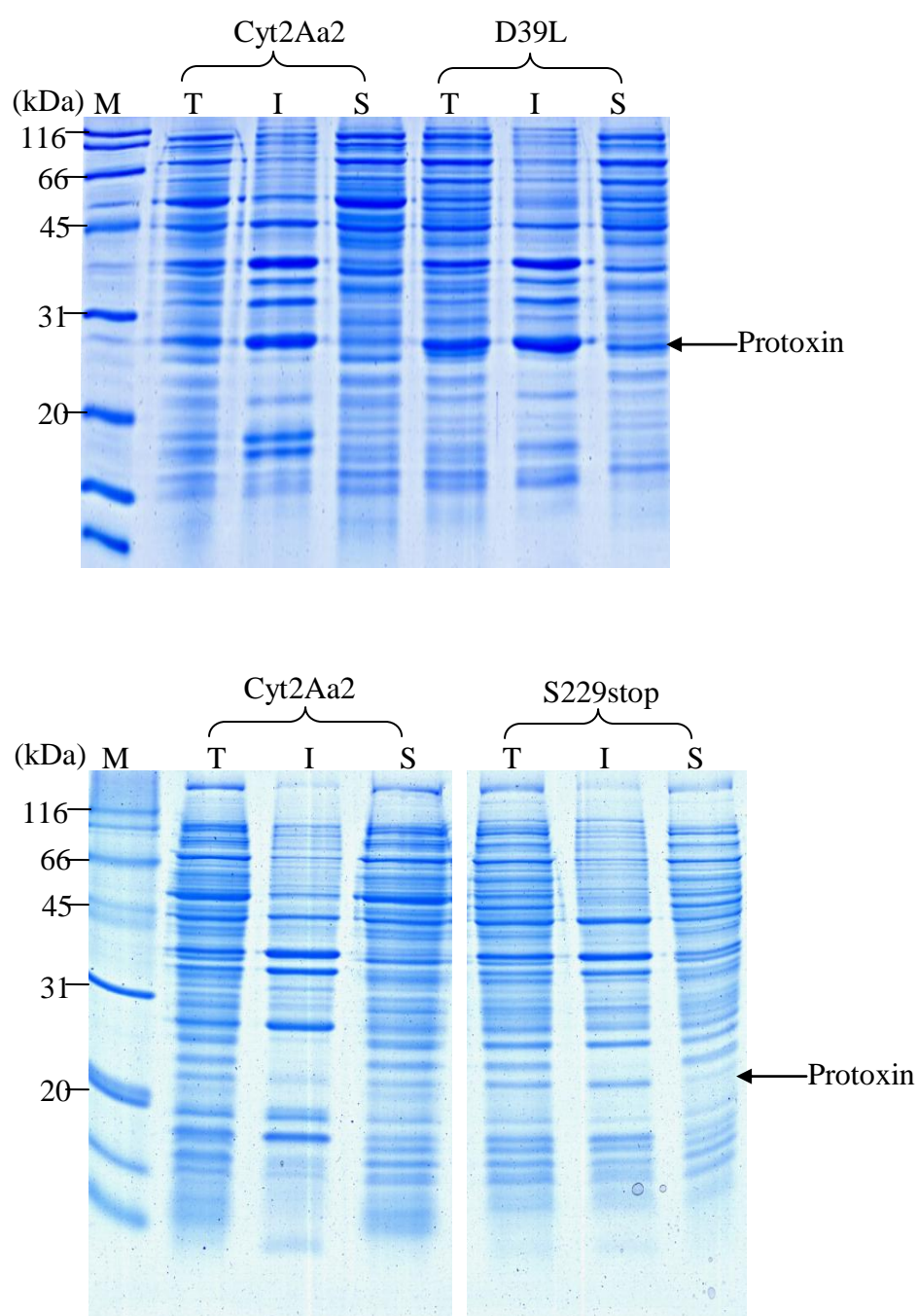


Figure 5.3: Protein profile of all mutants and Cyt2Aa2 on 15% polyacrylamide gel

M is broad-range protein marker lane. *E. coli* cell lysate was loaded in lane “ T ”. Total cell lysate was centrifuged to separate inclusions and soluble proteins. Insoluble fraction was resuspended in water and loaded in lane “ I ” while soluble fraction was loaded in lane “ S ”. The arrows indicate the band of prototoxin.

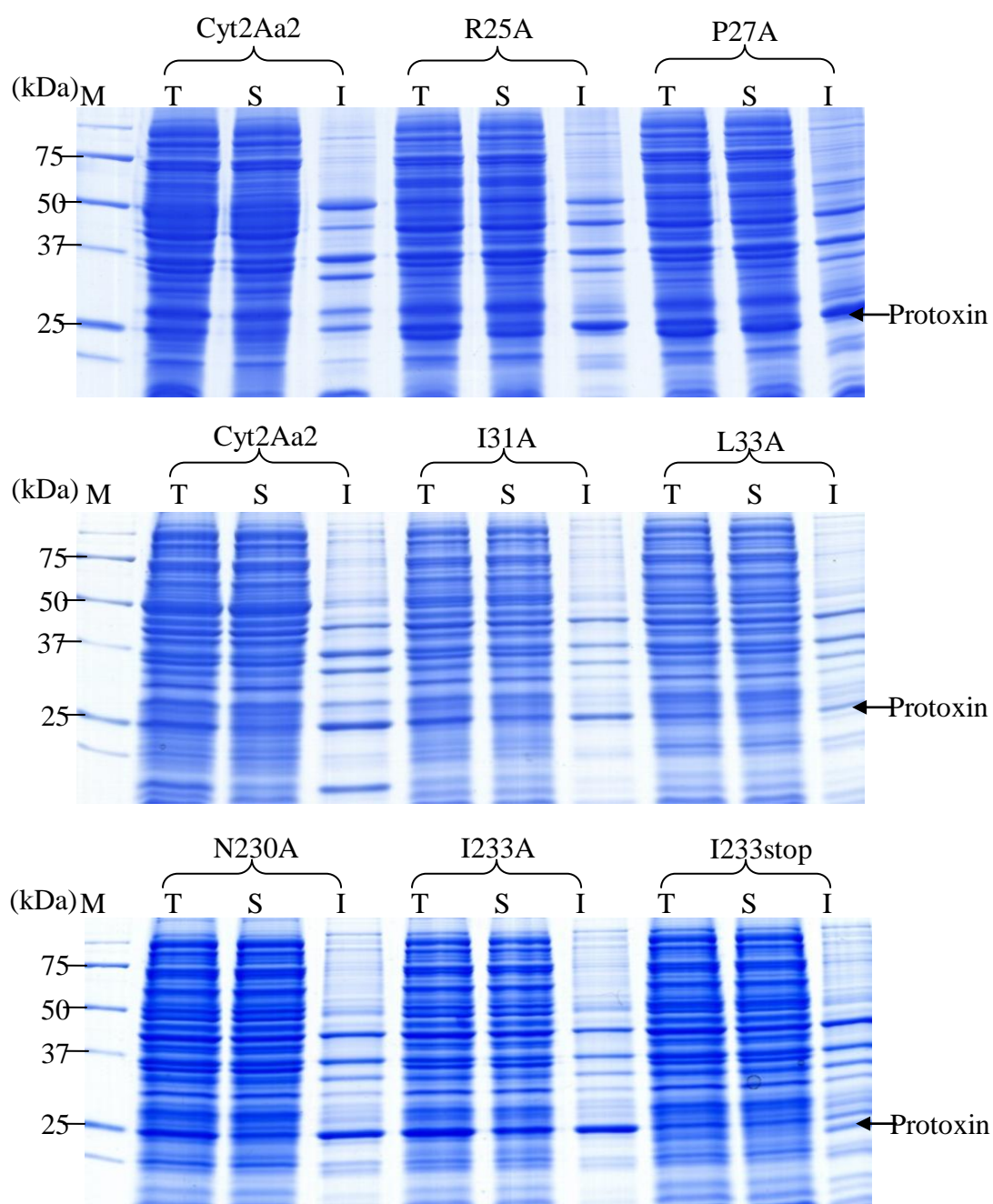


Figure 5.3: (Cont.) Protein profile of mutant and Cyt2Aa2 proteins on 12.5% polyacrylamide gel

M is broad-range protein marker lane. *E. coli* cell lysate was loaded in lane “ T ”. Total cell lysate was centrifuged to separate inclusions and soluble proteins. Insoluble fraction was resuspended in water and loaded in lane “ I ” while soluble fraction was loaded in lane “ S ”. The arrows indicate the band of prototoxin.

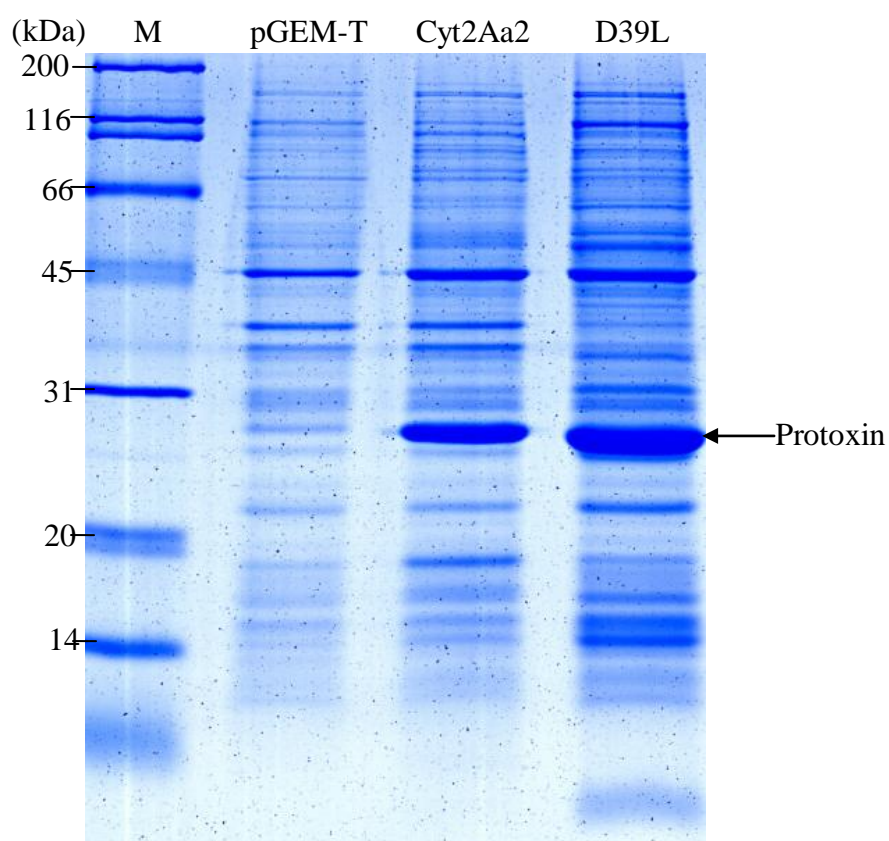


Figure 5.4: Partially purified inclusion of D39L mutant and Cyt2Aa2

Inclusions of D39L and Cyt2Aa2 on 15% polyacrylamide gel were observed at 29 kDa. M is broad-range protein marker lane.

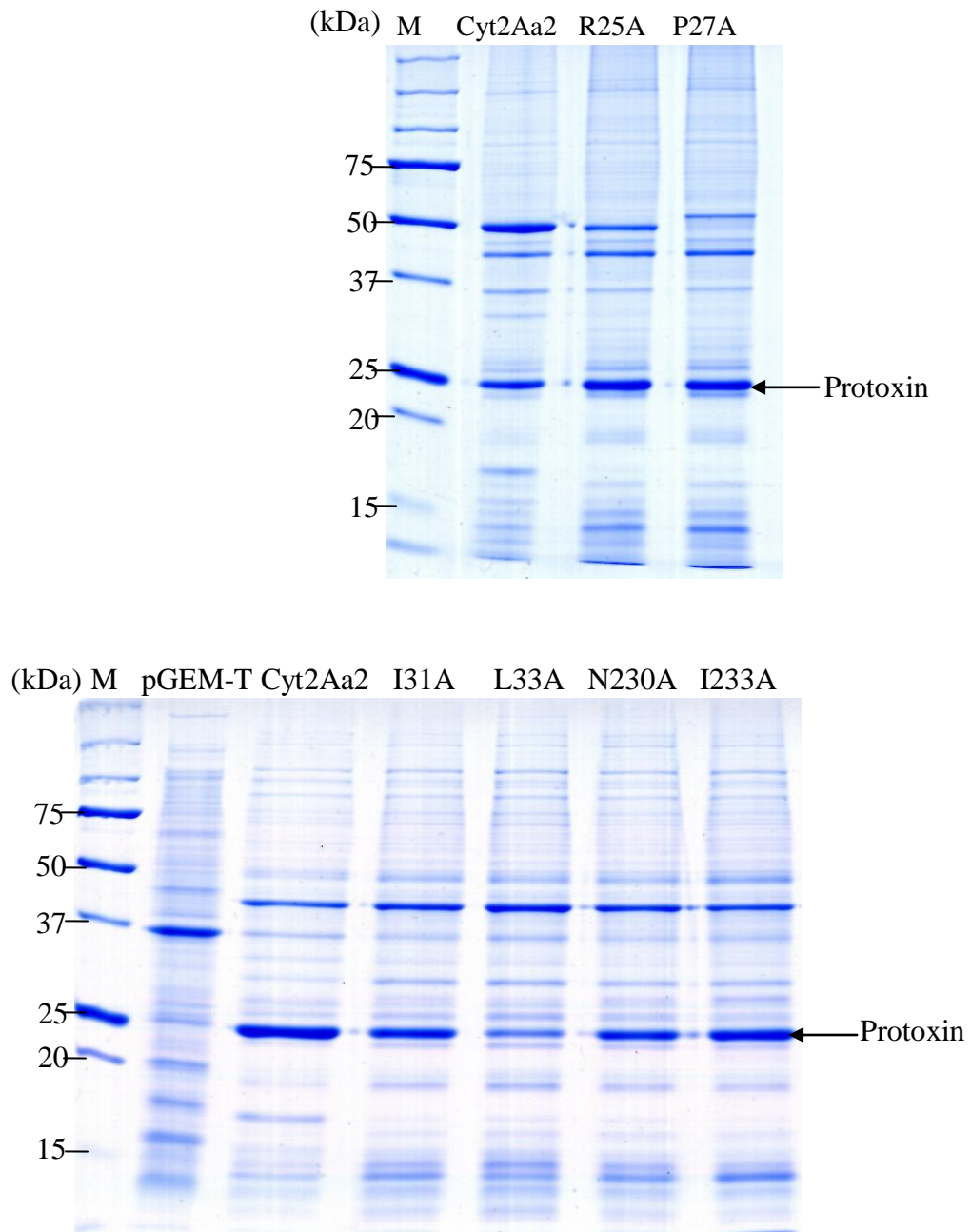


Figure 5.5: Partially purified inclusion of mutants and Cyt2Aa2

Inclusions of Cyt2Aa2 and each mutant were analyzed on 12.5% polyacrylamide gel. Inclusion of mutants and Cyt2Aa2 were observed at about 25 kDa. M is precision protein marker lane.

observed at lower molecular weight than that of Cyt2Aa2 protein that was shown at 25 kDa (**figure 5.6**). Western blot analysis technique was used to identify Cyt2Aa2 and mutant proteins. The proteins on polyacrylamide gel were transferred to the nitrocellulose membrane and then probed with anti-Cyt2A. The result revealed that inclusion of all mutants could react to anti-Cyt2A as shown in **figure 5.7**. S229stop protein was detected by chemiluminescent method because it was shown very faint band by colorimetric method.

5.3 Solubilization and proteinase K processing

To characterize the biochemical properties, inclusions of wild type were solubilized in 50 mM Na₂CO₃/NaHCO₃ buffer from pH 9 to 11 and provided protoxin as 25 kDa. After proteolytic processing by proteinase K, protoxin was converted to activated toxin that could be observed at molecular mass of 23 kDa on 12.5% polyacrylamide gel (**figure 5.8**). All mutants were solubilized in 50 mM Na₂CO₃/NaHCO₃ buffer, pH 9.5. The solubilized protoxins of R25A, P27A, I31A, D39L, and N238stop mutants were processed with 1% proteinase K. The protoxin and activated products could be observed at 25 kDa and 23 kDa, respectively. L33A, N230A, I233A and I233stop mutants gave less yield of activated toxin (**figure 5.9**). In addition, S229stop mutant was hardly solubilized and provided low amount of proteinase K activated toxin (**figure 5.10**).

5.4 Mosquito larvicidal toxicity

The mosquito larvicidal activity assay was performed to test toxicity of mutants and Cyt2Aa2 (wild type) *in vivo*. The 2nd instar *Aedes aegypti* mosquito larvae were fed with various concentrations of inclusions (0.49-250 µg/ml). The LC₅₀ values with their ranges for mutants and wild type are shown in **table 5.1**. The mosquito larvicidal activity result revealed that mosquito larvicidal activity of R25A, P27A, I31A, D39L, I233A and N238stop mutants was comparable to that of the wild-type protein whereas L33A, N230A, and I233stop showed lower toxicity than that of the wild type. Larvicidal activity was completely abolished for S229stop mutant.

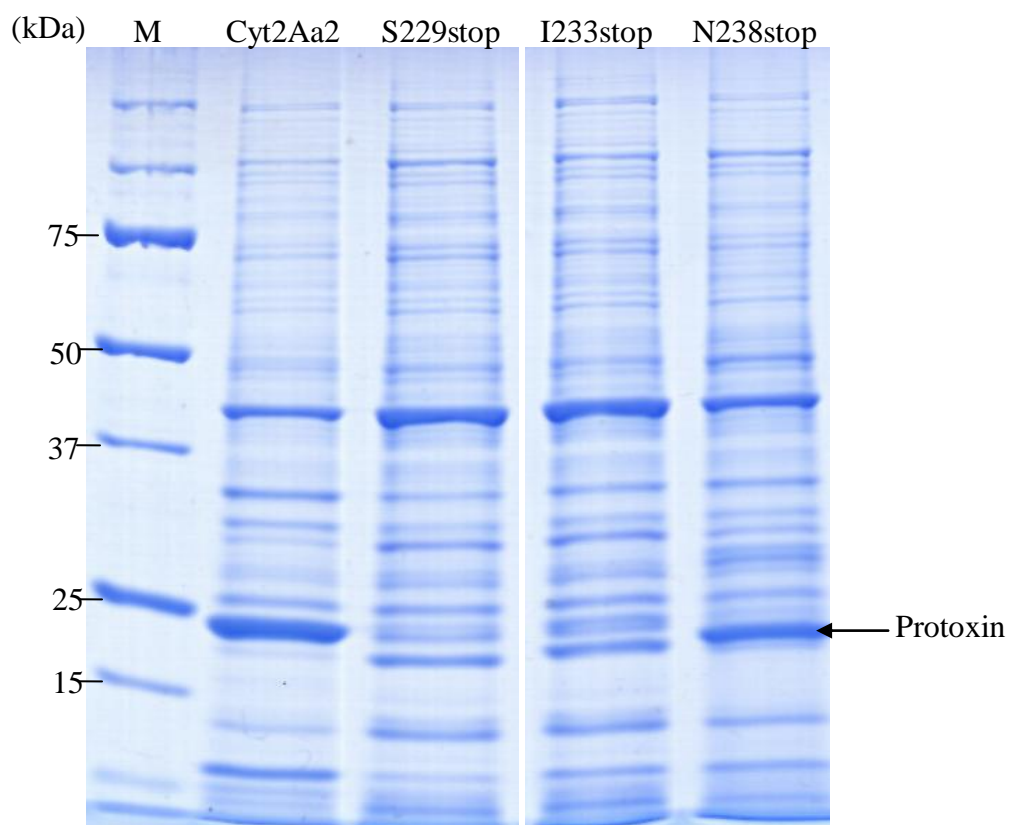


Figure 5.6: Partially purified inclusions of truncated mutants and Cyt2Aa2

Inclusions of truncated S229stop, I233stop, and N238stop proteins were analyzed on 12.5% polyacrylamide gel. Cyt2Aa2 lane represents a major band at 25 kDa. Truncated S229stop, I233stop, and N238stop mutants showed a lower band than wild type that could be observed at 25 kDa. M is precision protein marker lane.

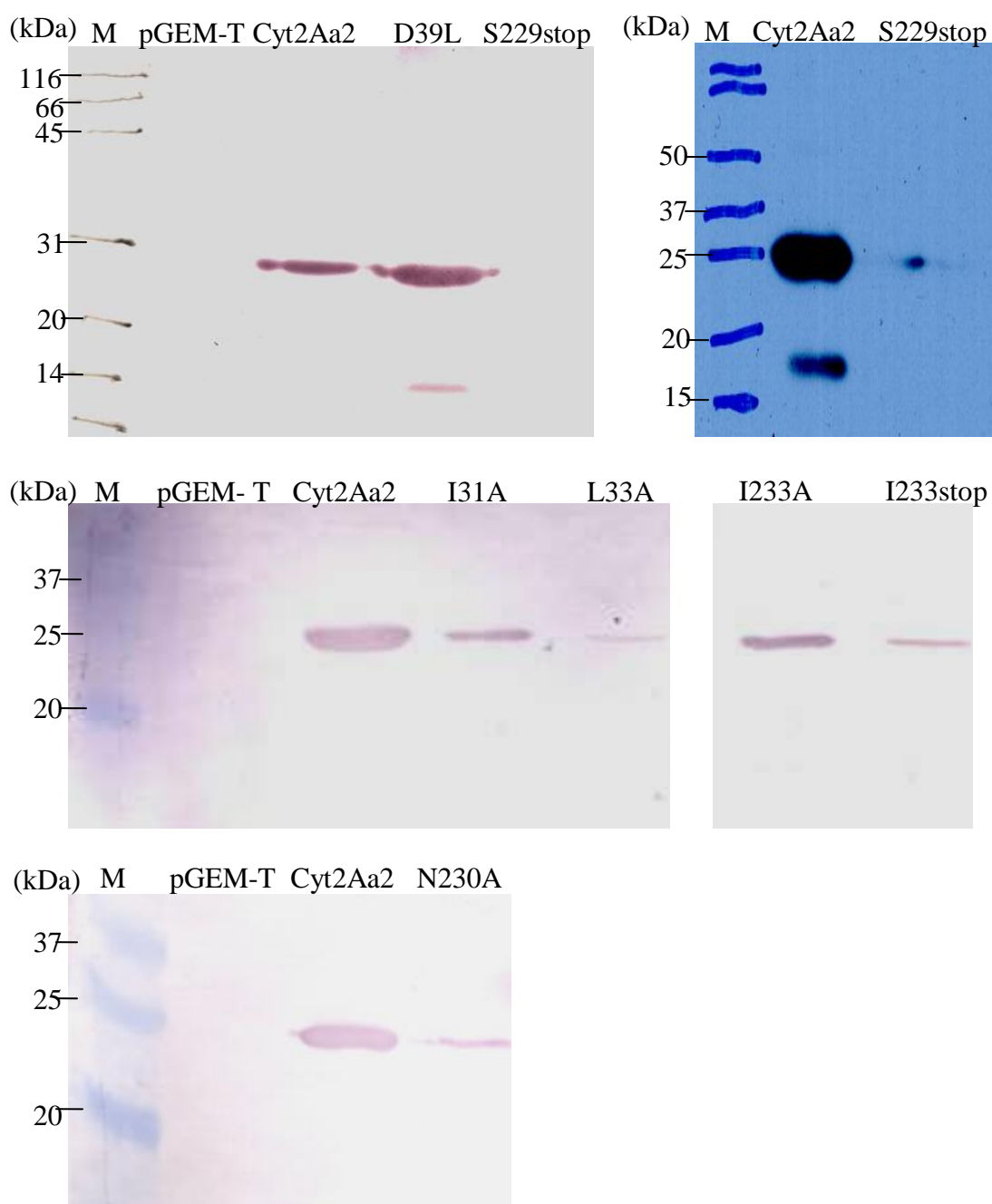


Figure 5.7: Western blot analysis of Cyt2Aa2 and mutant inclusions

Cyt2Aa2, I31, D39L, and I233A lanes showed the band at 25 kDa. L33A, N230A, S229stop, and I233stop lanes show very faint band at 25 kDa. M is protein marker lane.

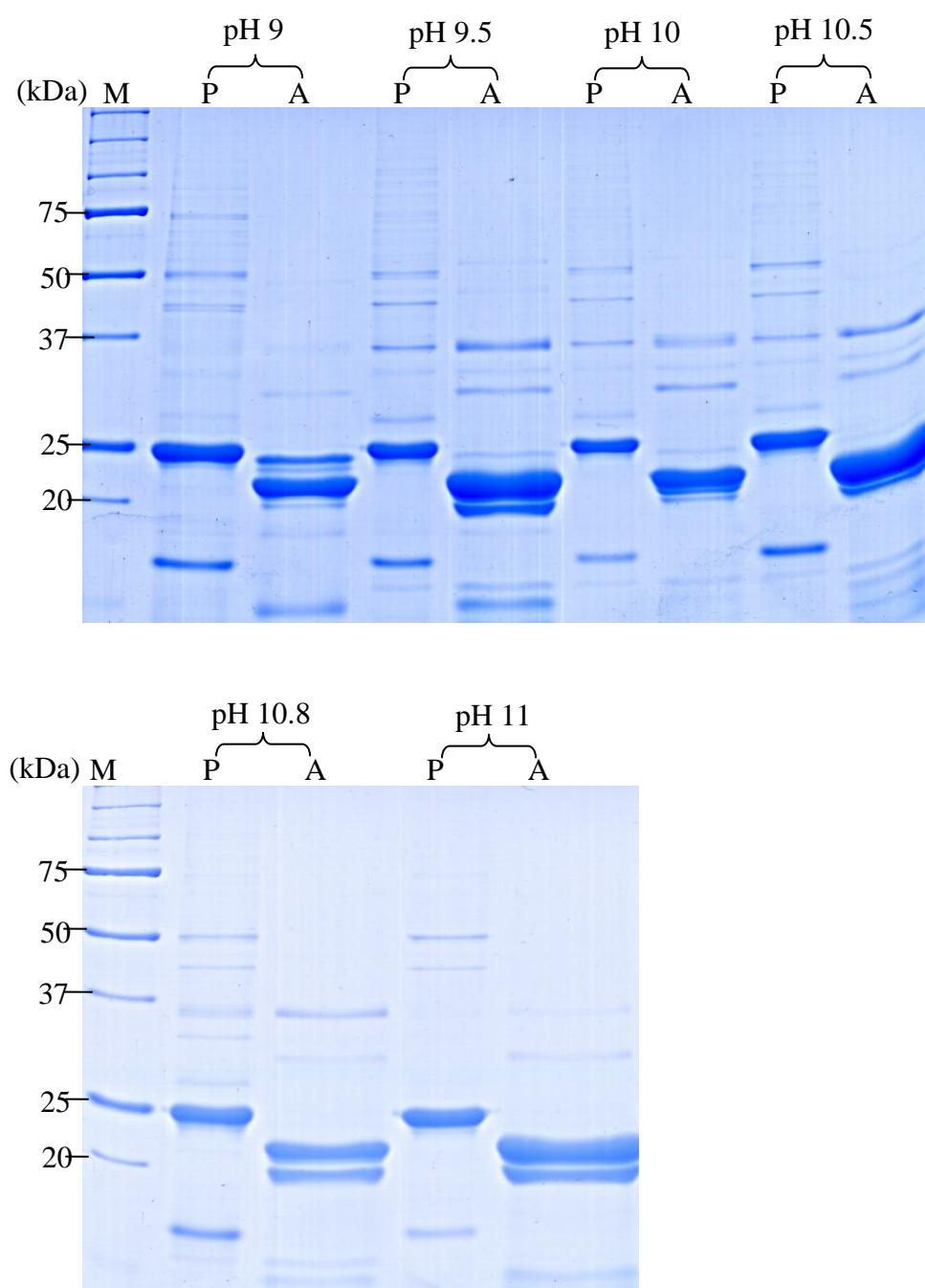


Figure 5.8: Protoxin and proteinase K activated product of Cyt2Aa2 protein

Cyt2Aa2 protoxin solubilized in 50 mM $\text{Na}_2\text{CO}_3/\text{NaHCO}_3$ buffer from pH 9 to 11 and activated by proteinase K (1% w/w) for 1 h at 37 °C. M, P and A represent to precision protein marker lane, protoxin and activated toxin, respectively.

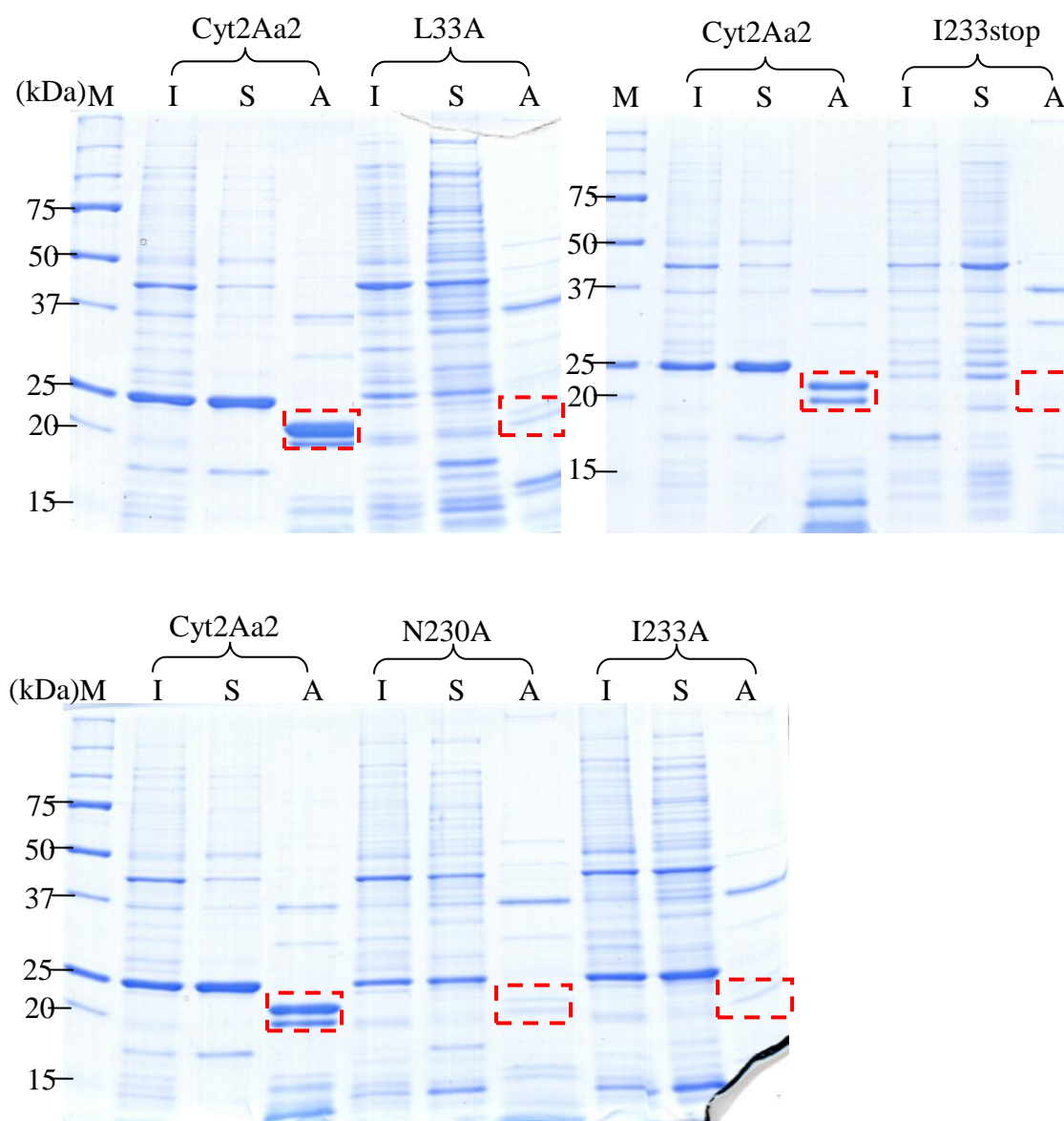


Figure 5.9: Solubilization in 50 mM $\text{Na}_2\text{CO}_3/\text{NaHCO}_3$ buffer pH 9.5 and proteinase K activation of mutants

Inclusions were solubilized in 50 mM $\text{Na}_2\text{CO}_3/\text{NaHCO}_3$ buffer for 1.5 h at 37 °C. Soluble proteins were separated by centrifugation at 15,300 g for 10 min and activated by proteinase K (1% w/w) for 1 h at 37 °C. M, I, S and A represent to precision protein marker, inclusion, soluble protein and activated toxin, respectively. The red boxes show the expected band size of activated toxin.

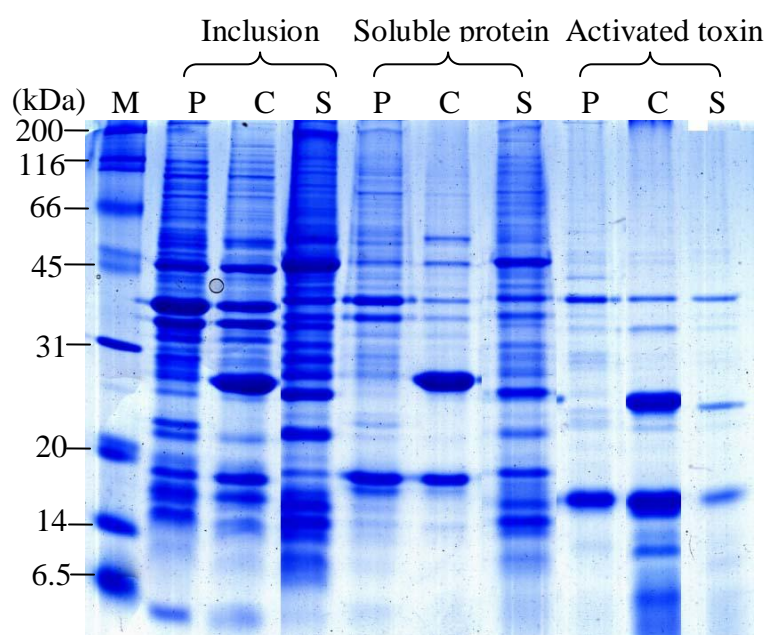


Figure 5.10: Protein solubilization and proteolytic processing of S229stop and Cyt2Aa2

Inclusions were solubilized in 50 mM $\text{Na}_2\text{CO}_3/\text{NaHCO}_3$ buffer for 1.5 h at 37 °C. Soluble proteins were separated by centrifugation at 15,300 g for 10 min and activated by proteinase K (1% w/w) for 1 h at 37 °C. P is cell carrying pGEM[®]-T Easy. C and S are Cyt2Aa2 and S229stop mutant.

Table 5.1: Mosquito larvicidal toxicity of Cyt2Aa2 and mutant proteins

Protein	Mosquito larvicidal activity; LC₅₀ (µg/ml)	Range of LC₅₀ (µg/ml)
Cyt2Aa2	0.71	0.02-0.87
R25A	0.38	0.20-0.47
P27A	0.94	0.05-1.52
I31A	1.11	0.94-1.30
L33A	32.41	26.58-40.37
D39L	0.56	0.03-1.54
N230A	10.71	8.83-12.98
I233A	0.42	0.32-0.53
I233stop	17.09	12.60-24.69
S229stop	Inactive	Inactive

In larvicidal activity assay, 2-folds serial dilution of each toxin was fed to 2nd instar larvae for overnight at room temperature. The larval mortality was calculated and reported as LC₅₀ value. In Hemolytic activity assay, 2-folds serial dilution of each toxin was incubated with sheep erythrocytes and left at room temperature for 24 hours. The end-point of haemolysis was monitored as the last well that was still red.

5.5 Haemolytic activity

In vitro haemolytic activity of protoxin and proteinase K activated toxins was tested against sheep red blood cells. Results revealed that wild type and mutant protoxins could lyse sheep red blood cells at high concentration. Activated toxin of R25A, P27A, I31A, D39L showed similar activity to Cyt2Aa2 whereas L33A, N230A, I233A, S229stop and I233stop showed lower activity than Cyt2Aa2. Haemolytic end points of Cyt2Aa2 and mutants are shown in **figure 5.11** and **table 5.2**.

5.6 Protoxin dimerization

Normally, solubilized Cyt2Aa2 protoxin showed one major band at 25 kDa on polyacrylamide gel after solubilization in 50 mM Na₂CO₃/NaHCO₃ buffer pH 9.5 and SDS-PAGE analysis in the presence of reducing agent (10 mM DTT). On the other hand, two major bands at 25 kDa and 50 kDa were clearly observed when performing SDS-PAGE analysis without reducing agent. L33A and N230A mutants showed very faint bands at 25 kDa and 50 kDa (**figure 5.12**) including truncated S229 stop and I233stop mutants (**figure 5.13**).

5.7 Toxin oligomerization

To investigate protein binding to membrane *in vitro*, proteins were incubated with multilamellar liposomes for 2 hours and then analyzed on SDS-PAGE. Results revealed that there was no band in liposome lane. Solubilized Cyt2Aa2 protoxin lane showed a very faint band at 25 kDa and a major band at 50 kDa whereas Cyt2Aa2 activated toxin provided one band at 23 kDa. Pellet of protoxin incubated with liposomes collected by centrifugation showed a band at 50 kDa, but pellet of activated toxin incubated with liposomes provided a laddering pattern of protein bands. On the other hand, supernatant of protoxin and activated toxin showed one band at 50 kDa and 23 kDa, respectively (**figure 5.14**). Pellet of D39L protoxin and activated toxin incubated with liposomes showed a similar result to the wild type toxin (**figure 5.15**).

Table 5.2: Haemolysis end-point of Cyt2Aa2 and mutant proteins

Protein	Haemolysis end-point ($\mu\text{g/ml}$)
Cyt2Aa2	0.12-0.39
R25A	0.12-0.39
P27A	0.12-0.39
I31A	0.06-0.48
L33A	2.25-15.63
D39L	0.12-0.48
N230A	0.42-0.56
I233A	1.78-3.25
I233stop	1.31-62.50
S229stop	7.82-15.63

In haemolytic activity assay, 2-folds serial dilution of each toxin was incubated with sheep erythrocytes and left at room temperature for 24 hours. The end-point of haemolysis was monitored as the last well that was still red.

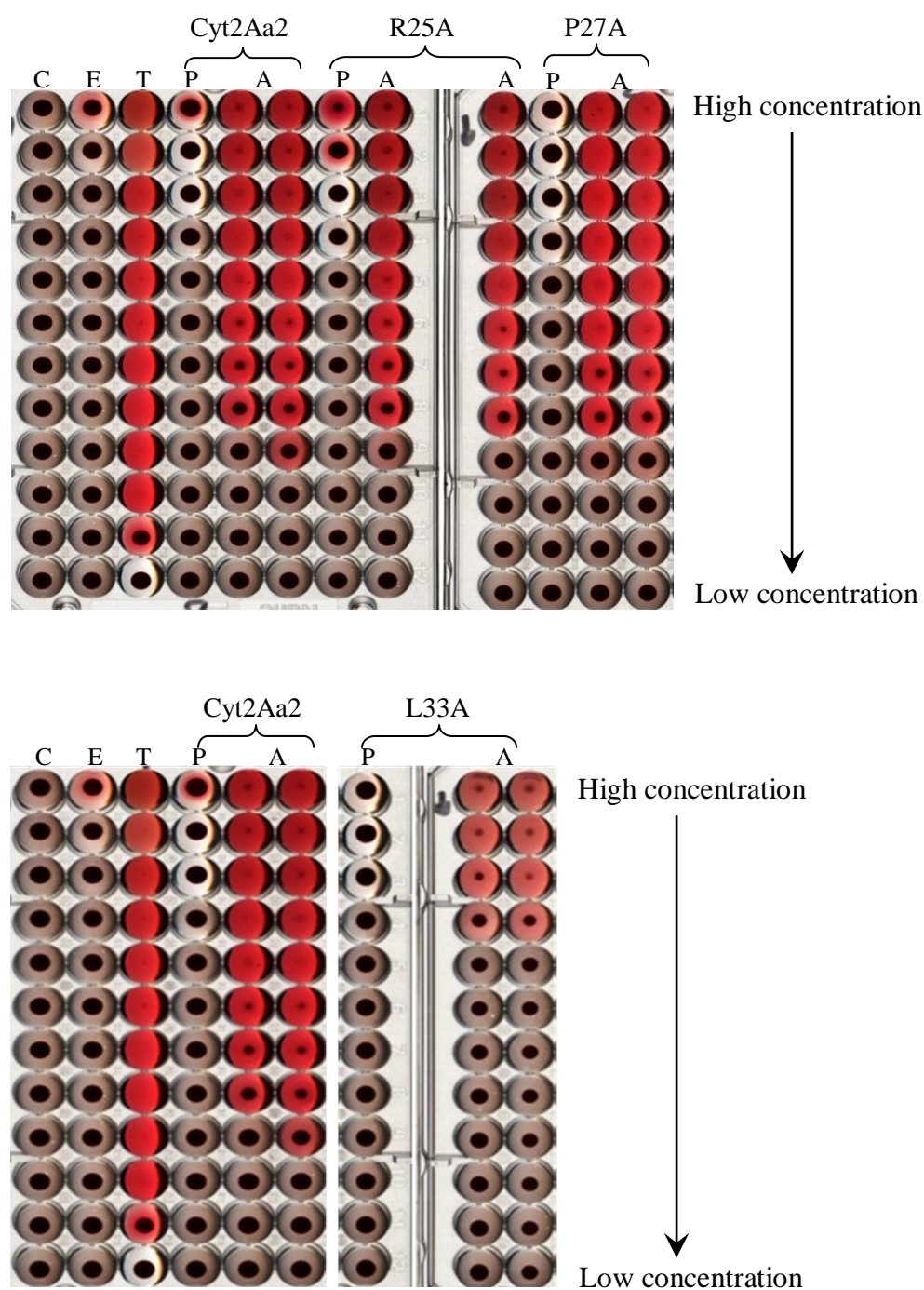


Figure 5.11: Haemolytic activity of mutant and Cyt2Aa2 proteins

The 2-folds serial dilution of each toxin was mixed with sheep erythrocytes. C, E, T, P, and A represents the well added with CO_3^{2-} buffer pH 9.5, CO_3^{2-} buffer pH 9.5+Proteinase K, Triton-X, protoxin and activated toxin. Starting concentration from each lane was different.



The 2-folds serial dilution of each toxin was mixed with sheep erythrocytes. C, E, T, P, and A represents the well added with CO_3^{2-} buffer pH 9.5, CO_3^{2-} buffer pH 9.5+Proteinase K, Triton-X, protoxin and activated toxin. Starting concentration from each lane was different.

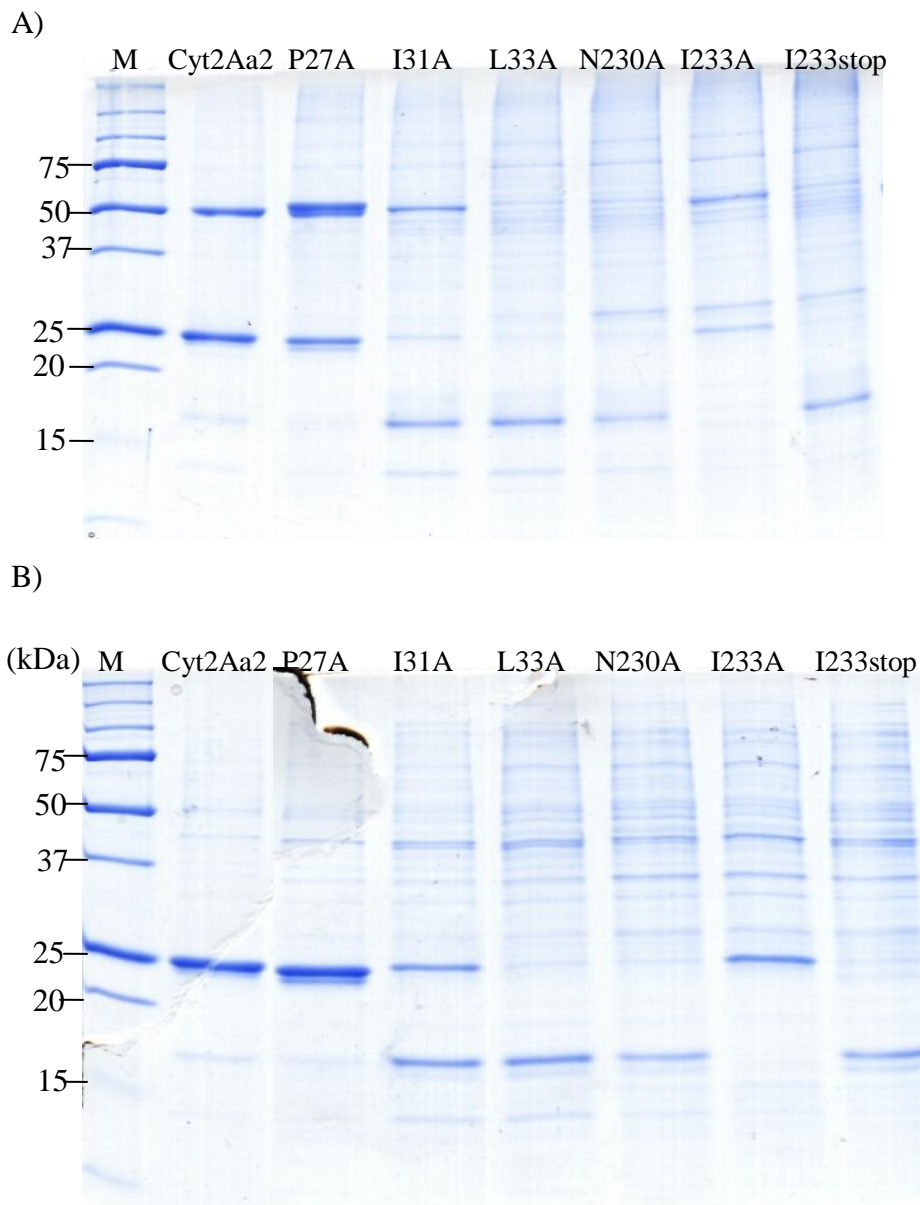


Figure 5.12: Cyt2Aa2 and mutant protoxins in the presence and absence of reducing agent on 12.5 % polyacrylamide gel

A) In the absence of DTT and no heating at 95 °C; Cyt2Aa2, P27A, I31A, and I233A lanes showed two bands at 25 kDa and 50 kDa, whereas L33A, N230A, and I233stop lanes did not show the band at 25 kDa and 50 kDa.

B) In the presence of DTT and heating at 95 °C; Cyt2Aa2, P27A, I31A and I233A lanes showed one band at 25 kDa, whereas L33A, N230A, and I233stop lanes did not show the band at 25 kDa.

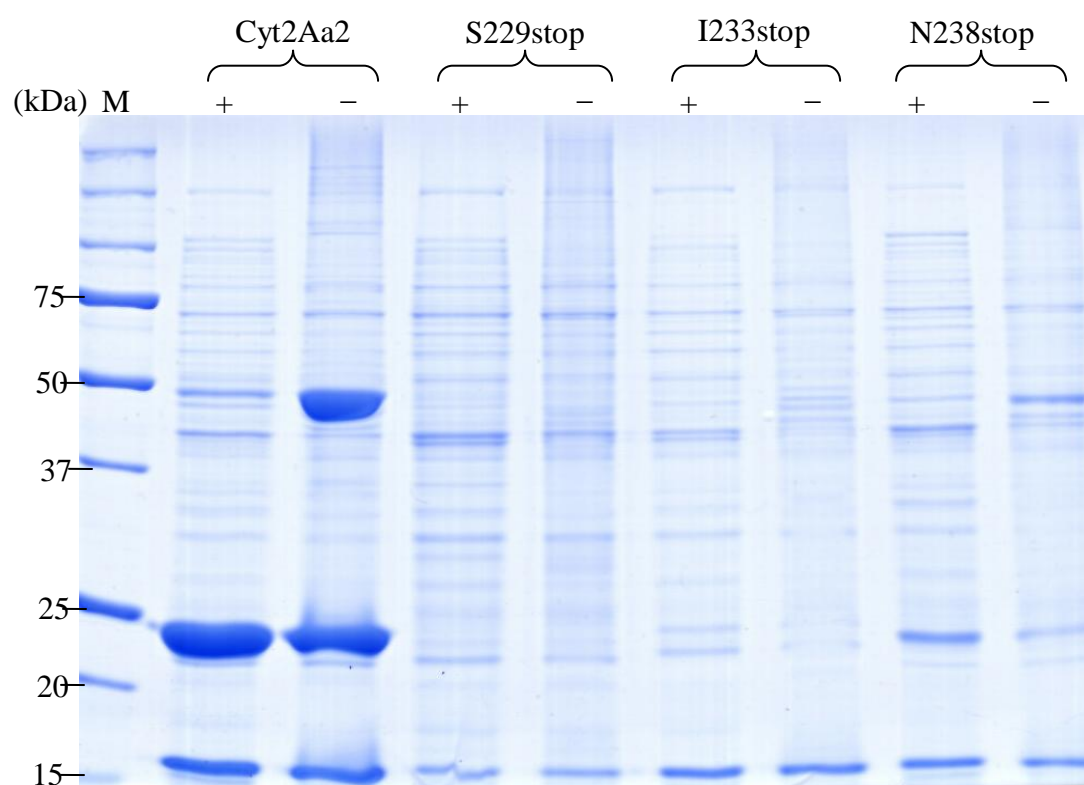


Figure 5.13: Cyt2Aa2 and truncated protoxins in the presence and absence of reducing agent on 12.5 % polyacrylamide gel

M is precision marker. + stands for heating sample at 95 °C and in the presence of DTT. - represent the lanes loaded protein that without heating sample at 95 °C and in the absence of DTT.

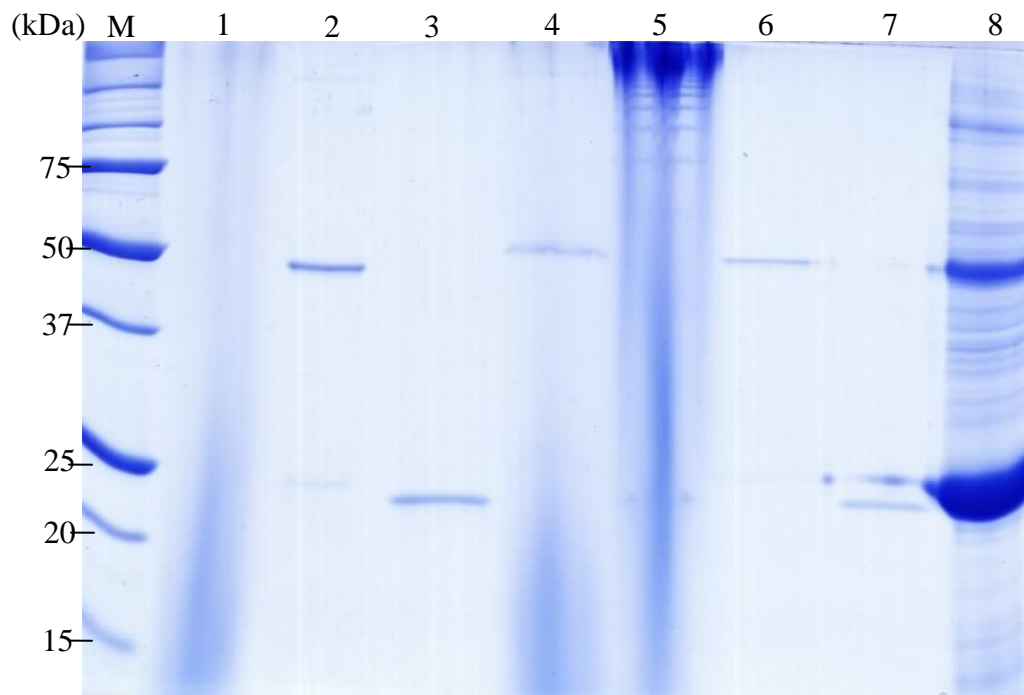


Figure 5.14: Toxin oligomerization test of Cyt2Aa2 toxin

Protein was incubated with liposome for 2 hours at room temperature.

M = precision protein marker.

Lane 1 = liposome alone

Lane 2 = protoxin alone

Lane 3 = activated toxin alone

Lane 4 = pellet of liposome + protoxin

Lane 5 = pellet of liposome + activated toxin

Lane 6 = supernatant of liposome + protoxin

Lane 7 = supernatant of liposome + activated toxin

Lane 8 = toxin inclusion

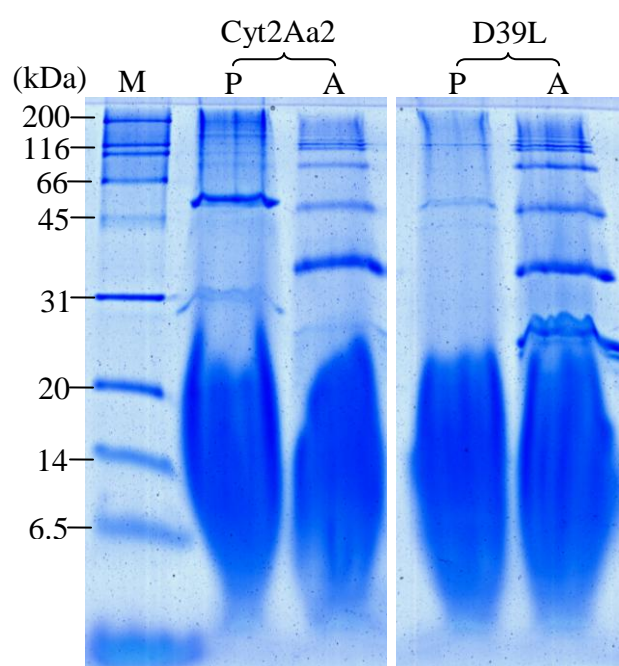


Figure 5.15: Toxin oligomerization test of D39L toxin compared with Cyt2Aa2 toxin

M is broad range protein marker. P and A represent the pellet of protoxin and activated toxin that were collected by centrifugation after incubated with liposomes for 2 hours at room temperature.

5.8 Intrinsic fluorescence spectroscopy

Tertiary structure of Cyt2Aa2 and mutants were investigated by intrinsic fluorescence spectroscopy. The purified protein samples were excited at 280 nm using excitation and emission slit width 2.5 nm. The fluorescent emission spectra were scanned from 300 nm to 550 nm. The emission spectra of Cyt2Aa2 protoxin showed a major peak at 330 nm and shoulder peak at 340 nm. R25A, P27A, I31A, and D39L gave a similar result to wild type, while the two peaks of N230A and I233A were not different. L33A and truncated S229stop, and I233stop toxin showed a major peak at 340 nm (**figure 5.16**).

5.9 Dynamic light scattering

Dynamic light scattering technique was used to reveal size distribution profile of mutant and Cyt2Aa2 protoxins in carbonate buffer pH 9.5. Cyt2Aa2 protoxin in carbonate buffer pH 9.5 has three populations and their diameter were about 4-10 nm, 40-100 nm, and 200-650 nm. I31A protoxin gave three peaks which were 4-10 nm, 30-100 nm, and 150-800 nm. L33A showed a large peak at 40-800 nm and N230A showed two populations which are 60-200 nm and 300-1,000 nm. I233A protoxin provided size about 150-350 nm (**figure 5.17**). All of them form large aggregate (major peak about 100-1,000 nm). Only wild type (Cyt2Aa2) and I31A protoxins showed monomer or dimer peak about 4-10 nm.

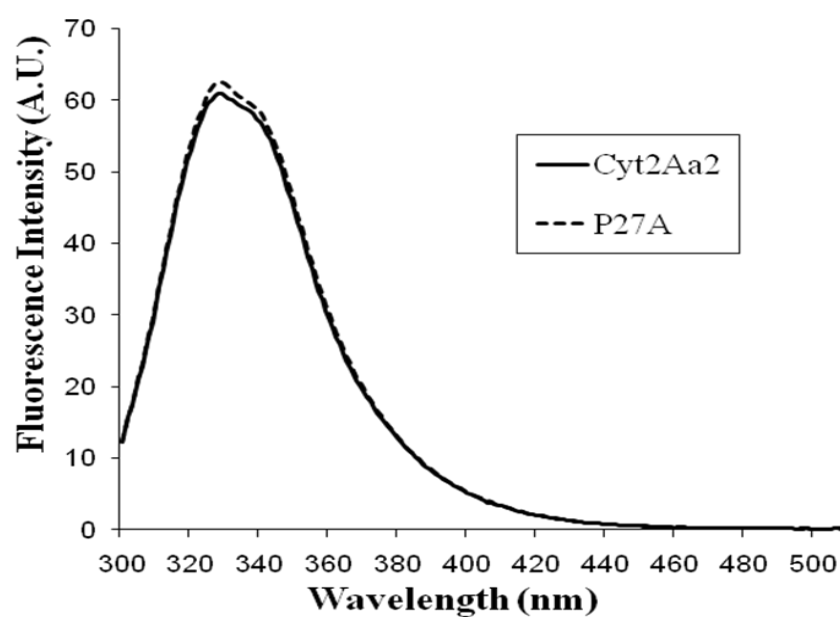
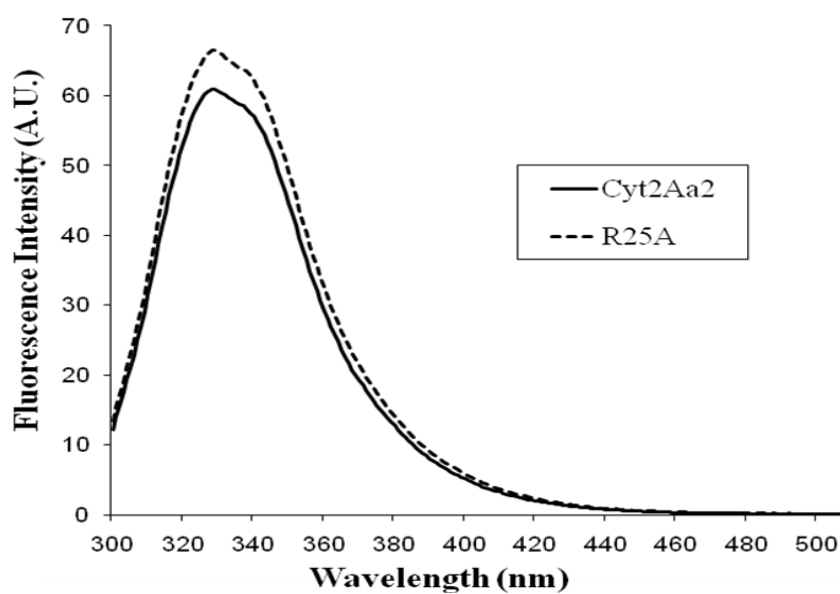


Figure 5.16: Intrinsic fluorescence spectra of mutant protoxins compared with Cyt2Aa2 protoxins (Conc. 10-40 $\mu\text{g/ml}$)

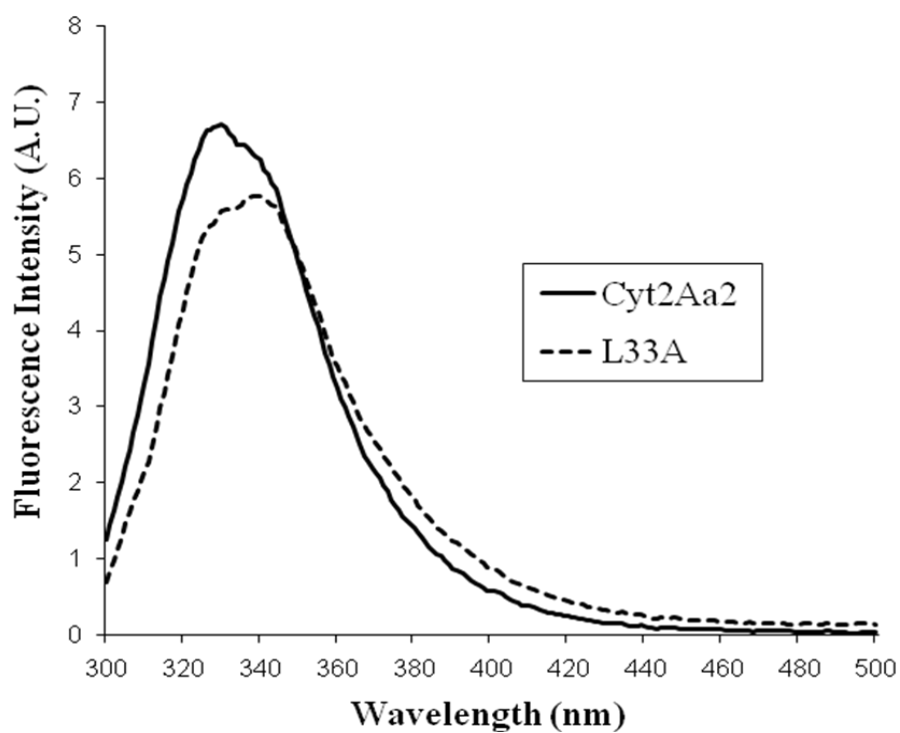
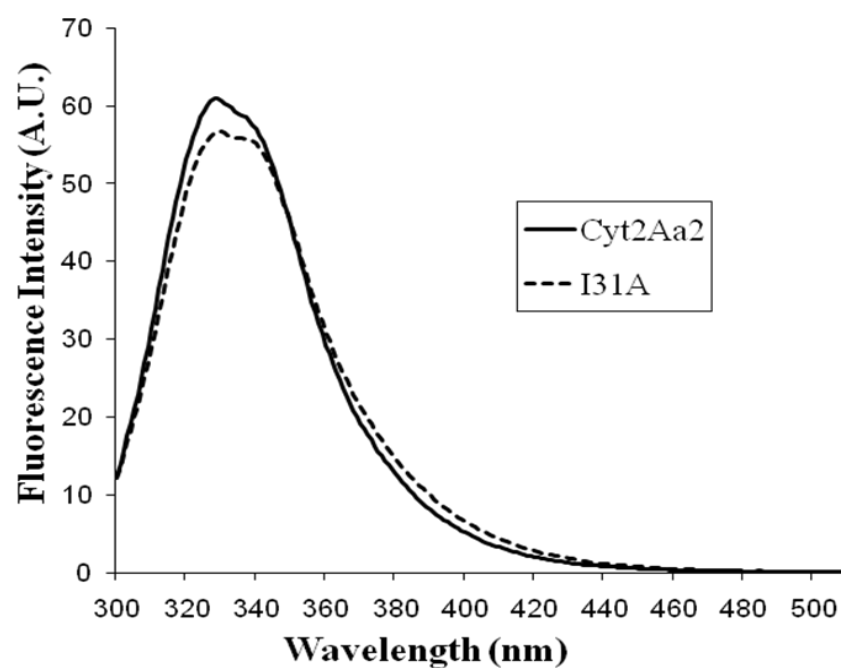


Figure 5.16: (Cont.) Intrinsic fluorescence spectra of mutant protoxins compared with Cyt2Aa2 protoxins (Conc. 10-40 μ g/ml)

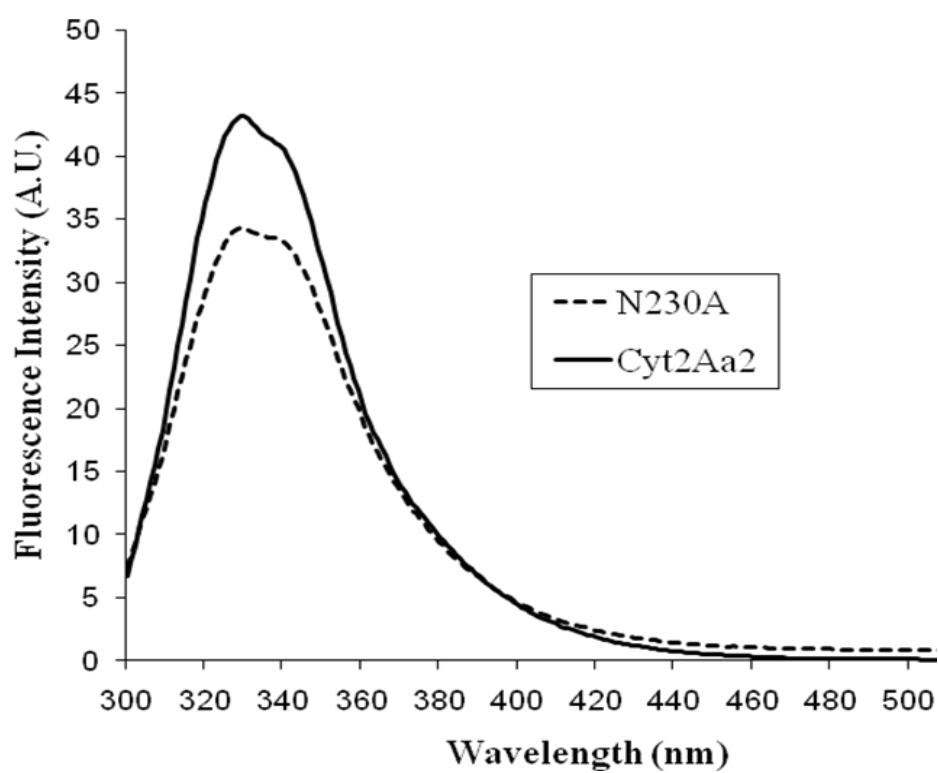
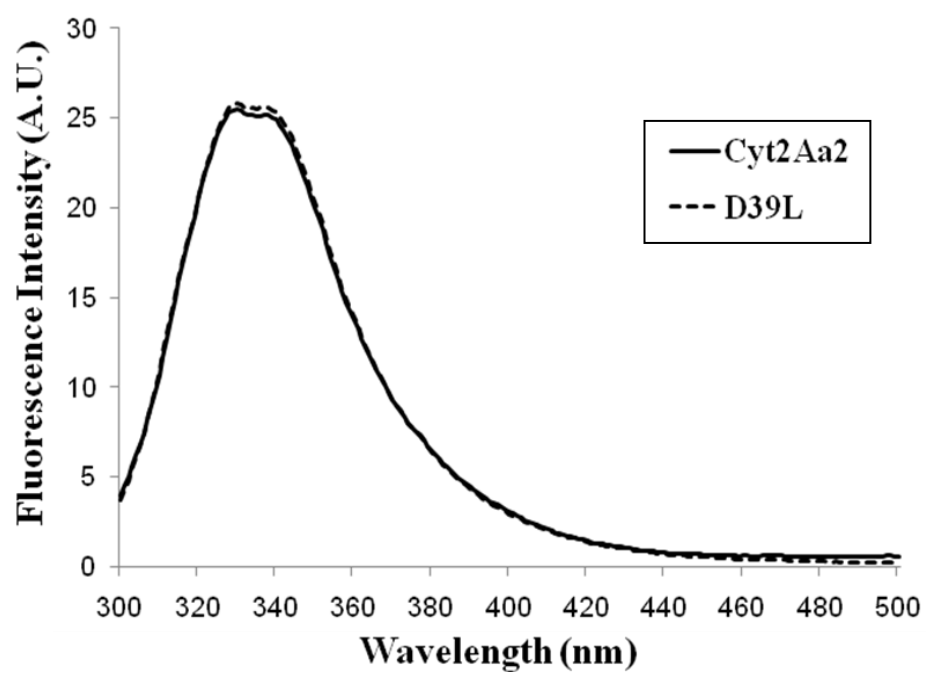


Figure 5.16: (Cont.) Intrinsic fluorescence spectra of mutant protoxins compared with Cyt2Aa2 protoxins (conc. 10-40 $\mu\text{g/ml}$)

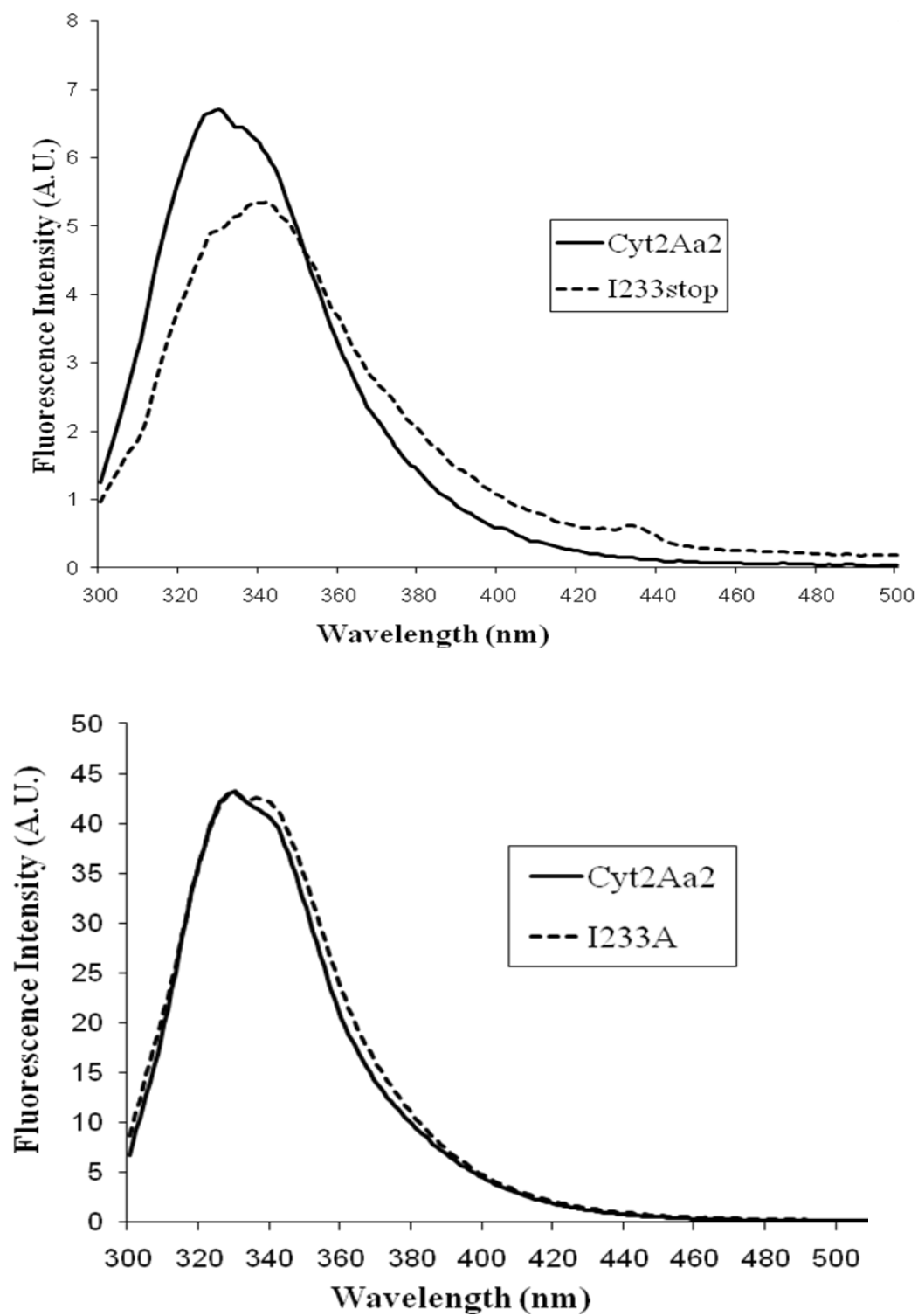


Figure 5.16: (Cont.) Intrinsic fluorescence spectra of mutant protoxins compared with Cyt2Aa2 protoxins (Conc. 10-40 $\mu\text{g/ml}$)

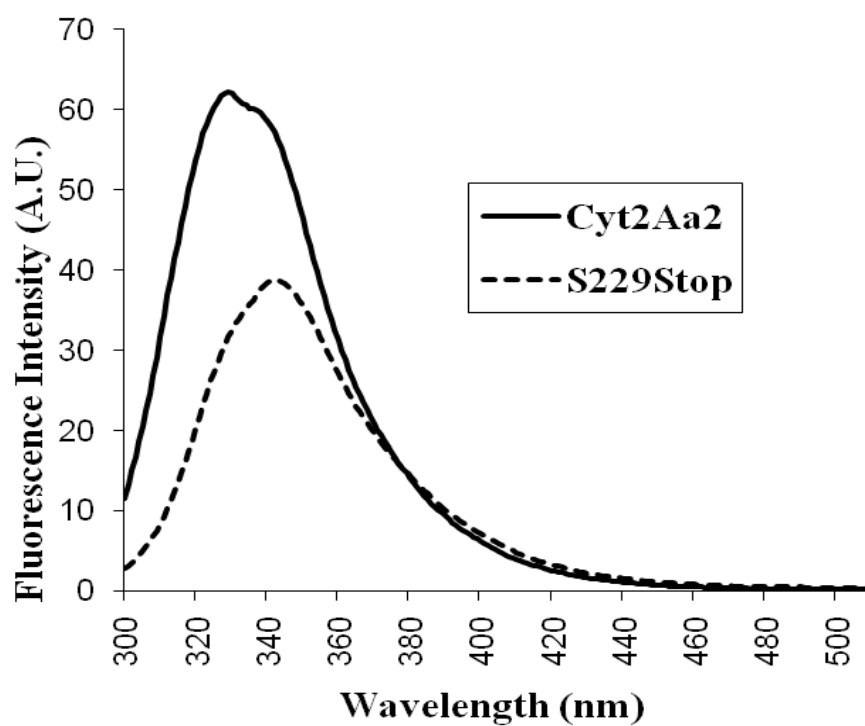
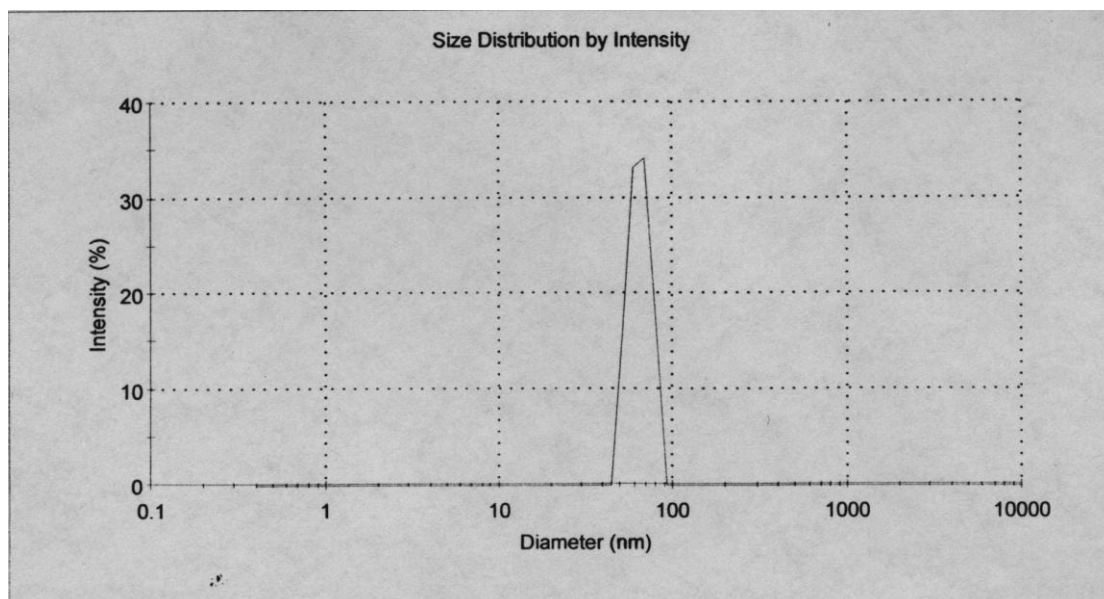


Figure 5.16: (Cont.) Intrinsic fluorescence spectra of mutant protoxins compared with Cyt2Aa2 protoxins (Conc. 10-40 $\mu\text{g/ml}$)

A)



B)

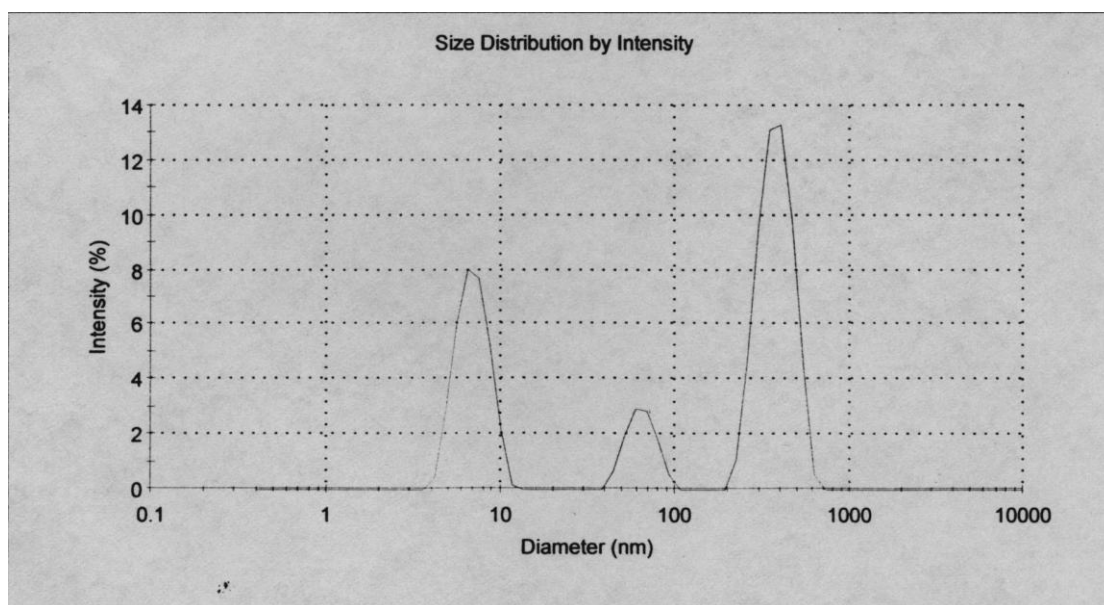
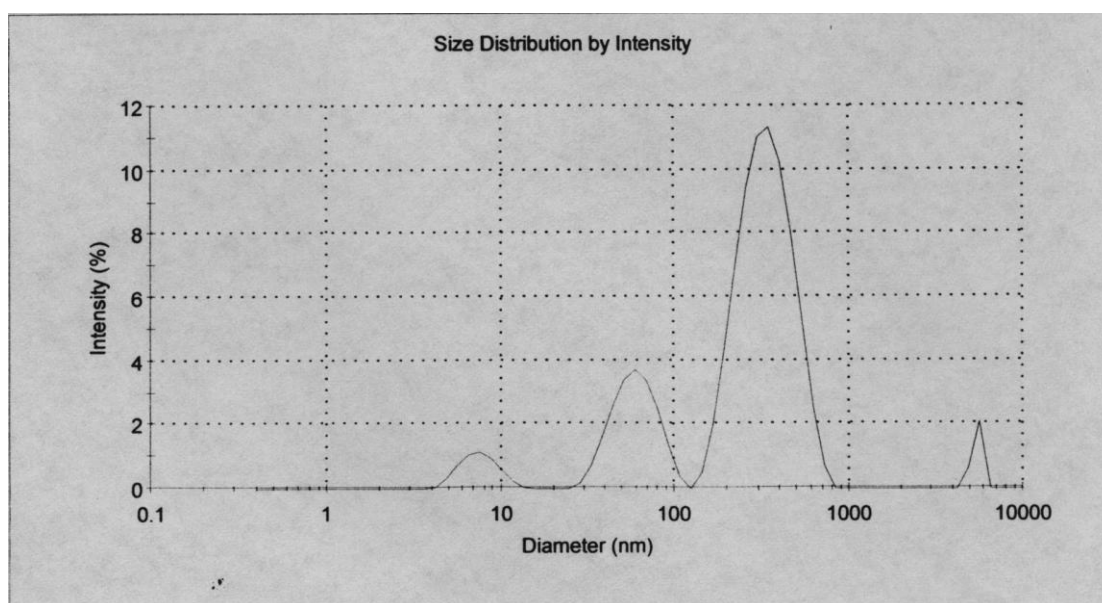


Figure 5.17: Size distribution profile of mutant and Cyt2Aa2 protoxins in 50 mM $\text{Na}_2\text{CO}_3/\text{NaHCO}_3$ buffer, pH 9.5

A) 50 mM $\text{Na}_2\text{CO}_3/\text{NaHCO}_3$ buffer, pH 9.5 B) Cyt2Aa2

C)



D)

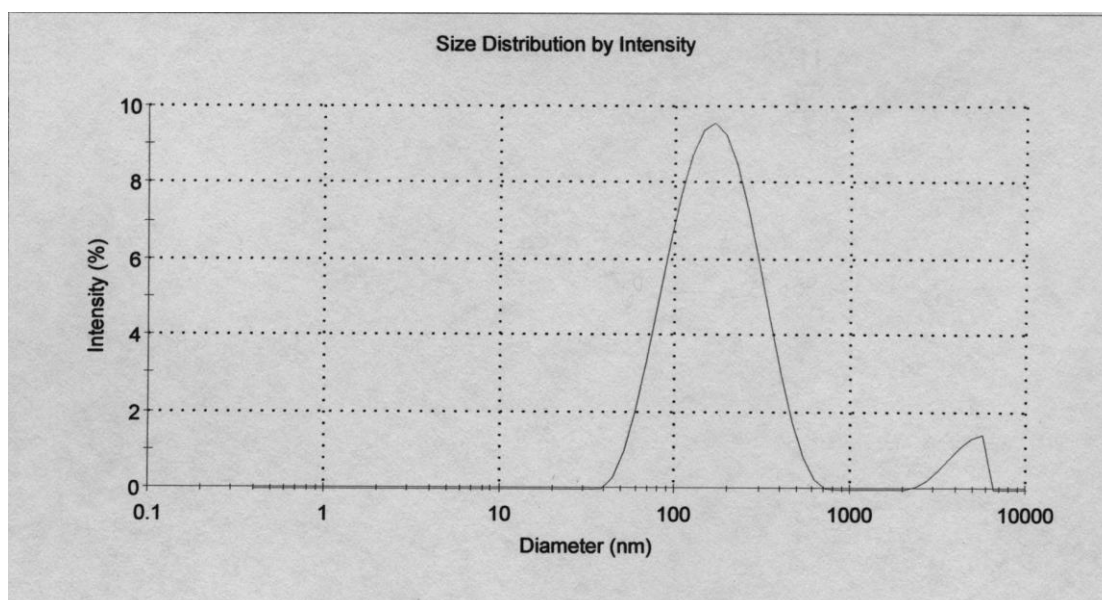
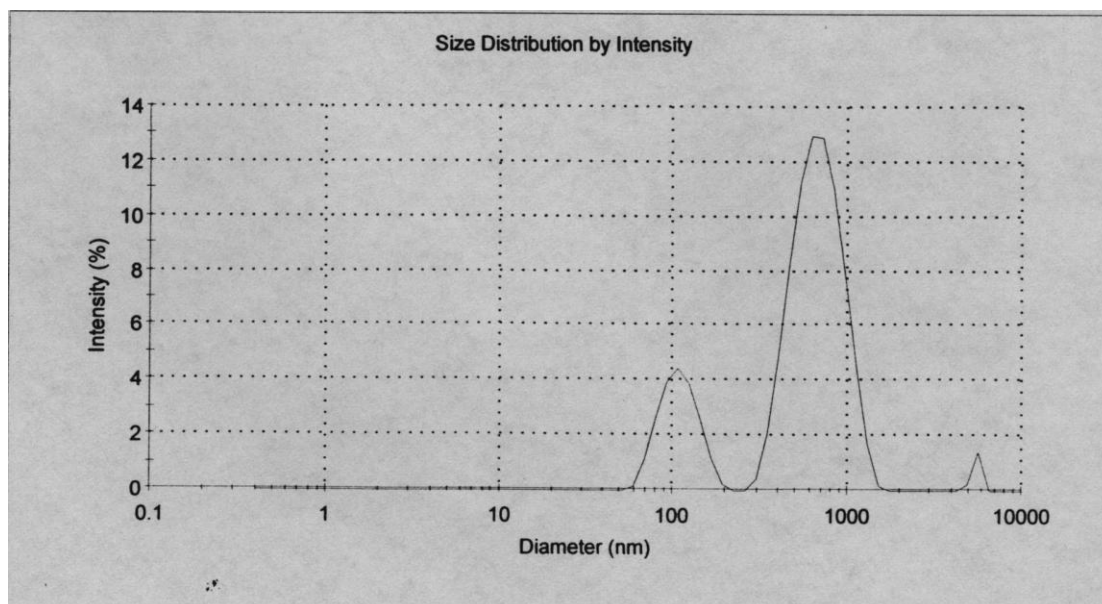


Figure 5.17: (Cont.) Size distribution profile of mutant and Cyt2Aa2 protoxins in 50 mM Na₂CO₃/NaHCO₃ buffer, pH 9.5

C) I31A D) L33A

E)



F)

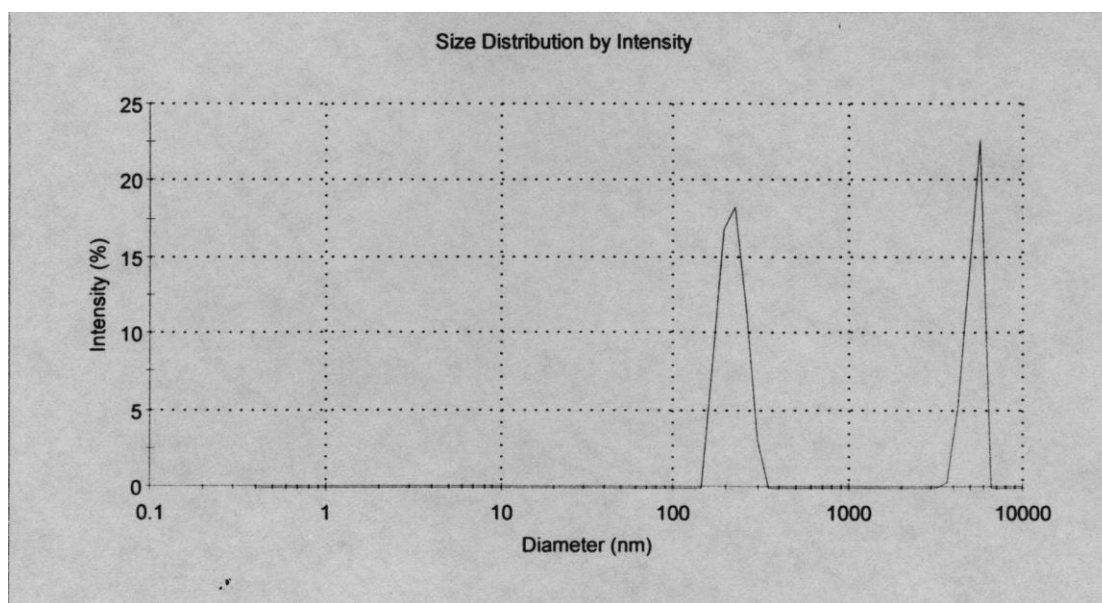


Figure 5.17: (Cont.) Size distribution profile of mutant and Cyt2Aa2 protoxins in 50 mM Na₂CO₃/NaHCO₃ buffer, pH 9.5

E) N230A F) I233A

CHAPTER VI

DISCUSSION

Cyt2Aa2 protein was found to give high toxicity to mosquito larvae, especially *Aedes aegypti* larvae. Gut-protease enzymes in the mid-gut of larvae were required for protein activation. Protease enzymes will cleave some parts at both N- and C-termini of Cyt2Aa2 protein out to trigger the protein function. It is interesting to know that why it needs to be cleaved out of N- and C-termini in order to be an activated toxin and what is the role of those amino acids at N- and C-termini.

Construction of mutants and truncated proteins

To investigate whether the amino acids located at N- and C-termini of Cyt2Aa2 protein are important for its structure and function, a number of point mutations were selected introduced into the molecular structure of Cyt2Aa2 protoxin. The point mutations, S229stop, S233stop and S238stop were selected to produce toxins with different length of truncation on the C-terminus. While those point mutations, R25A, P27A, I31A, L33A, D39L, N230A and I233A were designed to replace and test for the critical role of specific amino acids located on the N- and C-terminal regions. Site-directed mutagenesis was employed to generate the mutants in *E. coli* expression system. This expression system is common and well established with many related procedures for DNA transformation and expression induction. For Cyt2Aa2 protein, it is routinely expressed in *E. coli* with high yield and the toxin product is generally active. After PCR reaction using specific mutagenic primers, all mutants provided a major product at 3.8 kb on agarose gel, suggesting that the primer can bind specifically to the parental strand of Cyt2Aa2. The resulting product was the pGEM[®]-T Easy vector containing mutagenic Cyt2Aa2 gene. To confirm the mutation, PCR products were transformed to *E. coli* cells and the extracted DNA from *E. coli* culture were analyzed by restriction enzyme and automated DNA sequencing respectively. The results showed the mutation at the expected position for all mutants.

Biochemical properties (Protein production, solubilization and proteinase K activation)

R25A, P27A, I31A, D39L, I233A, N238stop mutants showed similar protein expression levels to that of wild type whereas L33A, N230A, S229stop, and I233stop mutants provided a lower protein expression level than that of wild type (**figure 5.2**). Amino acid substitutions to uncharged and small like alanine at positions R25, P27, I31, and I233 does not have any effect to the toxin production. The amino acids in these positions are proposed to involve with interaction between two toxin monomers through salt bridge and Van der Waals interaction [25]. A replacement with leucine residue at the position D39 also showed no effect on the inclusion formation. In contrast, alanine substitution at the position L33 located in β 1 of the N-terminal fragment leads to a significant decrease in protein production. In the detailed structure, L33 can form H-bonding with I31 and located in the van der Waals contact between the two monomers (**figure 6.1-6.2**). Based on the result from L33A mutation, this amino acid residue on β 1 of the N-terminus could play a crucial role in molecular folding and inclusion formation of Cyt2Aa2. This interaction through Van de Waals contact may also undergo with other dimers to assist in crystal protein formation [25]. N230A is another mutant that leads to low protein production. N230 on the C-terminus can form H-bond with V234 in α F of another monomer [25]. V234 is also in contact with Q200 to participate in crystal packing [25]. It is possible that when N230 was changed to alanine, the hydrogen bond with V234 will be missing, leading to an effect on the interacting network with Q200 and other residues. The result could be shown as a decreased level in protein production.

For the truncated proteins, S229stop and I233stop clearly gave a low expression of toxin. This may be a result from deletion of C-terminal tail. When compared with N238stop that showed a similar expression level to Cyt2Aa2, the effect of the truncated length seems to be important when the truncation reaches over the position 233. From x-ray structure, the residues from position 229 to 233 are identified as the C-terminal helix α F. Therefore, this result confirms that the C-terminal α F of Cyt2Aa2 is important for protein folding and inclusion formation [25]. In protein solubilization test in 50 mM $\text{Na}_2\text{CO}_3/\text{NaHCO}_3$ buffer pH 9.5, the solubility

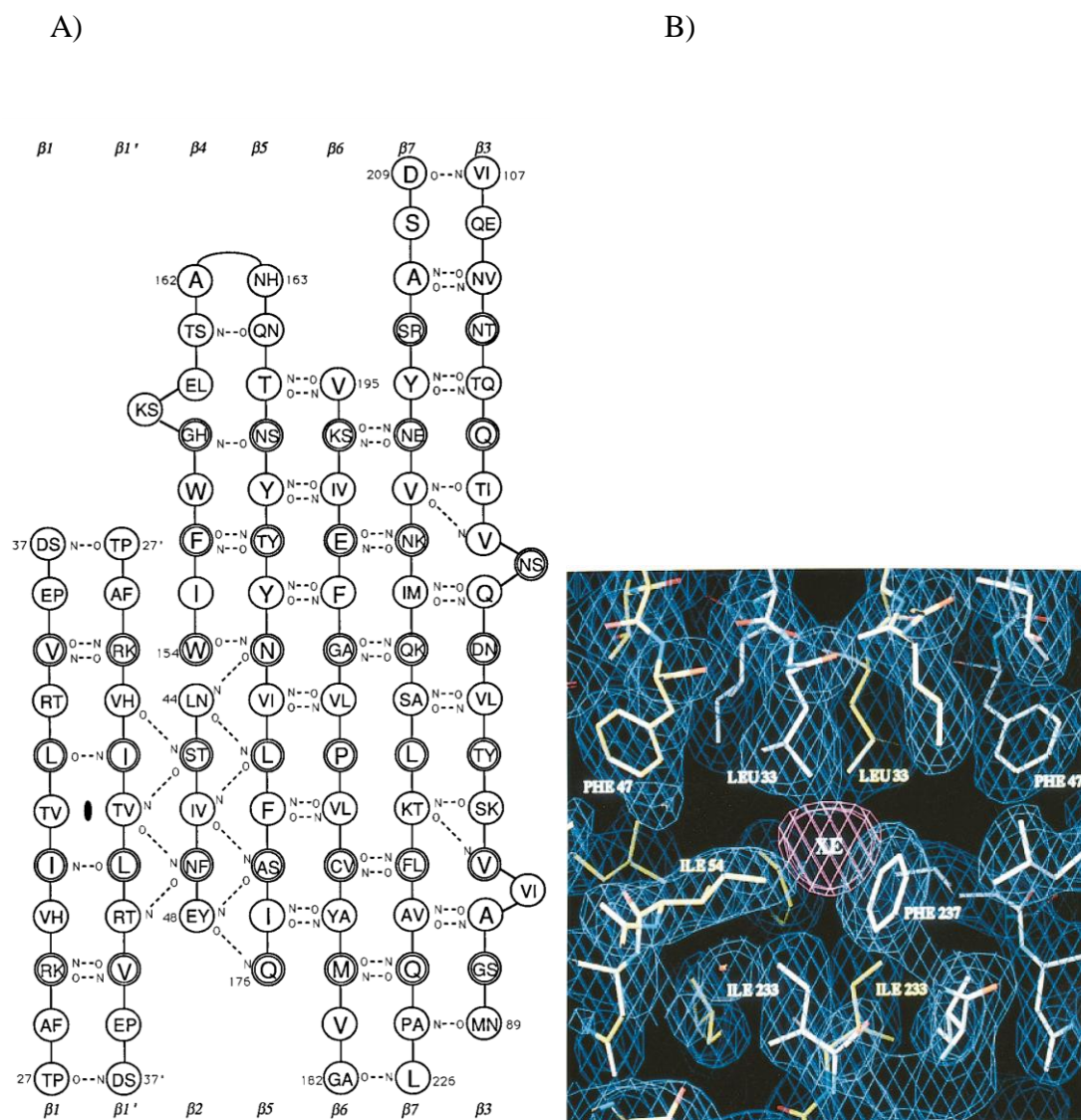


Figure 6.1: H-bond pattern in β -sheet of two monomers and van der Waals contacts on dimer interface of Cyt2 protein [25]

A) H-bond pattern in β -sheet. The amino acid residue of Cyt1 and Cyt2 is shown in the left and right, respectively.

B) A xenon atom bound in the hydrophobic cavity enclosed by van der Waals contacts on the dimer interface

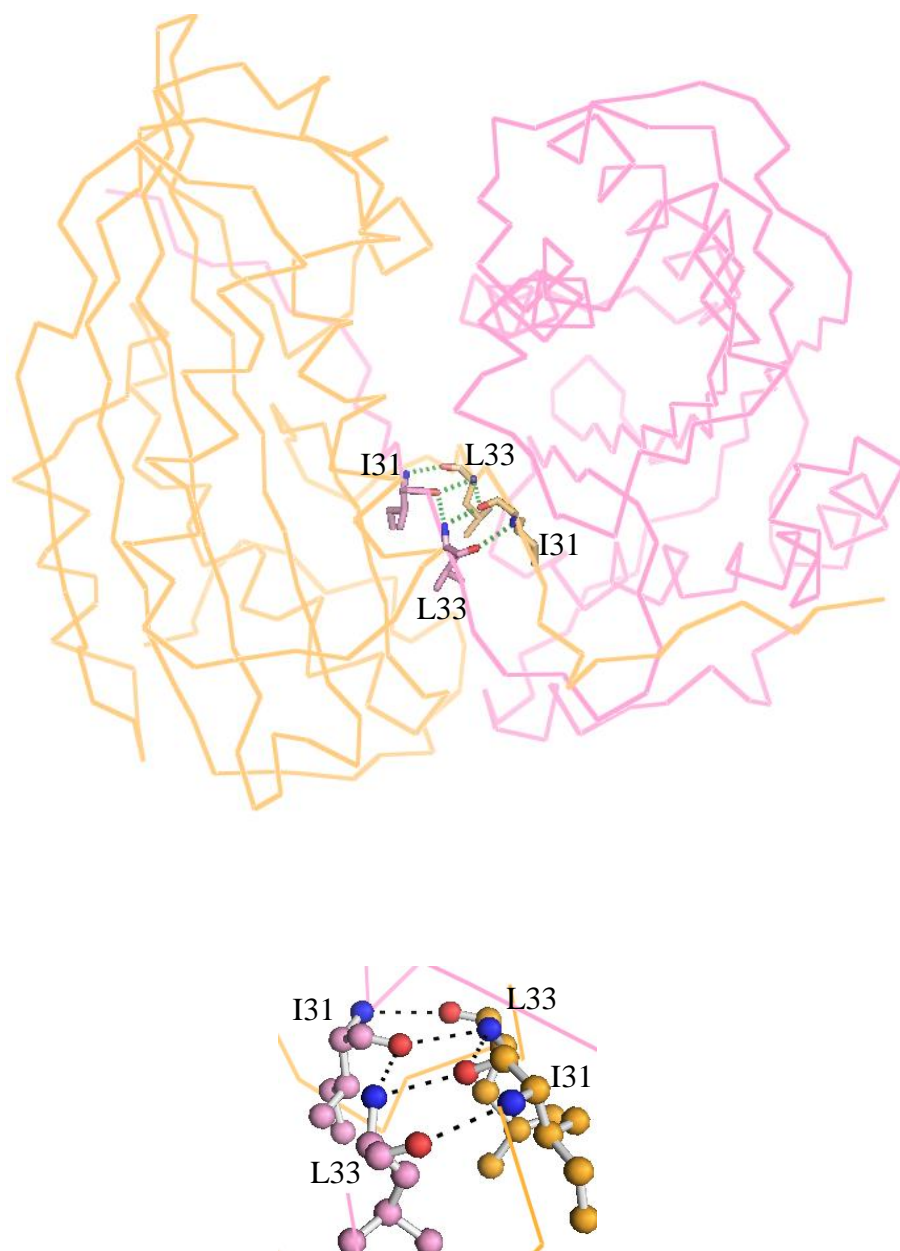


Figure 6.2: The H-bond interaction between I31 and L33 of Cyt2 protoxin created with PyMOL program

of R25A, P27A, I31A, L33A, and I233A proteins was comparable to that of Cyt2Aa2 but L33A, N230A, I233stop, and S229stop protein presented lower solubility than Cyt2Aa2. The mutations at these positions may be seen as a disturbance in the dimer contact as shown in **figures 5.12-5.13**. According to Li, et al., in an absence of these contacts, the monomer would have to adopt different conformation and had multiple conformations of protoxins in solution [25]. Therefore, these mutant proteins (L33A, N230A, I233stop, and S229stop) may adopt conformations that are different from Cyt2Aa2 in solution, affecting molecular stability and increased sensitivity to protease digestion. After proteolytic processing by proteinase K, a very faint band could be observed at 23 or 25 kDa on 12.5% SDS polyacrylamide gel (**figures 5.9-5.10**). Normally, Cyt2Aa2 yields proteinase K-activated product of about 25 kDa that contains amino acid residues from T34 to F237, and a minor band at 23 kDa for residues from S38 to S228. Both forms have a similar haemolytic activity [40]. It is interesting that disruption of H-bond between I233 (N atom) and A231 (O atom) by substitution to alanine did not affect the dimer contact whereas destroying the H-bond between N230 (O atom) and V234 (N atom) as shown in **figure 6.3** by substitution to alanine residue could not provide dimeric molecule. As shown in **figure 5.12**, I233A protoxin could be observed as a dimer at protein band about 50 kDa on 12.5% SDS-PAGE without the presence of DTT, but N230A did not show the protein band at 50 kDa. Consequently, it suggests that the hydrogen bond between N230 and V234 in another monomer is an important interaction for maintaining a dimeric structure and protoxin stability. For proteinase K digestion, I233A proteinase K-activated product showed a faint band at 25 kDa as shown in **figure 5.9**. It may be a result from its sensitivity to proteinase K processing. I233A protoxin still existed in dimeric form but it may be exposed some region accessible to protease digestion.

Biological properties

From haemolytic activity results of these mutagenic proteins, which are extracted from L33A, N230A, I233stop, and S229stop mutants, their protoxins could not lyse erythrocytes. It implies that although protoxins of these mutants may not be in the dimeric form, they are not in the right conformations to bind to the membrane or express their toxicities. The C-terminal truncated proteins which are S229stop and

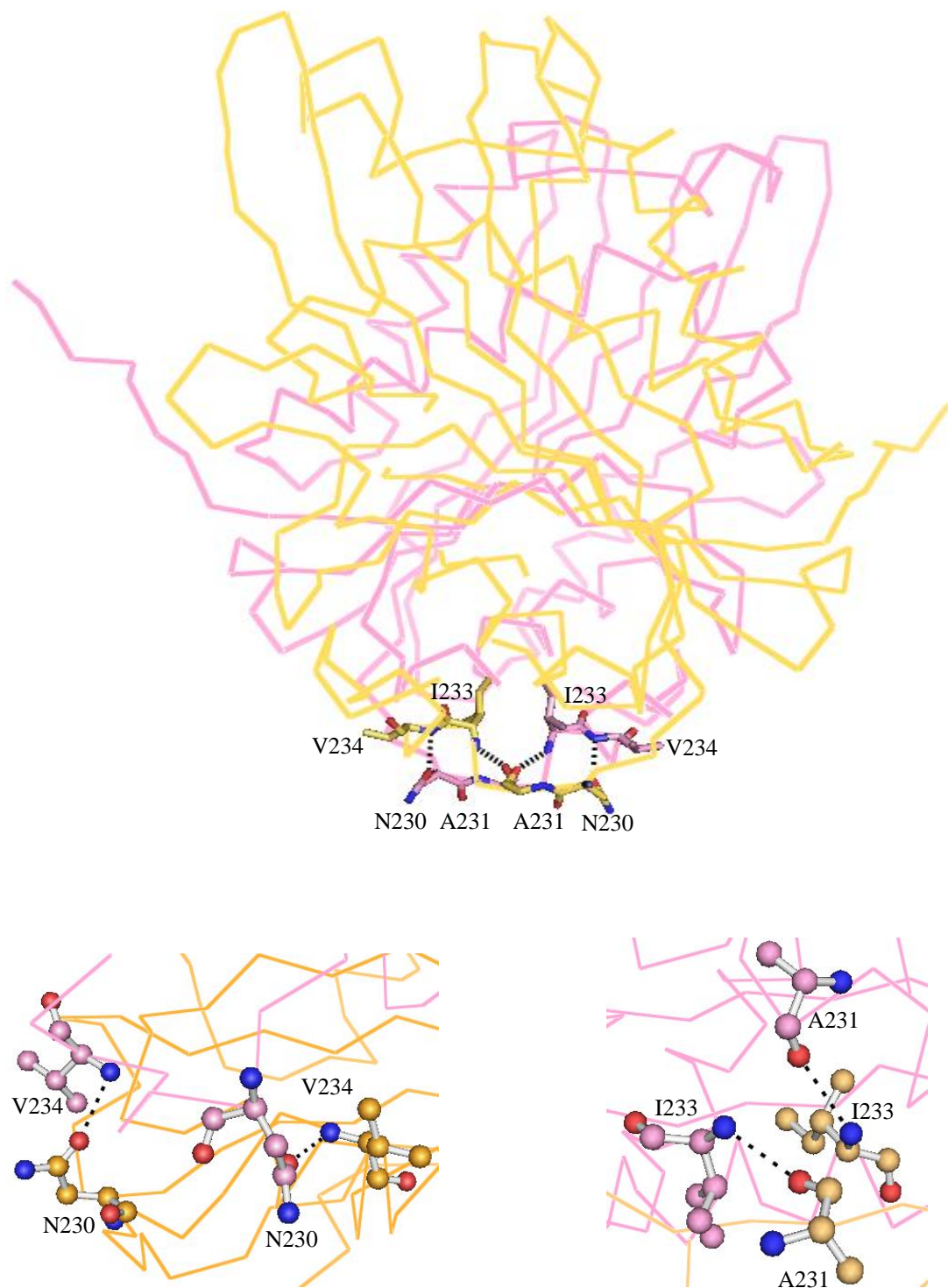


Figure 6.3: H-bond between α F of two monomers generated by PyMOL program

I233stop protoxins could not give the haemolytic activity and still requires proteolytic cleavage to cleave out at both N- and C-terminal fragments to become an active form. The fungal VVA2 toxin shares very similar structure to activated form of Cyt2Aa2 toxin. VVA2 monomer alone without proteolytic processing can provide the haemolytic activity [52]. On the other hand, the proteinase K-treated protoxins of these mutants which are L33A, N230A, I233A, I233stop, and S229stop mutants show lower haemolytic activity than Cyt2Aa2. It may be a result from various conformations or aggregation of protoxins in solution. The conformational change of mutant protein may affect protein stability and make protein more sensitive to proteinase K digestion. Therefore, they provided low amount of activated toxin.

Lipid binding test was used to investigate the behavior of protein when binding to the cell membrane. After incubated protein with liposome for 2 hours, Cyt2Aa2 protoxin showed a major band at 50 kDa that is a dimeric molecule on SDS-polyacrylamide gel, whereas Cyt2Aa2 activated toxin could form oligomeric molecules [62] or aggregation that was studied in Cyt1A [48, 71]. Therefore, a laddering pattern of protein band could be observed on SDS-polyacrylamide gel. D39L that has comparable toxicity to Cyt2Aa2 gave a similar result to Cyt2Aa2 when tested with liposomes (**figure 5.15**). It suggests that Cyt2 protein that can be functional or toxic can bind to the cell membrane and undergoes a specific process to lyse the cell either pore-forming model or detergent-like model [48, 71].

Mutant protoxins which were produced from L33A, N230A, S229stop, and I233stop showed more susceptibility to proteinase K digestion (**figure 5.9-5.10**). This could be explained why they have lower mosquito larvicidal activity than Cyt2Aa2 protein (**table 5.1**). After being solubilized at alkaline condition in mid-gut tract of mosquito larvae, the mutant proteins may exist in unfolded or unstable form of protoxin structure that leading to over digestion of gut-proteases. Particularly, S229stop protein could not kill mosquito larvae that showed a structural change in the result of intrinsic fluorescence spectroscopy (**figure 5.16**). It implied that protein had incorrect folding. S229stop mutant had low protein expression and was highly sensitive to protease digestion. Another reason is S229stop protein may be digested by gut-proteases to small inactive fragments that could not bind to the cell membrane

or undergo through the toxin mechanism which is either pore-forming model or detergent-like model.

Protein structure and particle sizes

Tertiary structural analysis of Cyt2Aa2 protein was investigated by intrinsic fluorescence spectrometer. The result showed that Cyt2Aa2 protoxin and proteinase-K activated product also showed a major peak at 330 nm and a shoulder around 340 nm. It suggests that there were more than one population or conformation of Cyt2Aa2 protoxins. All mutant protoxins were identified their structures to compare with that of Cyt2Aa2 protoxin. It could be classified into two groups. The first group is composed of R25A, P27A, I31A, D39L, N230A, and I233A mutants. They provided a major peak at 330 nm and a shoulder at 340 nm that were similar to those of wild type. R25A, P27A, I31A, and D39L mutants had comparable activity to Cyt2Aa2. This could be confirmed that they had a similar conformation to that of the wild type. On the other hand, N230A and I233A mutants showed a low solubility and over digestion after proteinase K treatment. They may have a partially conformational change but it did not disturb the environment around three tryptophan residues which are Trp132 located at α D, Trp154 and Trp157 located around β 4. Therefore, they can provide a similar spectrum to that of wild type. The second group of mutants includes L33A, S229stop, and I233stop protoxins. The major peak was observed at 340 nm whereas the shoulder was noticed around 330 nm. According to previous work of Cyt2Aa2 unfolding experiment, the maximum wavelength of native spectrum was observed at 327 nm and their structure was gradually unfolded with the red shift of their maximum wavelength to 347 nm when increasing GuHCL concentration [72]. These results imply that Cyt2Aa2 protoxin has a native structure that provided a maximum wavelength at 330 nm. Their emission spectra of L33A, S229stop, and I233stop protoxins were different from Cyt2Aa2 and they moved to red shift from wavelength at 330 nm to 340 nm. The positions of aromatic residues located in Cyt2Aa2 protoxin were changed that will alter their emission spectra. Replacing with alanine at leucine 33 made a conformational change and may result in protein aggregation. C-terminal truncated protoxin may adopt the incorrect folding of tertiary structure and tended to aggregate. Their haemolytic and larvicidal activities were

dramatically decreased and mutant protoxins were more sensitive to proteinase K digestion that may be the result from the structural change.

A protein size distribution profile was revealed by Dynamic Light Scattering (DLS) technique. Molecules in solution move as Brownian motion. When the laser hits a molecule, the intensity fluctuation of scattered light depends on the size of the molecule. It can determine the presence of aggregates and study oligomeric formation. Cyt2Aa2 protoxin profile showed three populations existed in 50 mM $\text{Na}_2\text{CO}_3/\text{NaHCO}_3$ buffer, pH 9.5 that showed their diameters around 4-10 nm (monomer or dimer), 30-100 nm (oligomer), 200-700 nm (oligomer). I31A protein was selected to test because it provided a similar tertiary structure and comparable activity to Cyt2Aa2 protein. Its protoxin also showed a similar size distribution profile to that of wild type. L33A showed a single broad peak between 40-600 nm and N230A showed two peaks at 60-200 nm and 300-1,100 nm, respectively (**figure 5.17**). L33A and N230A proteins had different tertiary structure from Cyt2Aa2. They are very sensitive to proteinase K digestion and showed much lower toxicity than that of Cyt2Aa2. In addition, size distribution profile of their protoxins was different from Cyt2Aa2 with diameter around 40-1,000 nm (oligomer) that was a wide range of a various size of molecules. L33A and N230A may be in the unfolded state and forming aggregation. Li., et al. reported that if Cyt2Aa2 protoxin is in the absence of dimer contact between two monomers, it will probably have multiple conformations, and the low solubility of main-chain results in aggregation [25]. I233A protoxin also showed different size distribution profiles from Cyt2Aa2 protoxin. Its diameter was about 150-350 nm and 5,000 nm (oligomer). The tertiary structure and haemolytic activity were also different from Cyt2Aa2. It suggests that I233A protoxin could not exist as a native form, thus it may provide more susceptibility to proteinase K than Cyt2Aa2 resulting in a reduction of haemolytic activity. Consequently, Cyt2Aa2 and I31A showed the monomer or dimer peak of protoxin (4-10 nm). They exist in the proper conformation and can yield the active fragment after proteinase K treatment. On the other hand, other mutants provided the larger size of protoxin. It could be oligomers or aggregation of incorrect protein folds.

Proposed role of N- and C-terminal regions ($\beta 1$ and αF)

Based on X-ray crystallographic structure analysis of Cyt2Aa2 protoxin in monomeric form, an interaction between the N-terminal fragment and the end of C-terminal fragment which is very closed in space is a factor that may keep the toxin in inactive form. D39 on N-terminal fragment located at proteolytic cleavage site can form hydrogen network with L40 on the N-terminal fragment and N241 on the C-terminal fragment (**figure 6.4**). D39 was mutated to disrupt the hydrogen bond network while keeping steric hindrance and size of its side chain. Haemolytic activity result showed that D39L protoxin did not contain haemolytic activity and it still requires proteolytic activation to become an active toxin. As a result, it can imply in many aspects, firstly, there is no interaction among D39, L40 on the N-terminal fragment and N241 on the C-terminal fragment. Secondly, there is the intra-interaction between three amino acids and breaking only the interaction at this position is not sufficient to convert inactive protoxin to active form because there are other interactions between N- and C-terminal fragments. Lastly, the inactive protoxin could not be active because of dimeric interaction of five regions between two monomers, especially on N- and C-terminal tails of each monomer [25].

The truncation of C-terminal fragment at position S229 located at proteinase-K cleavage site was engineered to delete the interactions between N- and C-terminal fragments. S229stop mutant is a low expression mutant, low solubility, and highly sensitive to proteinase K digestion. Low activity of this mutant could be just because there is no activated toxin to exhibit its activity. The result revealed that the deletion of 31 amino acids (S229 to N259) at C-terminal fragment gave a huge impact on protein production. The solubilized truncated C-terminal protoxin may not exist in a dimeric form after solubilized in 50 mM $\text{Na}_2\text{CO}_3/\text{NaHCO}_3$ buffer pH 9.5 (**figure 5.13**), but it was still inactive. The N-terminal fragment must be removed in order to turn the protein into the active form.

In addition, solubilized L33A and N230A protoxins did not exist in dimeric molecules (**figure 5.12**) and did not have the haemolytic activity. Consequently, it can be concluded that Cyt2Aa2 protoxin needs to be processed on both N- and C-termini to adopt the proper conformation that may be required for toxin

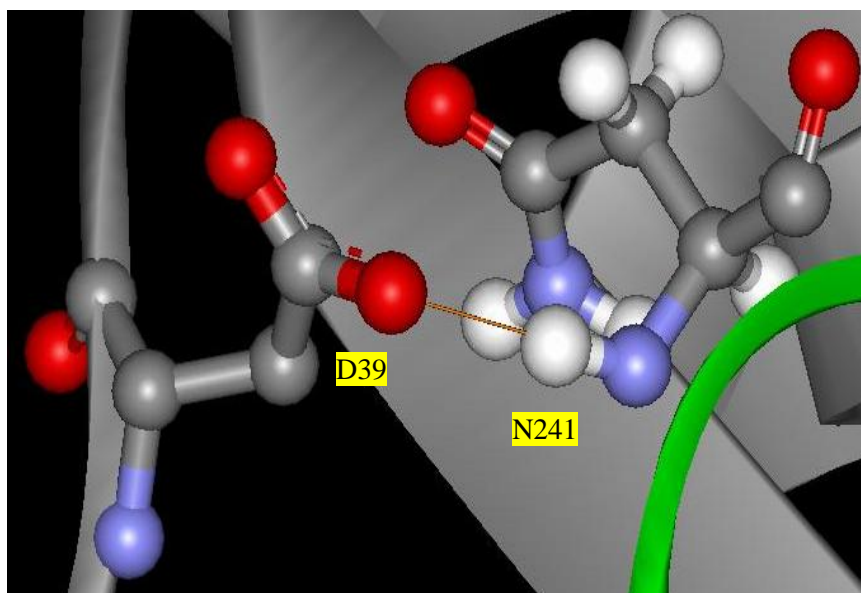
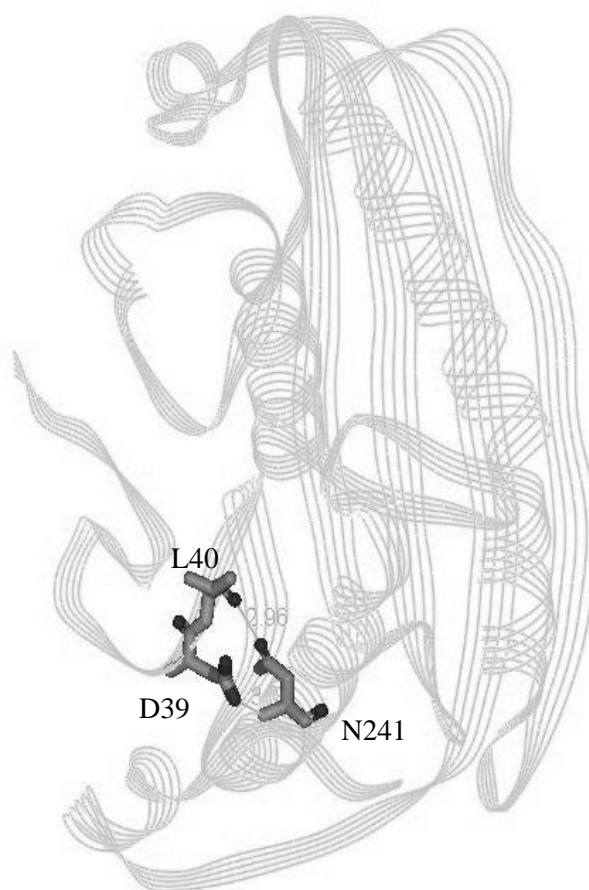









Figure 6.4: H-bond network between D39, L33 and N241 in Cyt2A monomer generated by WebLab ViewerPro software

binding to the membrane and toxin oligomerization process or aggregation. From previous study, the intertwined N-terminal fragments and β -1 and β -1' sheets of Cyt2A protoxin involved in dimerization were cleaved out to provide the active monomeric form. The C-terminal tails and α F and α F' of the protoxin were also removed to expose the mixed β layers core. Cyt2A showed only one trypsin cleavage site at His 30 on N-terminal fragment. When Cyt2A toxin was processed by trypsin, it provided an inactive product because it cannot remove the interaction between β -1 and β -1' sheets, therefore it still existed in dimeric form and it could not expose the mixed β layers core[25]. On the other hand, dimeric structure of Cyt2Aa2 protoxin is very essential for protein stability and maintaining protoxin in the right conformation to become the active toxin. Moreover, truncated C-terminal fragment S229 and I233 showed low efficiency in protein production, incorrect folding and less toxicity as shown in **table 6.1**. It suggests that α F is important for protein folding, inclusion formation, and protein stability. L33A and N230A proteins were not dimeric molecules and provided the different tertiary structure from Cyt2Aa2 that affects the solubility and toxicity. Therefore, N- and C-terminal fragments play important role during protein folding process. If Cyt2Aa2 protein does not have these N- and C-regions, the protein will become misfolded and denatured structure leading to protein aggregation, instability, and inactive form. β 1 at N-terminal fragment and α F at C-terminal fragment are important for protein folding and dimerization process to maintain the protein structure in the right conformation ready to be activated. Amino acid substitution and deletion at these regions could directly affect inter- and intra-molecular interactions required to hold the toxin in the right conformation. The mutated toxin will become mis-folded and inactive.

Table 6.1: List of truncated mutants of Cyt2Aa2 toxin

Truncated toxin	Amino acids	Solubilization	Proteinase K activation	Larvicidal activity	Haemolytic activity
Cyt2Aa2	← [1 - 259] → 	√	√	+++	+++
N238stop	← [1 - 237] → 	√	√	+++	+++
I233stop	← [1 - 232] → 	-	-	+	+
S229stop	← [1 - 228] → 	-	-	-	+
Q224stop	← [1 - 223] → 	-	-	-	-
K218stop	← [1 - 217] → 	-	-	-	-
E214stop	← [1 - 213] → 	-	-	-	-

“√” represents to ability to be solubilized in 50 mM Na₂CO₃/NaHCO₃ buffer, pH 9.5 or active toxin after proteinase K activation.

“-” represents to inability to be solubilized in 50 mM Na₂CO₃/NaHCO₃ buffer, pH 9.5 or active toxin after proteinase K activation.

“+” indicates the level of protein activity

CHAPTER VII

SUMMARY

1. Amino acid substitutions of Cyt2Aa2 at positions R25, P27, I31 and D39 did not affect protein structure and functions suggesting that they are not responsible for specific function. In contrast, amino acid replacements at positions L33, N230 and I233 affected protein folding, dimerization and reduced activity. These amino acids could play an important role to stabilize protein structure.
2. Deletion of 22 amino acids from C-terminal fragment of Cyt2Aa2 yielded truncated protein with similar toxicity to Cyt2Aa2, whereas deletion of 27 and 31 amino acids showed an effect on protein folding, protein production, and less toxicity. These amino acids located around α F at C-terminal fragment are essential for protein production, maintaining protein structure and protein integrity.
3. The correct protein folding of Cyt2Aa2 tertiary structure is required for protein production, solubilization, and activation. Constructed mutant toxins that give different fluorescence emission spectra from that of wild type showed the non-native properties in toxin solubilization and activation.
4. Dynamic Light Scattering of Cyt2Aa2 protoxins in solution demonstrated mixed populations of toxin monomer, dimer, and oligomer. Monomer or dimer forms of the toxin are suggested as the proper conformation for expression and activity.
5. Both N- and C-terminal regions of Cyt2Aa2 play a vital role in providing of correct protein folding and molecular stabilization.

REFERENCES

- 1 Carozzi, N.B., et al. (1991). Prediction of insecticidal activity of *Bacillus thuringiensis* strains by polymerase chain reaction product profiles. *Appl Environ Microbiol*, 57(11), 3057-61.
- 2 Kaelin, P., P. Morel, and F. Gadani. (1994). Isolation of *Bacillus thuringiensis* from stored tobacco and *Lasioderma serricorne* (F.). *Appl Environ Microbiol*, 60(1), 19-25.
- 3 Carlson, C.R., D.A. Caugant, and A.B. Kolsto. (1994). Genotypic diversity among *Bacillus cereus* and *Bacillus thuringiensis* Strains. *Appl Environ Microbiol*, 60(6), 1719-1725.
- 4 Schnepf, E., et al. (1998). *Bacillus thuringiensis* and its pesticidal crystal proteins. *Microbiol Mol Biol Rev*, 62(3), 775-806.
- 5 Crickmore, N., et al. (1998). Revision of the nomenclature for the *Bacillus thuringiensis* pesticidal crystal proteins. *Microbiol Mol Biol Rev*, 62(3), 807-13.
- 6 Schesser, J.H. and L.A. Bulla, Jr. (1978). Toxicity of *Bacillus thuringiensis* spores to the tobacco hornworm, *Manduca sexta*. *Appl Environ Microbiol*, 35(1), 121-3.
- 7 Somerville, H.J. and H.V. Pockett. (1975). An insect toxin from spores of *Bacillus thuringiensis* and *Bacillus cereus*. *J Gen Microbiol*, 87(2), 359-69.
- 8 Ulewicz, K. (1975). Studies of the infection of the cockroaches (*Blattella germanica*[L.]) with *Bac. thuringiensis*. *Zentralbl Bakteriol [Orig B]*, 160(4-5), 534-9.
- 9 Vervelle, C. (1975). [The role of spores and crystals of *Bacillus thuringiensis* Berliner in the infection of *Laspeyresia pomonella* L. (Tortricidae) (author's transl)]. *Ann Parasitol Hum Comp*, 50(6), 655-68.

- 10 Zhong, C., et al. (2000). Characterization of a *Bacillus thuringiensis* delta-endotoxin which is toxic to insects in three orders. *J Invertebr Pathol*, 76(2), 131-9.
- 11 Bravo, A., S.S. Gill, and M. Soberon. (2007). Mode of action of *Bacillus thuringiensis* Cry and Cyt toxins and their potential for insect control. *Toxicon*, 49(4), 423-35.
- 12 Gough, J.M., et al. (2005). Identification and characterization of proteins from *Bacillus thuringiensis* with high toxic activity against the sheep blowfly, *Lucilia cuprina*. *J Invertebr Pathol*, 90(1), 39-46.
- 13 Schesser, J.H. (1976). Commercial formulations of *Bacillus thuringiensis* for control of Indian meal moth. *Appl Environ Microbiol*, 32(4), 508-10.
- 14 Chilcott, C.N., et al. (1998). Activities of *Bacillus thuringiensis* insecticidal crystal proteins Cyt1Aa and Cyt2Aa against three species of sheep blowfly. *Appl Environ Microbiol*, 64(10), 4060-1.
- 15 Prieto-Samsonov, D.L., et al. (1997). *Bacillus thuringiensis*: from biodiversity to biotechnology. *J Ind Microbiol Biotechnol*, 19(3), 202-19.
- 16 Crickmore, N., et al. (1990). The construction of *Bacillus thuringiensis* strains expressing novel entomocidal delta-endotoxin combinations. *Biochem J*, 270(1), 133-6.
- 17 Insell, J.P. and P.C. Fitz-James. (1985). Composition and toxicity of the inclusion of *Bacillus thuringiensis* subsp. *israelensis*. *Appl Environ Microbiol*, 50(1), 56-62.
- 18 Gill, S.S., E.A. Cowles, and P.V. Pietrantonio. (1992). The mode of action of *Bacillus thuringiensis* endotoxins. *Annu Rev Entomol*, 37, 615-36.
- 19 Cao, J., et al. (2006). *Bacillus thuringiensis* protein production, signal transduction, and insect control in chemically inducible PR-1a/cry1Ab broccoli plants. *Plant Cell Rep*, 25(6), 554-60.
- 20 Cheong, H. and S.S. Gill. (1997). Cloning and characterization of a cytolytic and mosquitocidal delta-endotoxin from *Bacillus thuringiensis* subsp. *jegathesan*. *Appl Environ Microbiol*, 63(8), 3254-60.

- 21 Knowles, B.H., et al. (1989). A cytolytic delta-endotoxin from *Bacillus thuringiensis* var. *israelensis* forms cation-selective channels in planar lipid bilayers. *FEBS Lett*, 244(2), 259-62.
- 22 Slatin, S.L., C.K. Abrams, and L. English. (1990). Delta-endotoxins form cation-selective channels in planar lipid bilayers. *Biochem Biophys Res Commun*, 169(2), 765-72.
- 23 Von Tersch, M.A., et al. (1994). Membrane-permeabilizing activities of *Bacillus thuringiensis* coleopteran-active toxin CryIIIB2 and CryIIIB2 domain I peptide. *Appl Environ Microbiol*, 60(10), 3711-7.
- 24 Koni, P.A. and D.J. Ellar. (1993). Cloning and characterization of a novel *Bacillus thuringiensis* cytolytic delta-endotoxin. *J Mol Biol*, 229(2), 319-27.
- 25 Li, J., P.A. Koni, and D.J. Ellar. (1996). Structure of the mosquitocidal delta-endotoxin CytB from *Bacillus thuringiensis* sp. *kyushuensis* and implications for membrane pore formation. *J Mol Biol*, 257(1), 129-52.
- 26 Waalwijk, C., et al. (1985). Molecular cloning and the nucleotide sequence of the Mr 28 000 crystal protein gene of *Bacillus thuringiensis* subsp. *israelensis*. *Nucleic Acids Res*, 13(22), 8207-17.
- 27 Yu, Y.M., M. Ohba, and S.S. Gill. (1991). Characterization of mosquitocidal activity of *Bacillus thuringiensis* subsp. *fukuokaensis* crystal proteins. *Appl Environ Microbiol*, 57(4), 1075-81.
- 28 Kawalek, M.D., et al. (1995). Isolation and Identification of novel toxins from a new mosquitocidal isolate from Malaysia, *Bacillus thuringiensis* subsp. *jegathesan*. *Appl Environ Microbiol*, 61(8), 2965-9.
- 29 Riabchenko, N.F. and S.I. Alikhanian. (1984). [Bacteriocinogenic plasmids of *Bacillus thuringiensis*]. *Genetika*, 20(7), 1067-70.
- 30 Orduz, S., et al. (1992). A new serotype of *Bacillus thuringiensis* from Colombia toxic to mosquito larvae. *J Invertebr Pathol*, 59(1), 99-103.
- 31 Estruch, J.J., et al. (1996). Vip3A, a novel *Bacillus thuringiensis* vegetative insecticidal protein with a wide spectrum of activities against lepidopteran insects. *Proc Natl Acad Sci U S A*, 93(11), 5389-94.

- 32 Guerchicoff, A., A. Delecluse, and C.P. Rubinstein. (2001). The *Bacillus thuringiensis* cyt genes for hemolytic endotoxins constitute a gene family. *Appl Environ Microbiol*, 67(3), 1090-6.
- 33 Koni, P.A. and D.J. Ellar. (1994). Biochemical characterization of *Bacillus thuringiensis* cytolytic delta-endotoxins. *Microbiology*, 140 (Pt 8), 1869-80.
- 34 Tepanant, W. Investigation of folding pathway of Cyt2Aa2 Insecticidal protein from *Bacillus thuringiensis*. Nakron Pathom: MAHIDOL University 2004
- 35 Ward, E.S. and D.J. Ellar. (1986). *Bacillus thuringiensis* var. *israelensis* delta-endotoxin. Nucleotide sequence and characterization of the transcripts in *Bacillus thuringiensis* and *Escherichia coli*. *J Mol Biol*, 191(1), 1-11.
- 36 Earp, D.J. and D.J. Ellar. (1987). *Bacillus thuringiensis* var. *morrisoni* strain PG14: nucleotide sequence of a gene encoding a 27kDa crystal protein. *Nucleic Acids Res*, 15(8), 3619.
- 37 Galjart, N.J., N. Sivasubramanian, and B.A. Federici. (1987). Plasmid location, cloning, and sequence analysis of the gene encoding a 27.3-kilodalton cytolytic protein from *Bacillus thuringiensis* subsp. *morrisoni* (PG-14). *Current Microbiology*, 16(3), 171-177.
- 38 Thiery, I., et al. (1997). Identification of a gene for Cyt1A-like hemolysin from *Bacillus thuringiensis* subsp. *medellin* and expression in a crystal-negative *B. thuringiensis* strain. *Appl. Environ. Microbiol.*, 63(2), 468-473.
- 39 Payne, J.D., CA), Narva, Kenneth E. (San Diego, CA), Uyeda, Kendrick A. (San Diego, CA), Stalder, Christine J. (San Diego, CA), Michaels, Tracy E. (Ames, IA), *Bacillus thuringiensis* isolate PS201T6 toxin. 1995, Mycogen Corporation (San Diego, CA): United States.
- 40 Promdonkoy, B., et al. (2003). Cloning and characterization of a cytolytic and mosquito larvicidal delta-endotoxin from *Bacillus thuringiensis* subsp. *darmstadiensis*. *Curr Microbiol*, 46(2), 94-8.
- 41 Guerchicoff, A., R.A. Ugalde, and C.P. Rubinstein. (1997). Identification and characterization of a previously undescribed cyt gene in *Bacillus thuringiensis* subsp. *israelensis*. *Appl. Environ. Microbiol.*, 63(7), 2716-2721.

- 42 Yu, J., et al. (2002). Cloning and expression of cyt2Ba7 gene from a soil-isolated *Bacillus thuringiensis*. *Curr Microbiol*, 45(5), 309-14.
- 43 Juarez-Perez, V., et al. (2002). Characterization of Cyt2Bc Toxin from *Bacillus thuringiensis* subsp. *medellin*. *Appl. Environ. Microbiol.*, 68(3), 1228-1231.
- 44 McLean, K.M. and H.R. Whiteley. (1987). Expression in *Escherichia coli* of a cloned crystal protein gene of *Bacillus thuringiensis* subsp. *israelensis*. *J Bacteriol*, 169(3), 1017-23.
- 45 Adams, L.F., J.E. Visick, and H.R. Whiteley. (1989). A 20-kilodalton protein is required for efficient production of the *Bacillus thuringiensis* subsp. *israelensis* 27-kilodalton crystal protein in *Escherichia coli*. *J Bacteriol*, 171(1), 521-30.
- 46 Visick, J.E. and H.R. Whiteley. (1991). Effect of a 20-kilodalton protein from *Bacillus thuringiensis* subsp. *israelensis* on production of the CytA protein by *Escherichia coli*. *J Bacteriol*, 173(5), 1748-56.
- 47 Cohen, S., et al. (2008). High-resolution crystal structure of activated Cyt2Ba monomer from *Bacillus thuringiensis* subsp. *israelensis*. *J Mol Biol*, 380(5), 820-7.
- 48 Butko, P. (2003). Cytolytic toxin Cyt1A and its mechanism of membrane damage: data and hypotheses. *Appl Environ Microbiol*, 69(5), 2415-22.
- 49 Bourgouin, C., A. Klier, and G. Rapoport. (1986). Characterization of the genes encoding the haemolytic toxin and the mosquitocidal delta-endotoxin of *Bacillus thuringiensis israelensis*. *Mol Gen Genet*, 205(3), 390-7.
- 50 Knowles, B.H., et al. (1992). A broad-spectrum cytolytic toxin from *Bacillus thuringiensis* var. *kyushuensis*. *Proc Biol Sci*, 248(1321), 1-7.
- 51 Drobniowski, F.A. and D.J. Ellar. (1989). Purification and properties of a 28-kilodalton hemolytic and mosquitocidal protein toxin of *Bacillus thuringiensis* subsp. *darmstadiensis* 73-E10-2. *J Bacteriol*, 171(6), 3060-7.
- 52 Lin, S.C., et al. (2004). Crystal structures and electron micrographs of fungal volvatoxin A2. *J Mol Biol*, 343(2), 477-91.

- 53 Parker, M.W. and S.C. Feil. (2005). Pore-forming protein toxins: from structure to function. *Prog Biophys Mol Biol*, 88(1), 91-142.
- 54 Hofte, H. and H.R. Whiteley. (1989). Insecticidal crystal proteins of *Bacillus thuringiensis*. *Microbiol Rev*, 53(2), 242-55.
- 55 Andrews, R.E., Jr., M.M. Bibilos, and L.A. Bulla, Jr. (1985). Protease activation of the entomocidal protoxin of *Bacillus thuringiensis* subsp. *kurstaki*. *Appl Environ Microbiol*, 50(4), 737-42.
- 56 Armstrong, J.L., G.F. Rohrmann, and G.S. Beaudreau. (1985). Delta endotoxin of *Bacillus thuringiensis* subsp. *israelensis*. *J Bacteriol*, 161(1), 39-46.
- 57 Bulla, L.A., Jr., K.J. Kramer, and L.I. Davidson. (1977). Characterization of the entomocidal parasporal crystal of *Bacillus thuringiensis*. *J Bacteriol*, 130(1), 375-83.
- 58 Bravo, A., et al. (2004). Oligomerization triggers binding of a *Bacillus thuringiensis* Cry1Ab pore-forming toxin to aminopeptidase N receptor leading to insertion into membrane microdomains. *Biochim Biophys Acta*, 1667(1), 38-46.
- 59 Thomas, W.E. and D.J. Ellar. (1983). Mechanism of action of *Bacillus thuringiensis* var *israelensis* insecticidal delta-endotoxin. *FEBS Lett*, 154(2), 362-8.
- 60 Van Rie, J., et al. (1989). Specificity of *Bacillus thuringiensis* delta-endotoxins. Importance of specific receptors on the brush border membrane of the mid-gut of target insects. *Eur J Biochem*, 186(1-2), 239-47.
- 61 Gill, S.S., G.J. Singh, and J.M. Hornung. (1987). Cell membrane interaction of *Bacillus thuringiensis* subsp. *israelensis* cytolytic toxins. *Infect Immun*, 55(5), 1300-8.
- 62 Promdonkoy, B. and D.J. Ellar. (2003). Investigation of the pore-forming mechanism of a cytolytic delta-endotoxin from *Bacillus thuringiensis*. *Biochem J*, 374(Pt 1), 255-9.
- 63 Shai, Y. (1995). Molecular recognition between membrane-spanning polypeptides. *Trends Biochem Sci*, 20(11), 460-4.

- 64 Li, J., et al. (2001). Structural implications for the transformation of the *Bacillus thuringiensis* delta-endotoxins from water-soluble to membrane-inserted forms. *Biochem Soc Trans*, 29(Pt 4), 571-7.
- 65 Promdonkoy, B. and D.J. Ellar. (2000). Membrane pore architecture of a cytolytic toxin from *Bacillus thuringiensis*. *Biochem J*, 350 Pt 1, 275-82.
- 66 Du, J., et al. (1999). Biochemical characterization of *Bacillus thuringiensis* cytolytic toxins in association with a phospholipid bilayer. *Biochem J*, 338 (Pt 1), 185-93.
- 67 Ferre, J. and J. Van Rie. (2002). Biochemistry and genetics of insect resistance to *Bacillus thuringiensis*. *Annu Rev Entomol*, 47, 501-33.
- 68 Wirth, M.C., G.P. Georgiou, and B.A. Federici. (1997). CytA enables CryIV endotoxins of *Bacillus thuringiensis* to overcome high levels of CryIV resistance in the mosquito, *Culex quinquefasciatus*. *Proc Natl Acad Sci U S A*, 94(20), 10536-40.
- 69 Perez, C., et al. (2005). *Bacillus thuringiensis* subsp. *israelensis* Cyt1Aa synergizes Cry11Aa toxin by functioning as a membrane-bound receptor. *Proc Natl Acad Sci U S A*, 102(51), 18303-8.
- 70 Promdonkoy, B., P. Promdonkoy, and S. Panyim. (2005). Co-expression of *Bacillus thuringiensis* Cry4Ba and Cyt2Aa2 in *Escherichia coli* revealed high synergism against *Aedes aegypti* and *Culex quinquefasciatus* larvae. *FEMS Microbiol Lett*, 252(1), 121-6.
- 71 Manceva, S.D., et al. (2005). A detergent-like mechanism of action of the cytolytic toxin Cyt1A from *Bacillus thuringiensis* var. *israelensis*. *Biochemistry*, 44(2), 589-97.
- 72 Sangcharoen, A., et al. (2009). Investigation of the unfolding pathway of *Bacillus thuringiensis* Cyt2Aa2 toxin reveals an unfolding intermediate. *J Biotechnol*, 141(3-4), 137-41.

BIOGRAPHY

NAME	Miss Siriya Thammachat
DATE OF BIRTH	December 3, 1981
PLACE OF BIRTH	Bangkok, Thailand
INSTITUTIONS ATTENDED	Kasetsart University, 2000-2004: Bachelor of Science (Biology) Mahidol University, 2005-2010: Doctor of Philosophy (Molecular Genetics and Genetic Engineering)
SCHOLARSHIPS	National Center for Genetic Engineering and Biotechnology (NSTDA), 2006-2007 The Royal Golden Jubilee Ph.D. Program (RGJ), Thailand Research Fund (TRF), 2008-2010
HOME ADDRESS	90/77 Soi Kanchanawanit 23, Kanchanawanit Road, Khaorupchang, Songkhla 90000 Tel. 074-558144 E-mail: roongsung@hotmail.com
PUBLICATIONS	<u>Thammachat, S.</u> , Phuengthanaom, N., Pathaichindachote, W., Promdonkoy, B. & Krittanai C. Functional role of amino acids located at β -1 and α -F of Cyt2Aa2 toxin. <i>BMB. Rep</i> , accepted, (2010)

PUBLICATIONS

Thammachat, S., Pathaichindachote, W.,
Krittanaï, C. & Promdonkoy, B.
Amino acids at N- and C-termini
are required for the efficient
production and folding a cytolytic
delta-endotoxin from *Bacillus*
thuringiensis. *BMB. Rep.* **41**,
820-825 (2008)